Faculty of Health Sciences

Department of Human Biology

Division of Biomedical Engineering

University of Cape Town

Design and Development of an Automated MDI Delivery System with Breath Detection for Use with Oxygen Therapy

Minor Dissertation

Submitted to the University of Cape Town

In partial fulfilment of the academic requirements for MSc degree in Biomedical Engineering

by Coursework and Dissertation

Author: Muhammad Arshad Eyasim (EYSMUH001)

Supervisor: Professor Sudesh Sivarasu

24th July 2023

DECLARATION

I, *Muhammad Arshad Eyasim*, hereby declare that the work on which this dissertation/thesis is based is my original work (except where acknowledgements indicate otherwise) and that neither the whole work nor any part of it has been, is being, or is to be submitted for another degree in this or any other university.

I empower the university to reproduce for the purpose of research either the whole or any portion of the contents in any manner whatsoever.

Signature: Signed by candidate

Date: 24th July 2023

Abstract

Introduction: Metered Dose Inhalers (MDI) are pressurised canisters that contain a bronchodilator medication used to treat obstructive lung disease symptoms. The medication is delivered to the lungs' airways by simultaneously actuating the MDI and inhaling, and the medication's effectiveness depends on optimal actuation-inhalation coordination. With the emergence of Covid-19, the use of MDI has increased among ventilated patients with Chronic Obstructive Pulmonary Disease or Asthma. This emphasised the difficulty with actuation-inhalation coordination, in which a nurse must remain by the bedside to monitor inhalation, time the actuations, and synchronise the actuations with inhalation, which is inaccurate because it more often falls outside the desired range of 0.2 s, resulting in lower drug effectiveness. To address the inaccurate actuation-inhalation coordination and the limited number of Intensive Care Unit (ICU) resources, a need was identified for a device that can be used outside of ICU settings and can automatically deliver bronchodilator medications using MDIs.

Methods: An automated MDI delivery system with breath detection was designed and developed. The device comprises of an actuation mechanism, a breath detection system, and a user interface. A cam and servo mechanism actuates the canister, the breath detection system detects inhalation with a pressure and flow rate sensor, and the user interface (UI) consists of a display and a rotary encoder. The device was tested using a continuous positive airway pressure device and a breathing simulator to validate the accuracy of the breath detection system, the accuracy of the actuation mechanism, and the device's operation. The device was then validated against the existing manual solution by comparing the delay between the actuation and the inhalation signal to determine the effectiveness of the developed device.

Results: The developed device includes all the required functionalities and an intuitive UI. The device, however, is quite large and not impact-resistant; the noise during actuation can be disturbing, and it can only be used with canisters that do not require shaking before actuation. The device detects inhalation 0.11 s before the inhalation signal, and the servo actuates the canister in 0.25 s. This time difference of 0.14 s allows the medication to be delivered within the desired time after the onset of inhalation. Based on the user input settings, the device also operates as intended and the interval between actuations is the required 15 s. The automated test also shows a constant delay time of 0.14 s between the actuation and onset of inhalation, compared to the delays in the manual test, which vary and are mostly outside of the acceptable range.

Conclusion: The results show that the device works as intended and is more effective than the existing manual solution by providing an automated and improved solution for bronchodilator therapy, thus increasing the medication delivery's effectiveness. Future recommendations are made to improve the device's design, and future work includes further validating the device's effectiveness.

Acknowledgments

Alhamdulillah for giving me the strength and courage to complete this research.

First and foremost, I want to thank my parents for their determined support and prayers.

I wish to express my gratitude to Professor Sudesh Sivarasu for supervising, supporting and guiding me during my research. His expertise in the design of medical equipment was crucial to the success of this research, without which it would not have been possible.

I also want to thank Dr. Wandile Ganya for serving as the study's clinical partner. He provided helpful insights on the clinical aspect of the research and on the device's design. Additionally, I would like to thank all the lecturers at UCT who have taught me. I want to thank Jeran Cloete and Etienne Horn for providing valuable advice on my research as well as the UCT MedTech members.

I would like to thank UCT for the International Student Scholarship and Manufacturing, Engineering and Related Services (merSETA) for funding this research.

Table of Contents

List of Figures

List of Tables

List of Acronyms

BS	Breathing Simulator
CFD	Computational Flow Dynamics
COPD	Chronic Obstructive Pulmonary Disease
FMEA	Failure Modes and Effects Analysis
GUI	Graphical User Interface
ICU	Intensive Care Unit
MDD	MDI Delivery Device
MDI	Metered Dose Inhaler
MDL	Medical Devices Lab
MERS-CoV	Middle East Respiratory Syndrome Coronavirus
SARS-CoV-2	Severe Acute Respiratory Syndrome Coronavirus 2
UI	User Interface
VAT	Ventilator Assessment Tool

CHAPTER 1: INTRODUCTION

1.1 Background to Study

Bronchodilator therapy is commonly used in ventilated patients with obstructive lung diseases, such as Chronic Obstructive Pulmonary Disease (COPD) or Asthma, as it considerably decreases airway resistance by opening the airways of the lungs making breathing easier (Mouloudi et al., 2000). The use of bronchodilator medication is growing among Covid-19 ventilated patients with COPD or Asthma comorbidities as the number of Covid-19 infected cases rises (Villamañán et al., 2021). Metered Dose Inhalers (MDI) or nebulizers are used to administer aerosol bronchodilators to ventilated patients. MDI is preferred over nebulizers for bronchodilator delivery since it offers more benefits in terms of safety, affordability, and efficacy (Mouloudi et al., 2000).

One of the current methods to administer bronchodilator medication using an MDI is via an in-line MDI adapter connected to the circuitry. However, certain downsides have been identified with the current MDI administration method; a nurse must remain by the bedside to monitor inhalation, time the actuations, and synchronise the actuations with inhalation, which is inaccurate, resulting in lower drug effectiveness.

The current global pandemic is putting a growing strain on healthcare systems globally, particularly on Intensive Care Unit (ICU) resources such as ICU beds, nurses, and ventilators. At the outset of the pandemic, there was a global drive for the rapid acquisition of ventilators, and various novel and cost-effective ventilators were developed. However, many hospitals continue to struggle with a shortage of ICU beds and nurses. Many in-patients require MDI administration due to pre-existing lung diseases, and the addition of Covid-19 infected patients with COPD or Asthma comorbidities who also require MDI therapy places additional strain on limited ICU beds capacity and nurses.

Hence, to address the inaccurate actuation-inhalation coordination, the limited number of ICU beds and nurses, a device that can be employed outside of ICU settings and can automatically deliver bronchodilator medications using MDIs has been proposed. The device's ease of use also suits it for home use by users who require bronchodilator therapy in addition to their existing oxygen therapy.

1.2 Aim of the Study

The aim of this study is to design and develop an automated MDI delivery system with breath detection that can improve the synchrony of the actuation with inhalation during bronchodilator therapy of ventilated patients by detecting inhalation and subsequently actuating an MDI canister, improving the effectiveness of the MDI delivery.

1.3 Objectives of the Study

The objectives of this study are to achieve the design, validation, and pre-clinical testing objectives of an automated MDI delivery system.

The design phase includes several key components, such as an actuation mechanism capable of applying sufficient force to actuate the medication canister, a breath detection system that detects inhalation prior to actuation, and a user-friendly access point to reload the MDI canister. Other components include an alarm system to alert users of an unlocked door or low remaining dosage, a pulse oximeter add-on that displays a patient's oxygen saturation level and pulse rate, and an enclosure that safely and securely holds all the components.

The validation phase will test the accuracy of the breath detection system and the actuation mechanism and compare the output of the device to the operator-specified settings.

Lastly, the preclinical testing phase will determine the effectiveness of the automated solution by comparing the delay between the actuation and inhalation signals in the automated solution to the existing manual solution using a bench test.

1.4 Research Question

The research question that this study aims to address is: *Would an automated MDI delivery system be more effective than the present manual MDI delivery method?* The research question aims to address whether replacing the current manual solution with an automated solution is effective, not just by replacing the nurses but also if it is better in terms of the synchrony of the medication delivery, improving the treatment effectiveness.

1.5 Scope and Limitation of the Study

The scope of this research focuses on the design and development of an automated MDI delivery system with breath detection. To validate the operation of the device, the study will be conducted in a laboratory setting using a breathing simulator (BS) and a Continuous Positive Airway Pressure (CPAP) device. A bench test will be carried out to gather data on the synchrony of the actuation with inhalation between the automated solution and the current manual method. Subsequently, the collected data will be analysed to determine the device's effectiveness by comparing the synchrony of the actuation between the automated solution and the current manual solution with inhalation. It should be noted that the testing of the developed device will be limited to a CPAP device using air only.

1.6 Dissertation Overview

The dissertation begins with the Introduction to the study in Chapter 1, highlighting the problems identified, the aim and objectives, the research question, and the scope and limitations of the study. Chapter 2 consists of the literature review on topics focused on the problem identified, comprising an analysis of the prevalence of the target patients, the preference for using MDIs over nebulizers, the importance of the MDI actuation synchrony with inhalation, the extent of limited ICU resources and lastly, a review on the studies of similar devices. Chapter 3 details the design methodology followed to design and develop the device. Chapter 4 describes the design outcomes of the subsystems. Chapter 5 details the methodology followed to validate the device and the results are detailed and discussed in Chapter 6. Conclusions on the study are then drawn and recommendations are proposed in Chapter 7. Figure 1 shows a summary of the dissertation overview.

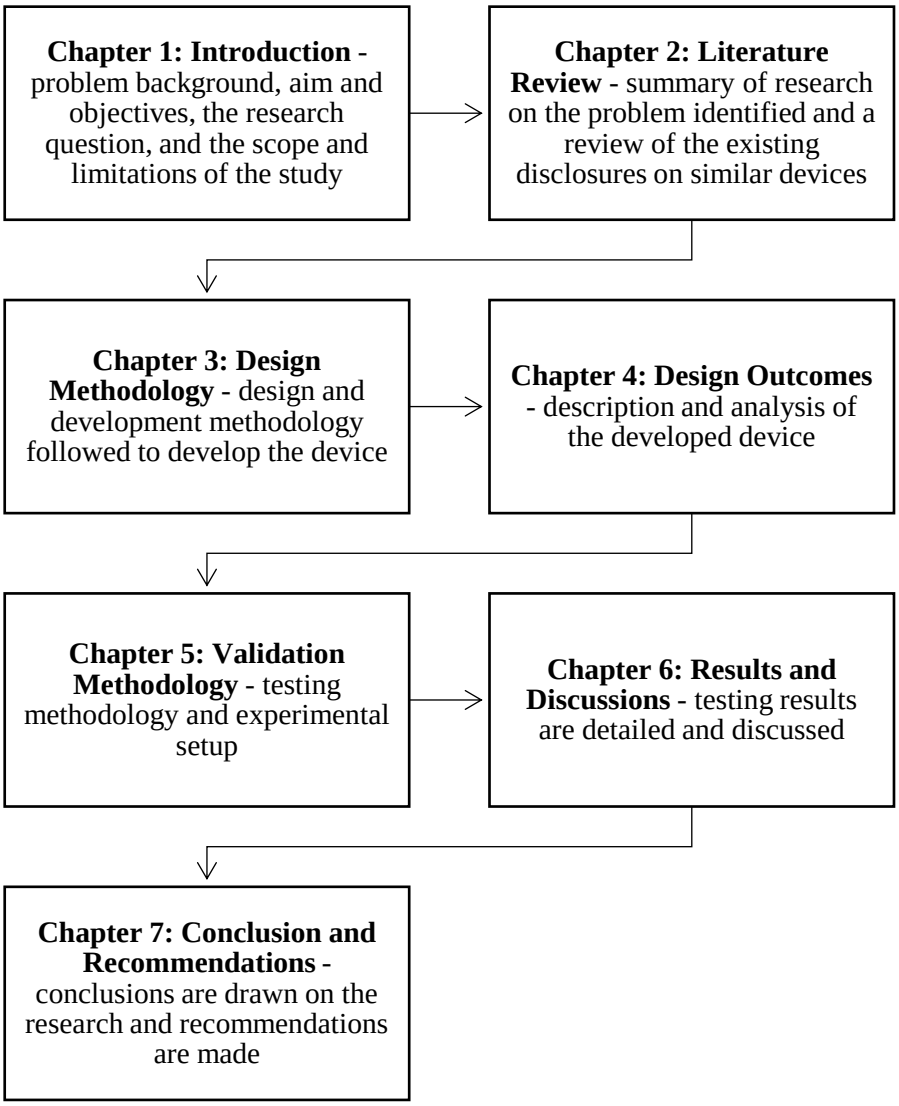

Figure 1: Dissertation overview

CHAPTER 2: LITERATURE REVIEW

The disease state analysis, advantages of using MDI over nebulizers, the importance of the MDI actuation synchrony with inhalation, the landscape of limited ICU resources internationally and in South Africa, and finally, a review of the studies of similar devices will be covered in the following literature study.

2.1 Disease State Analysis of Covid-19 Patients with Comorbid COPD or Asthma

The following sections detail the anatomy and physiology of the respiratory system, an epidemiology analysis of Covid-19 patients and comorbid COPD and Asthma, an overview of the pathophysiological mechanisms, and the clinical presentation and outcomes of the diseases.

Anatomy and Physiology of the Respiratory System

The Severe Acute Respiratory Syndrome Coronavirus 2 (SARS-CoV-2) virus is transmitted to a vulnerable person through droplets of saliva or airborne particles that are discharged when an infected person sneezes or coughs. The virus initially targets the human respiratory system before spreading to other parts of the body (Tabassum et al., 2022). The respiratory system consists of multiple organs, and its main function is to conduct gaseous exchange between the external environment and the bloodstream. Figure 2 illustrates the anatomy of the respiratory system.

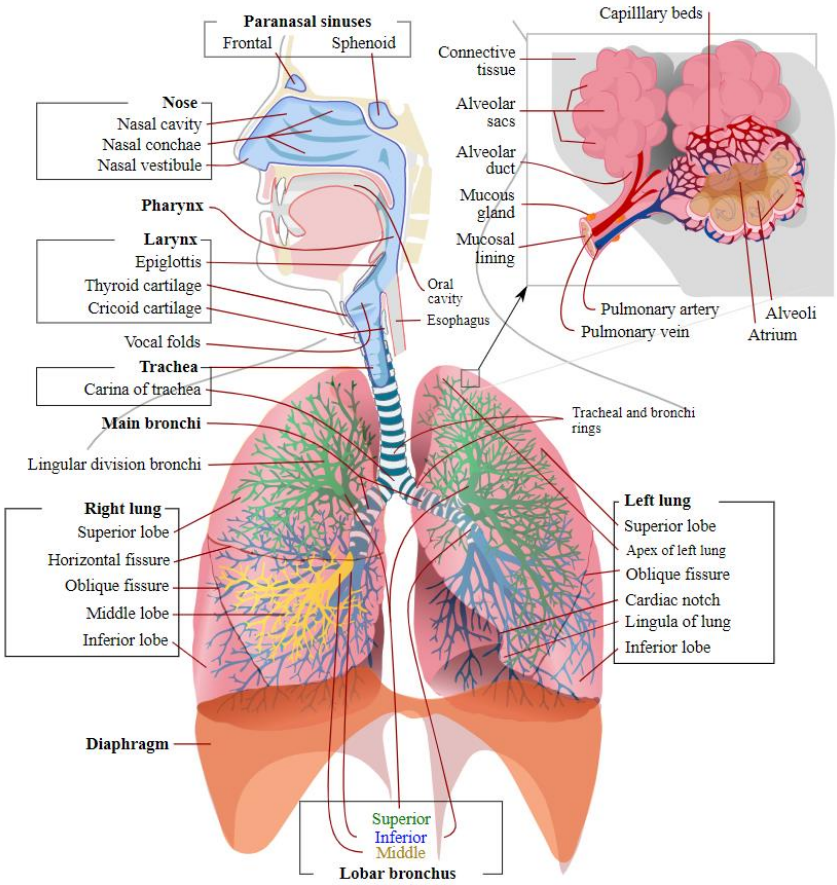

Figure 2: Anatomy of the respiratory system (Villarreal, 2007)

The respiratory system is responsible for maintaining the blood oxygen level and disposing of carbon dioxide through respiration, which comprises the following four mechanisms (Marianne Belleza, 2022):

1. Pulmonary ventilation.
2. External respiration.
3. Gas transport.
4. Internal respiration.

The mechanics of breath involves inhalation and exhalation. During inhalation, oxygen is drawn in, and the diaphragm and the external intercostal muscles contract, increasing the thoracic volume, which in turn stretches the lungs causing air to be drawn into the lungs (Marianne Belleza, 2022). During exhalation, carbon dioxide is disposed of, and the diaphragm and the external intercostal muscles relax, decreasing the thoracic volume, which in turn recoils the lungs causing air to be flown out of the lungs (Marianne Belleza, 2022).

The thoracic cavity and the lungs are attached, thus, the volume of the lungs changes together with the thoracic volume, which results in the pressure inside the lungs also changing. The relationship between the change in volume and pressure in the lungs causes that air to be drawn in or flown out is known as Boyle's law, which states that the volume of a gas is inversely proportional to pressure, whereby during inhalation, the volume of the thoracic cavity and the lungs increases, and the pressure inside the lungs decreases, causing air to be drawn in, and the opposite occurs during exhalation (Pandirajan, 2022).

The lungs are characterised by their respiratory volume and capacity. Figure 3 illustrates the respiratory volume and capacity of a typical person's lungs.

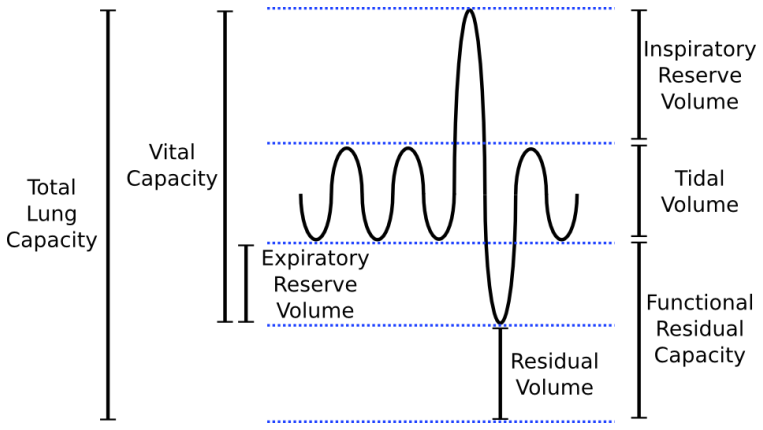

Figure 3: Respiratory volumes and capacities of the lungs (Lung Volumes, 2016)

Apart from the gaseous exchange, the respiratory system is also responsible for warming and humidifying the air during respiration, blocking out harmful substances through coughing, sneezing or filtering through small nasal hairs, and enabling the sense of smell ("How Lungs Work", 2022).

Epidemiology of SARS-CoV-2, COPD and Asthma Comorbidities in Covid-19 Patients

Multiple studies concluded that the origin of the SARS-CoV-2 virus is zoonotic (Paraskevis et al., 2020; Chan et al., 2020; Zhou et al., 2020; Lu et al., 2020) as the strain genome was very similar to bat-derived coronaviruses in addition to two previous SARS and Middle East Respiratory Syndrome (MERS) coronaviruses. Table 1 summarises the percentage similarity of the SARS-CoV-2 to bats and previous coronaviruses found in previous literature.

Table 1: Percentage similarity of SARS-CoV-2 to bat-derived and previous coronaviruses

	Bat-derived Coronaviruses			**Previous Coronaviruses**	
Study	**bat-SL-CoVZC45**	**bat-SL-CoVZXC21**	**batCoV RaTG13**	**SARS-CoV**	**MERS-CoV**
(Zhou et al., 2020)	-	-	96.2%	79.6%	-
(Lu et al., 2020)	88%	88%	-	79%	50%
(Paraskevis et al., 2020)	-	-	96.3%	-	-
(Chan et al., 2020)	89%	-	-	68%	-

The findings of the previous literature show that the batCoV RaTG13 virus is almost identical to the genome of the SARS-CoV-2 virus (Zhou et al., 2020; Paraskevis et al., 2020), while the bat-SL-CoVZC45 and bat-SL-CoVZXC21 (Lu et al., 2020; Chan et al., 2020) are very closely related to the SARS-CoV-2 virus, with an approximate 88% genome identity of 88% (Lu et al., 2020; Chan et al., 2020). The SARS-CoV virus is highly similar to SARS-CoV-2 (Zhou et al., 2020; Lu et al., 2020; Chan et al., 2020), with an approximate 68% to 79% genome identity. The findings show that it is very likely that the SARS-CoV-2 virus originates from bats.

The first case of a pneumonia outbreak, later on, associated with Covid-19, originated in Wuhan, a city in China (Dhar Chowdhury & Oommen, 2020). The Covid-19 virus, SARS-CoV-2, spread quickly both locally and globally through international travellers, with the first international case being reported in Thailand and afterwards, to the rest of the world (Dhar Chowdhury & Oommen, 2020; Helmy et al., 2020). The number of deaths due to the virus increased exponentially and the World Health Organisation (WHO) declared the SARS-CoV-2 outbreak a global pandemic (Helmy et al., 2020). During the first four months of the outbreak, there was an exponential increase in cases and

deaths outside China, whereas the cases and deaths in China did not increase significantly (Helmy et al., 2020). Globally, after the first four months, the number of cases and deaths increased drastically, with the numbers fluctuating irregularly and a few times, the numbers peaked very high, known as the Covid-19 wave.

As of 11th September 2022, reported by the latest weekly epidemiological update from WHO, there have been over 605 million cases and over 6.4 million deaths worldwide (WHO COVID-19 Weekly Epidemiological Update Edition 109, 2022). As of the same date, the number of cases and deaths globally are below the peaks that were previously experienced and the number of cases and deaths are showing a decreasing trend, relative to the previous seven days, in all WHO regions, except for Africa which is showing an increase in the number of deaths (WHO COVID-19 Weekly Epidemiological Update Edition 109, 2022).

The current trend of cases and deaths due to Covid-19 no longer reflects the actual numbers due to a decrease in the number of testing conducted, resulting in many undetected cases (WHO COVID-19 Weekly Epidemiological Update Edition 109, 2022). Moreover, the vaccination rate and easing of Covid-19 safety regulations will render the future trends of Covid-19 cases and deaths unpredictable.

With the outbreak of the pandemic, covid-19, many positive cases presented with COPD or Asthma comorbidities. The distribution of Covid-19 patients with COPD or Asthma was analysed by reviewing literature that conducted a comprehensive cohort study with Covid-19 patients and comorbid chronic diseases. Table 2 shows the data pooled from previous literature on the distribution of COPD and Asthma comorbidities in Covid-19 patients.

Table 2: Distribution of COPD and Asthma comorbidities in Covid-19 patients

Study	Region	Total No. of Patients, n	Asthma, n (%)	COPD, n (%)
(Choi et al., 2021)	Seoul, South Korea	7590	218 (2.9)	-
(Gerayeli et al., 2021)	Systematic review, worldwide	698042	14913 (2.1)	-
(Hansen et al., 2021)	Denmark	5104	354 (6.9)	432 (8.5)
(Lee et al., 2021)	National Health Insurance, South Korea	4610	-	141 (3.1)
(Patone et al., 2021)	10 regions, UK	198420	29792 (15)	1873 (0.9)
(Chhiba et al., 2020)	Chicago, US	1526	220 (14.4)	-
(Skevaki et al., 2020)	Wuhan, China	961	22 (2.3)	21 (2.2)

(Avdeev et al., 2020)	Moscow, Russia	1307	23 (1.8)	41 (3.1)
(Grandbastien et al., 2020)	Strasbourg, France	106	23 (21.7)	-
(Docherty et al., 2020)	166 hospitals, UK	16749	2345 (14)	3182 (19)
(Matsumoto & Saito, 2020)	Systematic review; China, USA & Mexico	17485	922 (5.3)	635 (3.6)

The review in Table 2 shows that the distribution of both comorbidities is higher in Europe and US compared to the other countries. In contrast, overall, the distribution of COPD comorbidities in Covid-19 patients is higher compared to Asthma.

Pathophysiology of SARS-CoV-2, Pneumonia, Hypoxemia, COPD, and Asthma

The disease states this study comprises are pneumonia and hypoxemia in Covid-19 patients with COPD or Asthma comorbidities. The pathophysiology of these diseases is discussed in the following section.

The covid-19 virus, SARS CoV-2, enters the host cells by attacking angiotensin-converting enzyme II (ACE-2) receptors in the airways (Tabassum et al., 2022). The virus enters the cytoplasm of the host cells, releasing genomic RNA and replicates (Liu et al., 2020), causing an initial innate immune response and, after further propagation down the respiratory tract, a more robust innate immune response is triggered by evoking Toll-like receptors (TLR) (Mason, 2020). Namely, TLR-4 leads to activating pro-inflammatory cytokines and immune cells in the infected site (De Wilde et al., 2017). The antigens of the virus are then presented to T cells by antigen-presenting cells, which causes the division of the T cells and consequently, an overactivated inflammation is induced, which is characterised by the massive release of pro-inflammatory cytokines, known as cytokine storm (Tabassum et al., 2022; Liu et al., 2020). These damage the alveoli causing hyperinflammation and multiple organ failure (Wisnu Wardana & Rosyid, 2021; Mason, 2020).

Pneumonia is a lung infection that occurs when the lungs become filled with fluid, causing the tiny air sacs to be inflamed. This restricts the lungs' ability to conduct gaseous exchange, resulting in severe shortness of breath, coughing and many other symptoms ("Coronavirus and pneumonia," 2020). In severe cases, the person must be put under oxygen therapy to supplement the blood oxygen level (Galiatsatos, 2022). Pneumonia induced by Covid-19 is more powerful than typical pneumonia as it can spread to both lungs, and the resultant lung injury takes much longer to ameliorate (Galiatsatos, 2022).

Hypoxemia is a low oxygen level in the blood caused by airway narrowing or a lack of gaseous exchange between the alveoli and the bloodstream ("Hypoxemia," 2022). Hypoxemia in Covid- 19 cases is mainly caused by ventilation-perfusion mismatch, in which gaseous exchange between the

alveoli and the bloodstream does not occur due to the alveoli not being ventilated (Dhont et al., 2020). Consequently, the tidal volume increases causing a rise in the negative inspiratory intrathoracic pressure, which, together with increased lung permeability caused by inflammation results in the progression of Edema (Gattinoni et al., 2020). After some time, the Edema will further increase lung weight, alveolar collapse, and atelectasis resulting in a gradual rise in the shunt fraction and continued loss in oxygenation that cannot be fully reversed by increasing FiO2 (Dhont et al., 2020). Specifically, in Covid-19 patients, many experience a phenomenon known as *"silent hypoxaemia"*, where the patients present with severe hypoxaemia but do not show any signs of respiratory distress, leading to sudden deterioration (Dhont et al., 2020).

COPD is a chronic lung disease characterised by persistent respiratory symptoms, lung inflammation, and airflow obstruction. Emphysema and chronic bronchitis are the two most common COPD conditions caused by tobacco use (Fekete et al., 2022). It is one of the most common comorbidities in patients with Covid-19, and it exacerbates the complications due to the restriction of oxygen supply, leading to rapid deterioration (Fekete et al., 2022). A study found that COPD patients and smokers had higher angiotensin-converting enzyme II (ACE-2) expression in their lower airways, and this enzyme is the main receptor of the SARS-CoV-2 virus that causes the infection, which also explains the higher severity risk of Covid-19 patients with COPD (Leung et al., 2020).

Asthma is a chronic disease characterised by the inflammation and narrowing of the respiratory tract causing airway hyperresponsiveness. It is mediated by type 2 immune response comprising of T helper 2 cells, type 2 B cells, group 2 innate lymphoid cells, type 2 macrophages, IL-4-secreting nature killer and natural killer T cells, basophils, eosinophils, and mast cells (Agache & Akdis, 2016). The inflammation results in the remodelling of the airway, which in turn causes the degranulation of mast cells, which eventually releases inflammatory deposits causing bronchial hyperresponsiveness and airway obstruction (Wisnu Wardana & Rosyid, 2021). This effect is further promoted by releasing cytokines from the immune response cells causing acute bronchospasm (Tabassum et al., 2022). Although there is no conclusive opinion on the impact of Asthma on Covid-19 patients, there is a higher probability that Asthma is not a severity risk for Covid-19 patients (Wisnu Wardana & Rosyid, 2021; Morais-Almeida et al., 2020; Tabassum et al., 2022), and also asthmatic patients showed a lessened expression of ACE-2 enzymes, suggesting a potential protective effect (Tabassum et al., 2022; Liu et al., 2020).

Clinical Presentation and Outcomes of Covid-19 Patients with COPD or Asthma

The most prominent to least prominent Covid-19 initial symptoms are fever, cough, myalgia, fatigue, dyspnoea, headache, diarrhoea, and vomiting (Huang et al., 2020; Sheleme et al., 2020). In an early study, 55% of the patients developed dyspnoea, and all of them had pneumonia (Huang et al., 2020). The study also found that the intervals between the onset of symptoms and the first hospital

admission ranged from 4 to 8 days, 5 to 13 days for dyspnoea, 8 to 14 days for acute respiratory distress, 7 to 14 days for ventilation, and 8 to 17 days for ICU admission (Huang et al., 2020). The severity of the illness can be categorised into asymptomatic, mild, moderate, severe and critical cases. Moderate cases present with respiratory distress and arterial oxygen saturation (SaO_2) ≥ 94%, severe cases present with a breathing rate > 24 breaths per min, severe pneumonia and hypoxia, SaO_2 < 94% and lung infiltrates > 50%, and critical cases present with respiratory failure and multiple organ failure (Samudrala et al., 2020; Huang et al., 2020).

Covid-19 patients are given antiviral therapy in the early stages, such as oseltamivir, darunavir-cobicistat, lopinavir-ritonavir, favipiravir and hydroxy-chloroquine to inhibit the replication of the SARS-CoV-2 virus by inactivating the proteases, and corticosteroids to prevent cytokine storms (Huang et al., 2020; Stasi et al., 2020). Moderate to severe cases require non-invasive mechanical ventilation and severe to critical cases require invasive mechanical ventilation (Huang et al., 2020). The clinical presentations of severe exacerbation due to Asthma overlap with the most prominent symptoms of Covid-19 (Shaker et al., 2020), whereas patients with COPD experience more severe symptoms (Zhao et al., 2020). These patients are given controlled oxygen therapy and are additionally administered a bronchodilator medication using an MDI (Shaker et al., 2020; Simons et al., 2020). MDIs are preferred as they do not pose a risk of viral transmission of the virus. However, nebulizers can be used in life-threatening cases (Simons et al., 2020).

2.2 Advantages of Using MDIs over Nebulizers

MDIs or nebulizers are most commonly used to administer aerosol bronchodilators during ventilation. An international survey on aerosol therapy use during ventilation found that MDIs are utilised more than nebulizers, with MDIs outnumbering nebulizers by 12% (Ehrmann et al., 2013). It was also found that 14% of physicians employ an external gas source with a jet nebulizer, delivering uncontrolled tidal volume to the patients, which can lead to clinical deterioration (Ehrmann et al., 2013). Furthermore, the effect of bronchodilation with MDIs is as effective as nebulizers with fewer dosages as it was found in a study that 4 doses from an MDI have the same effect as 6 to 12 times the same dose administered by a nebulizer (Dhand & Tobin, 1997).

MDIs have several advantages over nebulisers, including being less expensive, safer, and easier to use, as well as having greater dose accuracy, sterility, and efficacy (Ehrmann et al., 2013; Mouloudi et al., 2000) A study found that bronchodilators delivered using an MDI during pressure or volume-controlled ventilation mode effectively decreases airway resistance consistently, confirming its effect is independent of the ventilator mode compared to when using nebulizers (Mouloudi et al., 2000). The study also found that there is no effect on bronchodilation if the inhalation flow/time profile is altered (Mouloudi et al., 2000).

2.3 Importance of the MDI Actuation Synchrony with Inhalation

The effectiveness of bronchodilator medication delivered using MDI depends on the deposition of the medication in the targeted areas, which is, in turn, dependent on the actuation timing with inhalation as the medication needs to be carried with the inhaled air, to enable deposition on the muscles of the airways, causing them to relax and making breathing easier. The current manual method used in the ICU settings is often inaccurate in the coordination of the MDI actuation and inhalation (Dhand, 2017; Ari, 2015; Georgopoulos et al., 2000), where the MDI is actuated after inhalation starts, resulting in lower drug deposition due to some of it being lost into the exhalation phase, thus, resulting in lower drug effectiveness. This asynchrony is mainly attributed to nurses' improper MDI actuation-inhalation coordination technique, reaction time, or fatigue.

There are many previous studies (Maccari et al., 2015; Capstick & Clifton, 2012; Cho-Reyes et al., 2019; Broeders et al., 2011; Fernández Tena & Casan Clarà, 2012) that showed there is a correlation between the deposition of the medication in the airways and the timing of the MDI actuation with inhalation. A recent study (Talaat et al., 2022) conducted a CFD analysis to study the effect of the timing of the MDI actuation on the drug deposition by actuating the MDI at 0, 1.5, and 2.5 s after inhalation. The results showed that actuating the MDI at 1.5 s and 2.5 s resulted in a very low deposition in the airways, with most medication being lost in the mouth, whereas actuating at 0 s, deposits more medication to the tracheobronchial region and the five lobes, which are the desired target for the drug deposition and thus, having a higher potential for increased effectiveness of the medication (Talaat et al., 2022). Another study (Leach et al., 2005) used radiolabelled MDI canisters to correlate actuation time to lung deposition and found that lung deposition was highest with both a breath-activated MDI and a normal MDI, with actuation times of 0.18 s and 0.32 s, respectively. Another study (Broeders et al., 2003) defined an acceptable range of 0 to 0.2 s for the actuation-inhalation coordination.

The deposition of the MDI medication in the airways may be influenced by factors such as the inhalation flow rate, the period of inhalation, the coordination of the MDI actuation with inhalation, the period of inhalation pause, and the aerosol particle size (Laube et al., 2011; GINA., 2016, as cited in Biswas et al., 2017). The first four factors are controlled by the patient while using the MDI and the particle size depends on the formulation and the design of the MDI used (Smith et al., 1998, as cited in Biswas et al., 2017). These factors were studied (Biswas et al., 2017), and it was found that higher inhalation flow rate and increased period of inhalation increased the deposition of the medication, but this increase was lower than the deposition during better coordination. The study concluded that actuating the MDI immediately after the start of inhalation with a high inspiratory flow rate is the optimum condition for maximum drug deposition, which agrees with the previously mentioned study (Talaat et al., 2022). Another study also concluded that maximum bronchodilation, resulting from increased drug deposition, may be achieved using a high dosage and actuating the MDI at the start of inhalation (Mouloudi et al., 2000).

Based on the available evidence, it can be concluded that the optimal time interval for actuation and the onset of inhalation is within the range of 0 to 0.2 s. This interval ensures maximum lung deposition and maximises bronchodilator medication's effectiveness.

2.4 MDI Actuation-Inhalation Coordination Errors Among Nurses

The optimum actuation-inhalation coordination can only be achieved by the nurses actuating the MDI in the ICU settings. However, improper MDI actuation-inhalation coordination by nurses can result in inadequate medication delivery, leading to poor clinical outcomes for patients. This can be attributed to factors such as competency, fatigue, and reaction time.

The majority of studies found that nurses were not properly actuating the MDI on ventilated patients in an ICU setting (Johnson et al., 2022; Swami et al., 2021; Pérez-Malagón et al., 2021; Rajbanshi & KC, 2017; De Tratto et al., 2014). In a study on the competency of healthcare workers in using MDIs (Pérez-Malagón et al., 2021), it was found that 30% of nurses used an incorrect technique to actuate the MDI. According to a similar study (Swami et al., 2021), approximately 53% of nurses actuated the MDI incorrectly. These findings were attributed to a lack of knowledge and training on proper MDI administration techniques.

With the recent pandemic, many nurses worked long hours and were prevalently fatigued (Jamebozorgi et al., 2022; Lee & Choi, 2022; Galanis et al., 2021; Ghassemi, 2021). These conditions, particularly with ICU nurses, have contributed to the incorrect MDI delivery technique as fatigue affected their reaction time. According to a recent study (Lee & Choi, 2022) on nurses' fatigue during the pandemic, 62% of 234 nurses reported a high prevalence of fatigue. A similar study (Jamebozorgi et al., 2022) found that approximately 75% of nurses experienced burnout.

The findings of this literature review suggest that there were various factors that contributed to improper MDI administration by nurses in an ICU setting on ventilated patients. This technique must be performed correctly and accurately because incorrect medication delivery can result in poor clinical outcomes for patients.

2.5 Limitations of ICU Resources

In most cases, hospitals have sufficient ICU resources such as ICU beds, facilities, and nurses, which are regularly in use (Vincent & Creteur, 2020). However, the current global pandemic, Covid-19, is putting additional strain on both general and ICU wards around the world, and these constraints cause many ethical dilemmas owing to triage, hence respiratory support outside of ICU resources is strongly recommended (Vincent & Creteur, 2020). In a global survey of 2700 respondents on the impact of Covid-19 on critical care resources, 32% reported a lack of ICU nurses and 17% reported a shortage of ICU beds (Wahlster et al., 2021).

Because of the ongoing pandemic, many nurses worked long hours and were unable to take time off, increasing the negative effects on their mental and physical well-being (Turale & Nantsupawat, 2021). According to a study on patient care and clinical outcomes for patients with Covid-19 infection admitted to high-care or ICUs in ten African nations, delays in admission due to a lack of critical care resources resulted in increased mortality, in addition to comorbidities (Biccard et al., 2021). It has been determined (Naidoo & Naidoo, 2021) that approximately 16% of Covid-19 infected cases require ICU hospitalisation and that this percentage will put further strain on South Africa's already limited ICU resources. Therefore, in the context of limited ICU beds and short staffing of nurses who are mentally and physically fatigued, the manual administration of MDI medication is not feasible.

2.6 Current Disclosures on Similar Devices

A few similar devices have been developed, but none are commercially available. An automated MDI delivery device for home usage has been developed (Karle et al., 2007) for use at home with Continuous Positive Airway Pressure (CPAP) devices, consisting of two motors for an agitation feature that uses a vibrating gear mechanism and a rotating cam for the actuation of the canister, respectively. A breath detector, which uses a temperature-detecting thermistor to detect temperature changes to indicate inspiration or exhalation, was also included in the design (Karle et al., 2007). The breath detection system matches the patient's breath; however, the thermistor is very sensitive depending on where it is placed. The device had several design flaws, including noise, battery level, actuation lag owing to the motor utilised, and the in-line actuator was not fastened to the device's base, causing it to be ejected after each actuation (Karle et al., 2007).

Three patents on the design of automated MDI delivery systems were disclosed by iDTx Systems Inc., with Michael Spandorfer as the main inventor. The first patent (Spandorfer & iDTx Systems, Inc., 2008) describes an automated drug delivery and monitoring system for use with mechanical ventilation, which includes a linear actuator and a feature that allows multiple canisters containing different medications to be placed in the delivery unit and administered individually according to the specified settings. The second patent (Spandorfer et al., 2015) describes a self-contained automated MDI adapter for ventilators that includes an actuator device and a gas flow sensor that can both detect inhalation and measure the patient airway resistance, which can then be used to change the dosage settings manually or automatically by the controller. The third invention filed (Spandorfer et al., 2019) is similar to the second one, but it employs a different actuation system, in which a pivotal movement actuates the canister.

Another invention using an automated mechatronic adaptor for MDI administration was also developed (Zhang et al., 2016), it uses the hall effect to detect breath and sends a signal to the MDI actuation mechanism through a microcontroller. The MDI is actuated by a gear system in the actuation mechanism. The automated adaptor for MDI administration had a satisfactory aerosol-release time,

which depends on the switch on flow rate that activates the hall sensor, the MDI canister mechatronics hysteresis, and the intentional delay (Zhang et al., 2016). The key design flaw noted in this technology is that it does not allow for the reloading of the canister unless the entire system is dismantled (Zhang et al., 2016).

2.7 Conclusion and Motivation of Study

The literature review further highlights the significance of the problem identified. The disease state analysis details the severity and clinical outcomes, highlighting the complicated clinical management of the target patients, especially with the treatment method. Ultimately, using MDIs are the preferred method to administer bronchodilator medications to moderate to severe cases of Covid-19 patients with COPD or Asthma requiring ventilation. They are preferred as they do not pose a risk of viral transmission of the virus, they are not expensive, safer, easier to use, as well as having better sterility, and efficacy. However, it is crucial to have an accurate actuation-inhalation coordination with this method for optimum bronchodilator medication effectiveness. Based on the evidence in the literature, it was determined that the optimal range between the actuation and the onset of inhalation is between 0 to 0.2 s. This interval ensures maximum lung deposition and therefore, maximizes the effectiveness of bronchodilator medication.

However, the challenge that has been identified regards specifically this actuation-inhalation coordination time interval which is inaccurate and has been highlighted due to the pandemic as nurses were working long hours, resulting in fatigue, which together with prior incorrect technique used, contributed to improper MDI administration by nurses in ICU settings, which were also under strain. Therefore, the inaccurate actuation-inhalation coordination and limited ICU resources drive the study's motivation to solve this problem, as this problem can result in poor clinical outcomes for patients. Thus, to address the inaccurate actuation-inhalation coordination and the limited number of ICU beds and nurses, a device that can be used outside of ICU settings and can automatically deliver bronchodilator medications at the onset of inhalation using MDIs has been proposed. There are a few disclosures on devices that employ a similar principle of automatically delivering MDI medication by detecting breath and actuation a canister, but none are commercially available.

Hence, the research aims to develop an automated MDI delivery system using an improved actuation mechanism and breath detection system, to improve the effectiveness of medication delivery, free up nurses and reduce ICU admissions

CHAPTER 3: DESIGN METHODOLOGY

This chapter outlines the considerations and requirements for developing an MDI delivery system with breath detection.

The initial considerations of the device to be developed are that it must have an actuation mechanism to actuate the canister and an automated breath detection system that distinguishes it from the existing disclosures on similar devices. Based on a prior art search, a servo and cam actuation mechanism and together a pressure and flow rate sensor for the breath detection system were considered for the device. Some of the existing disclosures were not suitable for the intended application due to their bulkiness and functionality. As such, the developed device must be small, modular, and include a user interface (UI) for displaying adjusting various settings. Furthermore, the placement and reloadability of the canister must also be considered as some of the existing disclosures do not allow for the canister to be easily reloaded. The complexity of the device is related to the timing of the actuation and breath detection systems, which can only be validated after the design and development of the device. The following sections outline the design methodology followed to develop the device, including an overview of the system, design requirements, design process, and a description of the requirements and considerations of the components required to build the device.

3.1 Device System Design

3.1.1 System Overview

The design of the device was guided using the literature with considerations of Intellectual Property (IP). Figure 4 illustrates the architecture of the device showing the components of the system, namely the actuation mechanism, UI, and breath detection subsystem.

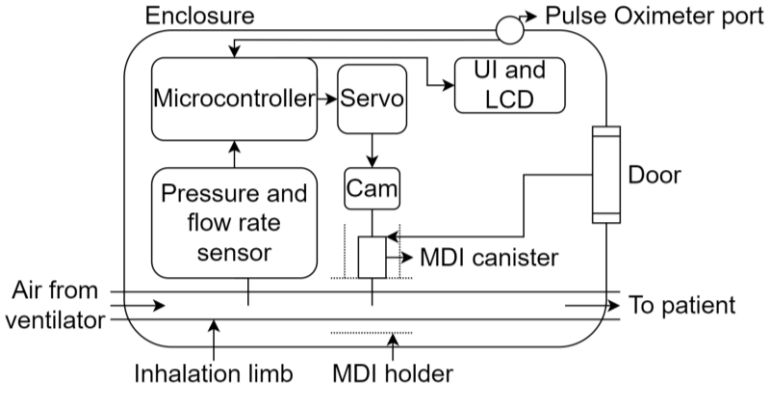

Figure 4: Block diagram of device architecture

The device is comprised of several key components that work together to achieve its intended function. The first component is the actuation mechanism of the device, which is made up of a servo and cam, which work together to actuate the canister. A pressure and flow rate sensor are included in the device to enable the breath detection system. To ensure that the canister is held in line with the air

pathway, the device also includes an MDI holder. The device also features a door that provides easy access to the MDI canister for reloading, a UI that allows the user to input various settings, and an LCD display that shows these settings. The device also includes a pulse oximeter port that connects a pulse oximeter signal cable. All the components are controlled by a microcontroller, which is responsible for the automated controls system of the device.

3.1.2 Design Requirements

The specifications for the design requirements of the MDI delivery system were drawn based on the input from the clinical partner and the user requirements. The design requirements for the MDI delivery system are the following:

- The device shall hold the canister and actuates it in line with the air pathway. This helps to maintain the proper positioning of the canister, which is crucial for the canister's proper operation.
- The canister shall be easily accessible and reloadable. This allows the user to reload the canister without difficulty.
- The device shall be able to exert sufficient force to actuate an MDI canister. This mechanism is critical to the device's function, as it enables the release of the medication from the canister in a controlled and precise manner.
- The device shall be able to measure the pressure and flow rate of the air pathway to detect inhalation. This combination of sensors helps to detect the patient's inhalation and to ensure that the medication is delivered at the right time within the desired range of the patient's inhalation cycle.
- The access to the canister shall be closed and locked during the operation of the device. This prevents any accidental or unauthorised access during the device's operation.
- The device shall incorporate safety features. This alerts the nurse, clinician, or user of any deviation from the device's intended operation to prevent any harm to the patient or user.
- The device shall have a port to connect a pulse oximeter to read and show the readings on the device's display. This feature is particularly useful for home-based patients, as it enables the monitoring of their oxygen saturation levels.
- The device shall have a simple and intuitive user interface (UI). This simplifies its use by any user without any training.
- The device shall have a microcontroller. This controls and automates the device's operation.
- The device shall have a rechargeable battery. This prevents interruptions in patient care during load-shedding.
- The device shall house all the components in a safe enclosure. This prevents damage or tampering.

3.1.3 Design Process

The design process was initialised by conducting a literature review on current designs as presented in Chapter 2. Figure 5 illustrates the design process followed. Considering the input from the clinical partner together with the literature review in the background research, the design process was then divided into 8 subsystems, namely, the MDI actuation mechanism, breath detection system, safety features, pulse oximeter, UI, microcontroller selection, power supply, and the enclosure to obtain the design outcome.

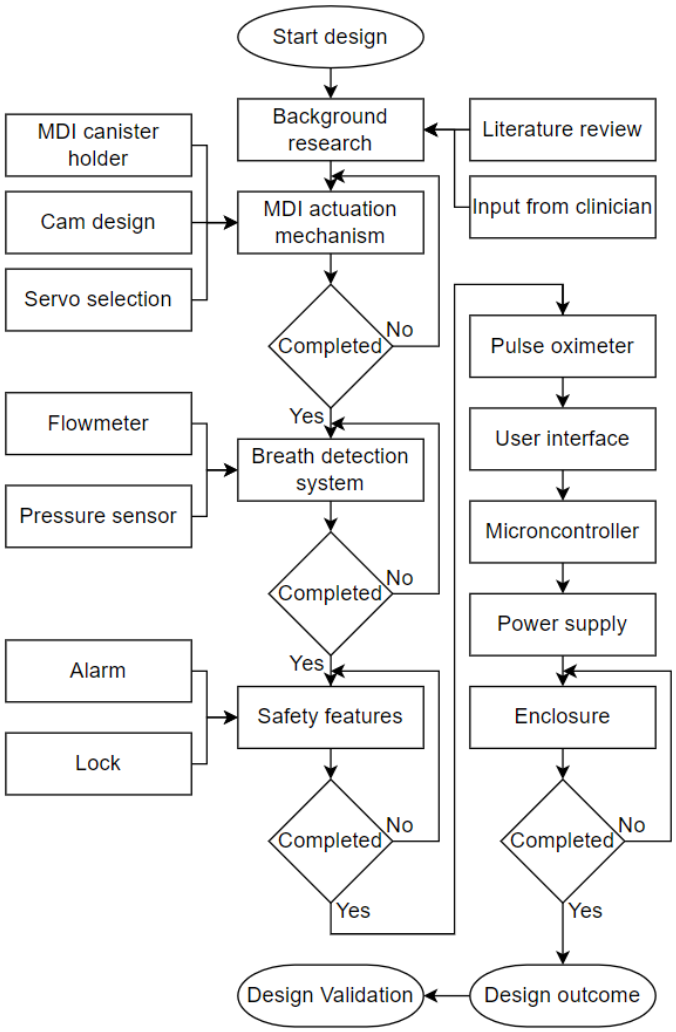

Figure 5: Design process

3.2 MDI Actuation Mechanism

3.2.1 Design Considerations

The MDI actuation mechanism comprises three subsystems:

1. The MDI canister holder.
2. The cam's design.
3. The selection of a servo.

Table 3 summarises the design considerations for the subsystems of the MDI actuation mechanism.

Table 3: Design considerations for the MDI actuation mechanism

Subsystem	Design Considerations
MDI Canister Holder	Hold the canister vertically
	Allow the canister to be easily reloaded
	Actuate the canister in line with the air pathway of the breathing circuit
Cam	Small so that the door does not impede its rotation during an actuation
	Is not blocked by the canister when reloading
Servo Selection	Exert sufficient force to actuate the canister
	Allow the canister to be easily accessed without any dismantling

The system must also monitor the number of actuations that have occurred and alert the user when the number of dosages left is low.

3.2.2 Technical Specifications

The specifications of the actuation mechanism were drawn by reviewing studies on the dosage and interval between the dosage used for bronchodilator therapy during ventilation (Cardin, 2021; Dhand, 2017; Maccari et al., 2015; Dhand et al., 1995).

Based on the review, the number of actuations which is equal to the number of dosages ranges from 1 to 10 and the interval between dosages ranges from 1 to 10 hours.

3.3 Working Principle of Breath Detection System and Requirements

The breath detection system operates based on changes in the pressure and airflow rate of the air pathway across the MDI Delivery Device (MDD).

Figure 6 shows the pressure and flow rate waveforms during CPAP mode.

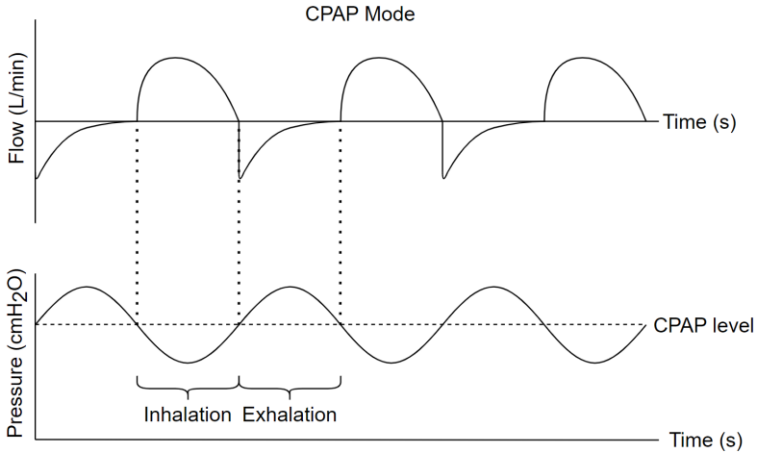

Figure 6: Pressure and flow rate waveforms of CPAP

Inhalation causes a drop in pressure and an increase in air flow rate during CPAP therapy. This change will be monitored using a pressure sensor and a flowmeter and will be used as the determining factor for detecting inhalation.

The requirement for the pressure sensor is that it must be able to measure pressures between 3 and 20 cmH_2O, which is the range for CPAP therapy, and the requirement for the flowmeter is that it must be able to measure flow rates up to 60 L/min, which is the flow rate that CPAP therapy can go up to, in order to match the patient's need based on their breathing effort (Volsko, 2019; Chen et al., 2012).

3.4 Safety Requirements

The design must incorporate various safety features to prevent device failure or patient harm. The door must be locked, and the device must activate an alarm if the following occurs:

- The number of dosages left is low.
- There is a power failure.
- Inhalation is not detected over a short period.

3.5 Pulse Oximeter

The pulse oximeter is an add-on feature that allows the device to display the patient's oxygen saturation level (SpO2) and pulse rate of the patient for diagnosis purposes. The pulse oximeter is an accessory that will be connected to the device via a data cable.

3.6 User Interface

The user interface will be designed to be simple and intuitive to use. It must display the various parameters and allow the user to navigate through the menu navigation to select and adjust the settings. The settings that the user must specify are the number of dosages and the interval between the dosages.

The UI must also enable the following:

- Display the number of dosages left.
- Allow the user to deliver an additional dose when required.
- A selection to unlock the door for reloading the canister.
- Display the pulse oximeter readings.

3.7 Microcontroller Requirements

A microcontroller is needed to provide the processing power required to control the functions of all the system's electronic components. The microcontroller must be suitably selected to have a sufficient number of digital and analogue pins for all the electronic components.

3.8 Power Supply Requirements

The device can be typically powered from a wall electrical outlet, however, in South Africa where load shedding is prominent, a power supply is required to run the device during the load shedding periods. The specifications of the power supply will depend on the electrical components used. The power supply must be integrated inside the device, rechargeable, can operate for a minimum of 2 hours on battery power and provide the required voltage and current needed by all the electrical components used.

3.9 Enclosure Design Considerations

All the mechanical and electrical components must be enclosed securely in an enclosure. The enclosure must be:

- Lightweight.
- Compact.
- Rigid.
- Have no sharp edges or corners.

3.10 Conclusion

In conclusion, the design methodology in this chapter has described the requirements to design and develop the device. Initially, an overview of the device’s system and a detailed set of design requirements were obtained. These were used to develop the design process to develop the device and the requirements and considerations of the components required to build the device were detailed. The next chapter will present the design outcome, describing each component that made up the developed device, demonstrating how the design methodology outlined in this chapter has resulted in the development of the device.

CHAPTER 4: DESIGN OUTCOMES

This chapter outlines the design outcomes of the design process, from implementing the design considerations and requirements to developing the MDI delivery system with breath detection.

4.1 MDI Actuation Mechanism

The following section details the design outcomes for the subsystems of the MDI actuation mechanism.

4.1.1 MDI Canister Holder

The MDI canister holder was designed with additional design considerations for the pressure and flowmeter connection. Figure 7 illustrates the rendering of the MDI canister holder.

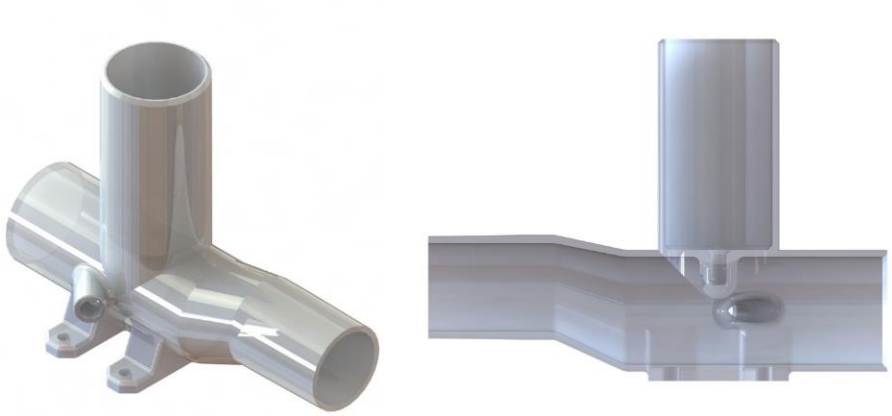

Figure 7: MDI canister holder

The design holds the canister vertically, allows for easy reloading of the canister by simply sliding in or out the canister, and the protruded nozzle inside the air pathway allows for in-line actuation. The inlet of the part was designed to hold the in-line flowmeter and a port was added on the side to connect the pressure sensor. The design was then validated using Solidworks Flow Simulation to analyse the effect of the protrusion, which incorporates the nozzle to deliver the medication from the canister, and the pressure port, whereby the pressure sensor is placed on the velocity and pressure pattern of the air pathway inside the MDI canister holder. An extra part was added at the outlet of the part to model the breathing circuit connection. An internal type of analysis was used with oxygen as the fluid. The pressure used is 20 cmH_2O, equivalent to 1961 Pa, a standard pressure setting for CPAP devices, and the inlet flow rate utilized is 30 L/min, representing the prevalent flow rate typically attained during CPAP therapy (Lebret et al., 2021; Volsko, 2019; Brusasco et al., 2015; Chen et al., 2012; Glover & Fletcher, 2009).

Table 4 summarises the conditions used for the simulation. The simulation's thermodynamic parameters, static pressure: 1961.00 Pa and temperature: 293.20 K were the same at the boundaries.

Table 4: Flow simulation conditions

	Parameters	Specifications
Initial Conditions	Velocity	Velocity in X & Y direction: 0 m/s Velocity in Z direction: 1.200 m/s
Boundary Conditions at Inlet Type: Inlet Volume Flow Face: Inlet face	Flow	Flow vectors direction: Normal to face Volume flow rate: 0.0005 m^3/s Fully developed flow: Yes
Boundary Conditions at Outlet Type: Static Pressure Face: Outlet face	Boundary layer	Turbulent

Figure 8, Figure 9, Figure 10, and Figure 11 illustrate the results for the velocity and pressure contour obtained after 241 iterations.

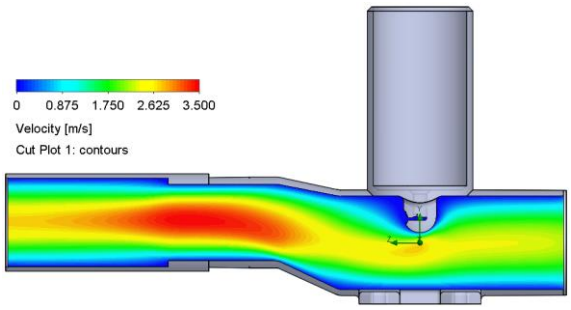

Figure 8: Velocity contour along the right plane inside the MDI canister holder

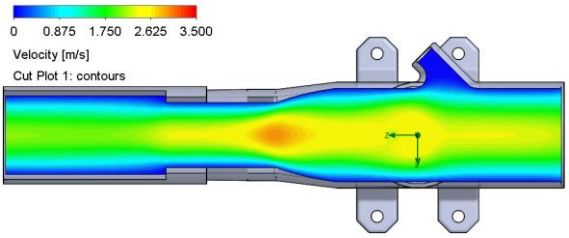

Figure 9: Velocity contour along the top plane inside the MDI canister holder

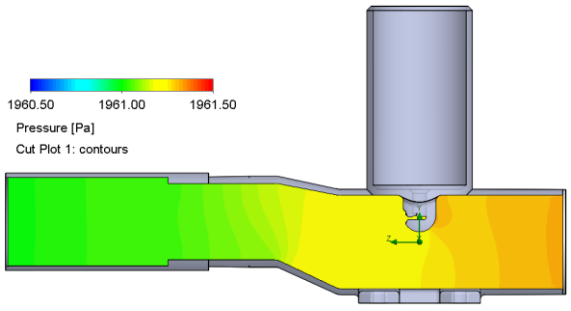

Figure 10: Pressure contour along the right plane inside the MDI canister holder

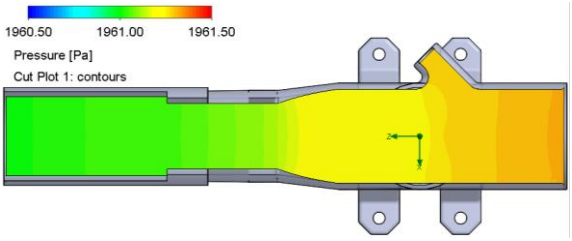

Figure 11: Pressure contour along the top plane inside the MDI canister holder

The simulation yields the following results: the global goal for the average velocity is 1.372 m/s and the global and inlet surface goals for static pressure are 1961.16 Pa and 1961.33 Pa, respectively. These values are expected based on the conditions used. As illustrated in Figure 8 and Figure 9, the velocity pattern inside the part is mostly uniform, with an increase around the neck, due to the change in diameter, which becomes uniform again near the exit. As illustrated in Figure 10 and Figure 11, the pressure drop from the inlet to the outlet is very small and thus, can be considered

negligible. Hence, the design of the MDI canister holder is validated to be suitable to hold the canister and measure pressure without affecting the velocity and pressure of the air pathway.

4.1.2 Cam

The size of the base circle and the lift are the two primary sizing parameters of a cam design, and they are determined by the servo width and the actuation travel distance, respectively. The cam's base circle was chosen to be 21 mm in diameter, whereby the radius is within the distance between the cam's centre to the servo mounting's edge, as illustrated in Figure 12, allowing for the required rotation of the cam.

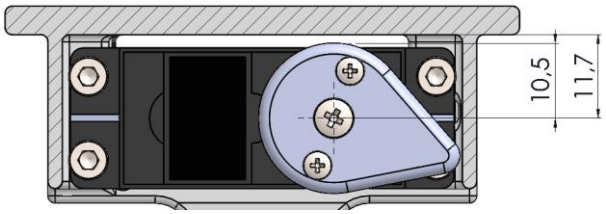

Figure 12: Distance between cam and servo mount

The MDI canister used in this research is labelled Glenbute, reg. no.: 54/10.2.1/0852, and is manufactured by Glenmark Pharmaceuticals South Africa (Pty) Ltd. The canister's actuation travel distance was measured to be 4 mm, and the perpendicular distance between the canister's outer end and the inside of the canister's concave surface was measured to be 3 mm. With a 1 mm gap between the cam and the canister to allow the door to be opened without any obstruction, the lift was designed to be 8 mm. Figure 13 illustrates the design and dimensions of the cam.

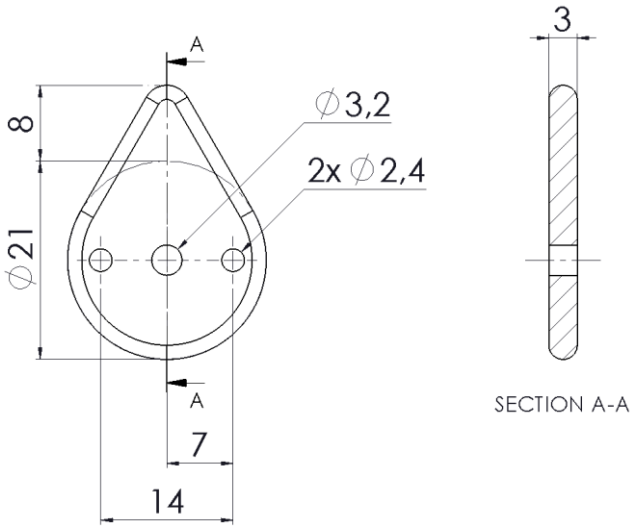

Figure 13: Design and dimensions of the cam

The thickness of the cam was set to 3 mm as it is the minimum size to keep the cam rigid and small. The centre hole is for securing the cam to the servo through a wheel with an M3 bolt and the two holes of the sides are to lock the rotation of the cam to the servo and the wheel with M2 bolts.

4.1.3 Servo Selection

The torque required to actuate the canister was inferred using data from previous works of literature on the force required to actuate various MDI canisters and the radius of the torque arm of the cam, which is equal to 18.5 mm. A stall factor was also introduced to avoid any stall during actuation. The torque is calculated as shown in Equation 1.

$$\tau = \frac{F \times r \times n_{stall}}{g} \times 100 \ [kg.cm] \qquad \textit{Eq. 1}$$

Where:

F [N] is the force required to actuate the canister,

r [m] is the radius of the torque arm,

n_{stall} is the stall factor, and

g [m/s^2] is the acceleration due to gravity.

Figure 14 illustrates the results of the torque required for various MDIs actuation.

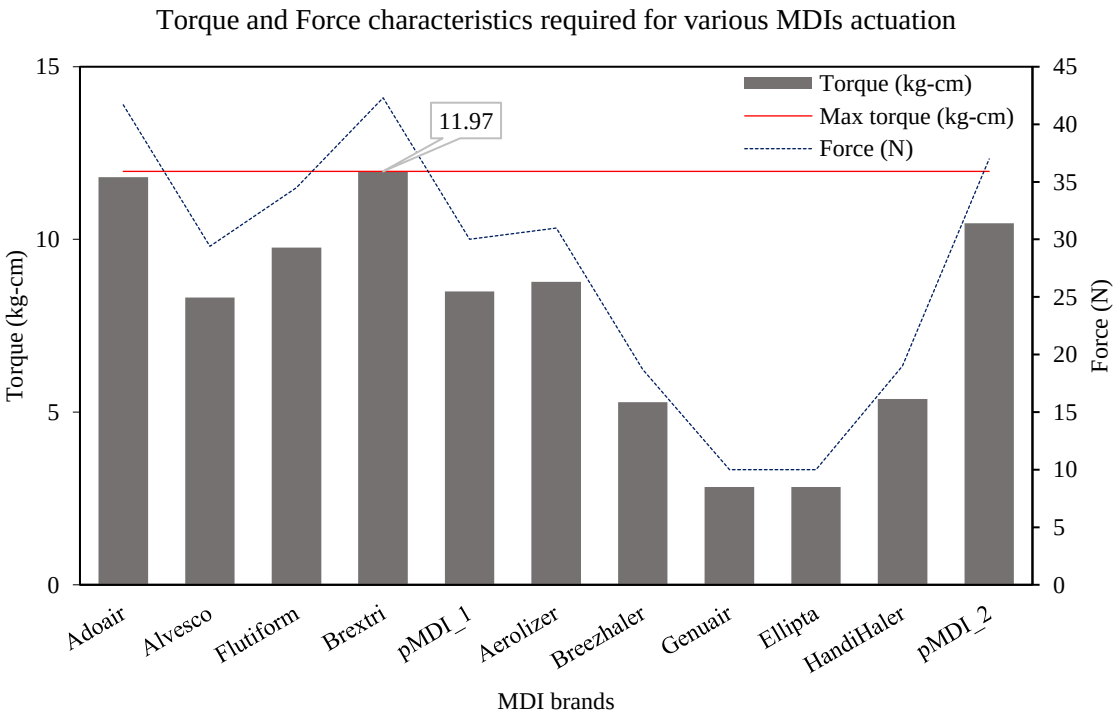

Figure 14: Torque and Force characteristics required for various MDIs actuation

Based on Figure 14, a servo of a minimum toque of 12 kg.cm is required. Thus, a Tower PRO MG995 13 kg.cm metal gear servo motor was procured due to its specifications and availability. It is a metal gear servo with an operating voltage of 5 V.

Figure 15 illustrates the rendering of the actuation mechanism comprising the cam, servo, and servo mount which is integrated into the device's door.

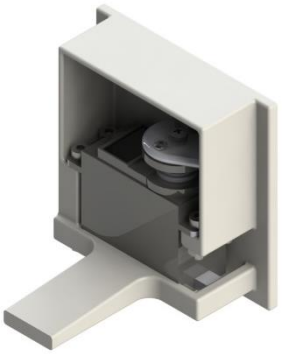

Figure 15: Actuation mechanism

The long protrusion at the end serves as the lock mechanism, with a second servo actuating against it to lock or unlock the door. As shown in Figure 15, the actuation mechanism was then tested successfully with the MDI holder and a canister to validate if the mechanism can actuate the canister.

4.2 Breath Detection System

Based on the requirement for the pressure sensor and availability, an NXP MPX5010DP pressure sensor was procured. This sensor can effectively measure pressures ranging from 0 to 100 cmH_2O. It operates as an analogue sensor, generating an output voltage that directly corresponds to the measured pressure. Additionally, its microchip features digital calibration, ensuring full calibration and temperature compensation. Figure 16 illustrates the pressure sensor used in the device.

Figure 16: NXP MPX5010DP pressure sensor

The pressure reading is obtained as shown in Equation 2.

$$Pressure = \frac{\frac{Sensor\ value - Sensor\ offset}{Sensitivity}}{mmH_2O\ to\ cmH_2O\ conversion\ factor}\ [cmH_2O] \qquad \textit{Eq. 2}$$

Where:

The sensor value is obtained by multiplying the analogue reading of the sensor by the conversion multiplier specific to the microcontroller's Analogue-to-Digital Converter [mV],

the sensor offset is 200 [mV] (obtained from the sensor's datasheet),

the sensitivity is 4.413 [mV/mmH2O] (obtained from the sensor's datasheet), and

the mmH_2O to cmH_2O conversion factor is 10 [cmH_2O/mmH_2O].

A Sensirion SFM3000-200C flowmeter was procured to measure the airflow. It is a bidirectional low-pressure drop digital flowmeter with a range of +/- 200 slm that can work with air and oxygen media, making it suitable for medical applications. This sensor is a digital sensor equipped with digital calibration within its microchip, ensuring full calibration and temperature compensation. It interfaces with external devices through digital protocols such as I2C (Inter-Integrated Circuit). Figure 17 illustrates the flowmeter used in the device.

Figure 17: Sensirion SFM3000-200C flowmeter

The flow reading is obtained as shown in Equation 3.

$$Flowrate = \frac{Measured\ value - Offset\ flow}{Scale\ factor\ flow}\ [Lpm] \qquad Eq.\ 3$$

Where:

the measured value is the sensor reading,

the sensor offset is 32000 (obtained from the sensor's datasheet), and

the scale factor flow for oxygen is 142.8 [1/Lpm] (obtained from the sensor's datasheet).

Both components have an operating voltage of 5 V. Additionally, these two components are readily available for high-quality mass production for commercial applications. The software required to operate these components was obtained from an open-source platform.

4.2.1 Determining the Inhalation Phase

An exponential filter was applied to the pressure and flow readings to determine the inhalation phase. The effect of the exponential filter, which is determined by the filter's weight, will enable changes in the readings to be determined and related to their raw readings, which can then be used to identify inhalation. The MegunoLink library, which is available in the Arduino libraries, was used to filter the readings.

The filter is the implementation of a linear recursive exponential filter, which is a data processing method that combines linear processing with recursive updating and exponential weighting to produce a smooth output signal (Martinsen, 2016). The filter effectively smooths out the reaction to sudden fluctuations, such as noise, in the input signal. The smoothing depends on the weight used, whereby a higher weight prioritizes latest data, leading to a quicker response to input changes with minimal smoothing (Martinsen, 2016). Conversely, a lower weight prioritizes older data, resulting in substantial smoothing and a slower response to input changes, regardless of whether they are noisy or not (Martinsen, 2016).

The filtered value is obtained as shown in Equation 4 (Martinsen, 2016).

$$y_n = w \times x_n + (1 - w) \times y_{n-1} \qquad \textit{Eq. 4}$$

Where:

y_n is the filtered reading at time n,

x_n is the new input reading at time n,

y_{n-1} is the previous filtered reading, and

w is the weighting factor ranging from 0 to 100.

As a result, the approach used is first to determine the weight required for the pressure and flow readings, which will allow the inhalation phase to be determined. The pressure sensor was connected between a CPAP device and a breathing simulator. The Arduino was programmed to output both raw and filtered pressure readings for a range of filter weights. The CPAP device was initially configured at 8 cmH_2O and the breathing simulator was configured at 20 bpm and I:E ratio of 1:2 to simulate normal breathing conditions.

Figure 18 illustrates a snippet of the results of the raw and filtered pressure readings and inhalation signals from BS between two inhalations.

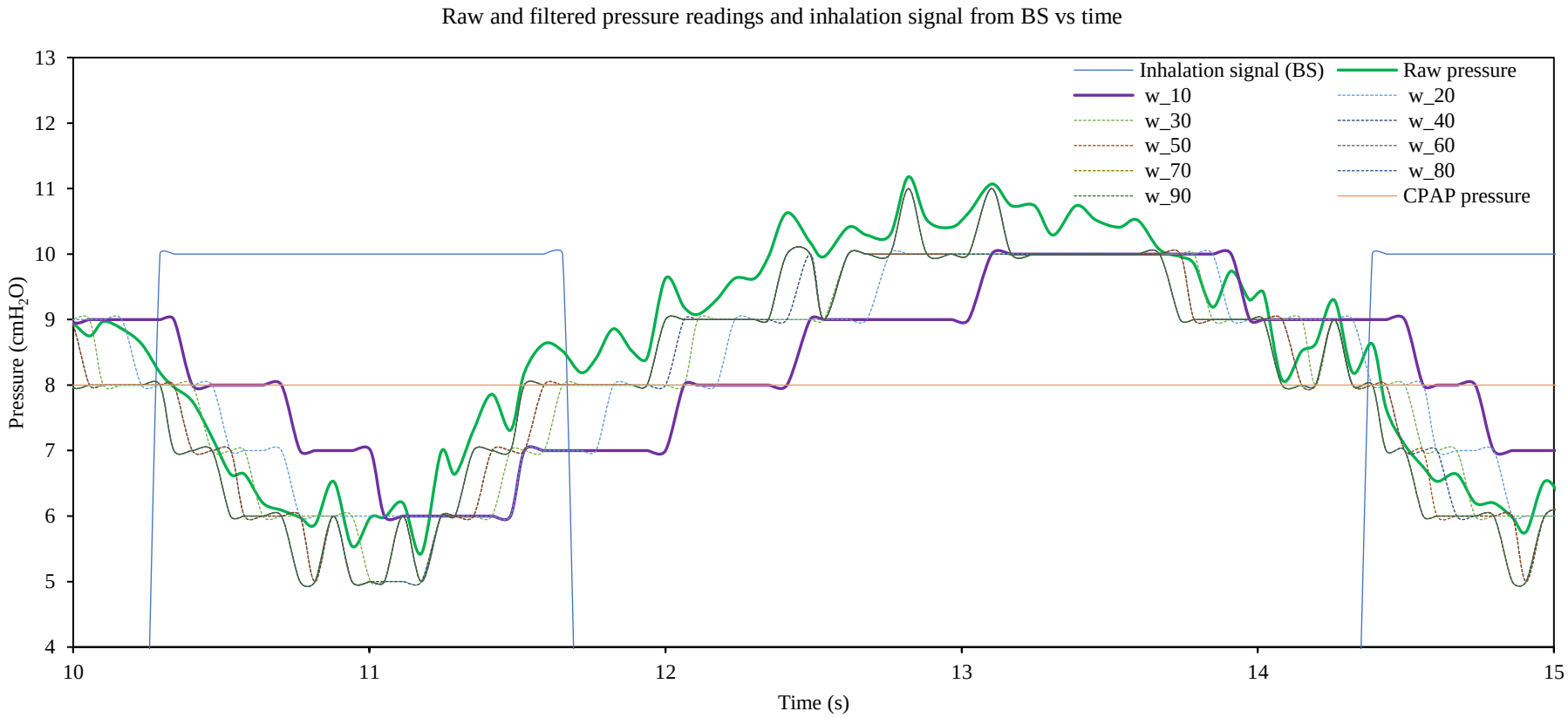

Figure 18: Raw and filtered pressure readings and inhalation signal from BS vs time

Based on the results shown in Figure 18, a weight of 10 was selected as it responds slowly to changes, is very smooth, and is the only filtered pressure reading that is greater than the raw pressure at the intersection with the inhalation signal, making it a distinct identifier that can be related to the raw pressure reading to identify the start of the inhalation phase.

The same process is repeated with the flow readings to obtain the weight that enables the raw reading to be related to the filtered readings to identify inhalation. Figure 19 illustrates a snippet of the results of the raw and filtered flow readings and inhalation signals from the BS between two inhalations.

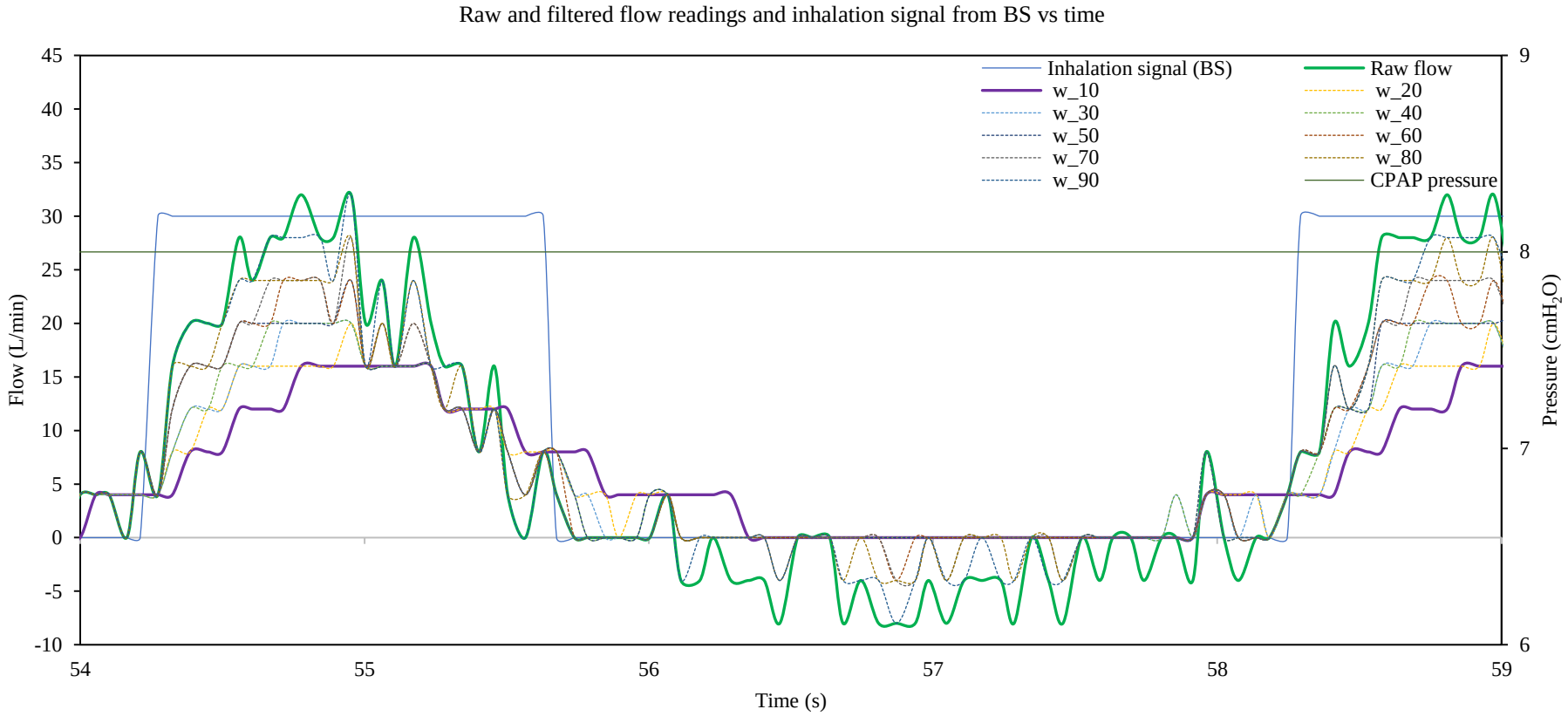

Figure 19: Raw and filtered flow readings and inhalation signal from BS vs time

Based on the results shown in Figure 19, a weight of 10 was selected as it again, responds slowly to changes, is very smooth, and is the only filtered flow reading that is smaller than the raw flow at the intersection with the inhalation signal, making it a distinct identifier that can be related to the raw flow reading to identify the start of the inhalation phase. A flow reading less than 0 is also used as an identifier, as it indicates the change from exhalation to inhalation.

After obtaining the weights for the pressure and flow readings, a relationship was established between the raw and filtered readings to determine the start of the inhalation phase. Figure 20 illustrates a snippet of the raw and filtered readings of the pressure, flow, and inhalation signal from the BS between two inhalations.

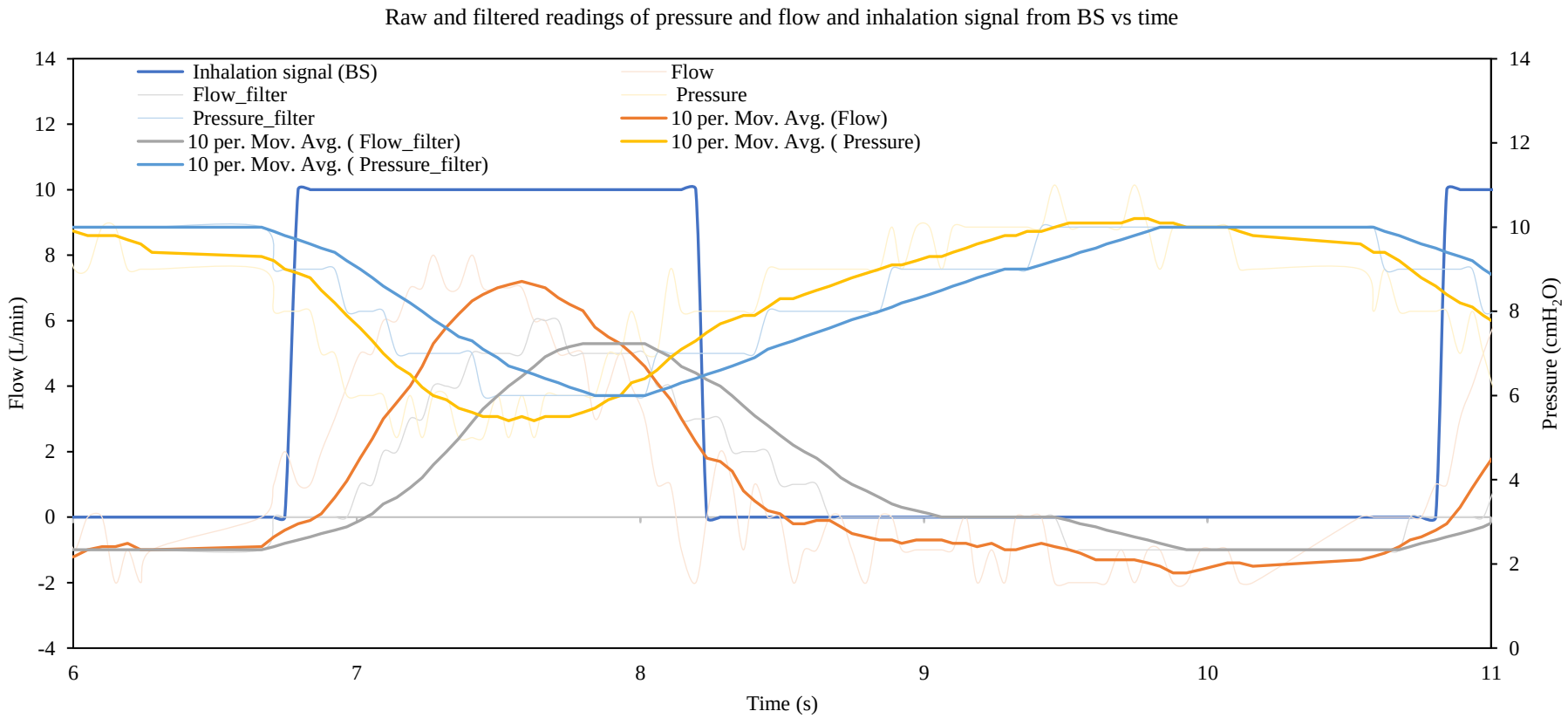

Figure 20: Raw and filtered readings of pressure and flow and inhalation signal from BS vs time

Based on the results shown in Figure 20, the conditions for the start of the inhalation are when the filtered pressure reading is greater than the raw pressure reading, when the filtered flow reading is less than the raw flow reading, and also when the flow reading is less than 0.

4.2.2 Combining the Actuation Mechanism with the Breath Detection System

The code for the actuation mechanism and the breath detection system were combined. Figure 21 illustrates the coding steps.

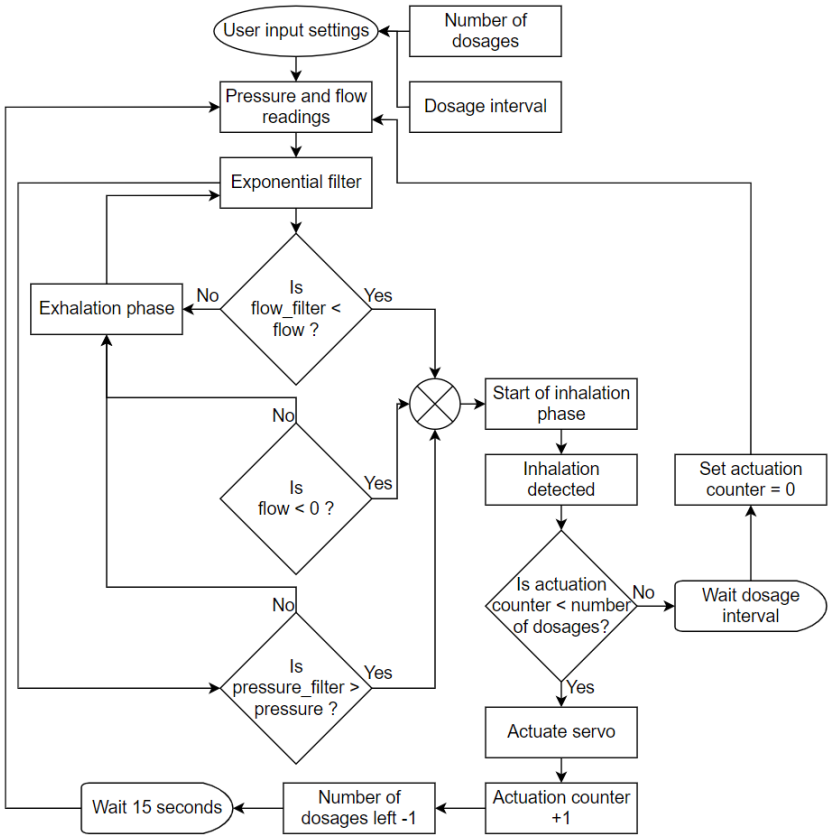

Figure 21: Breath detection system program flowchart

4.3 Safety Features

4.3.1 Door Lock Mechanism

A limit switch is positioned at the door's closing position, and as the door closes, it activates the switch, signalling a second servo to lock the door. Figure 22 and Figure 23 illustrate the door in its open and closed positions, respectively.

Figure 22: Door open

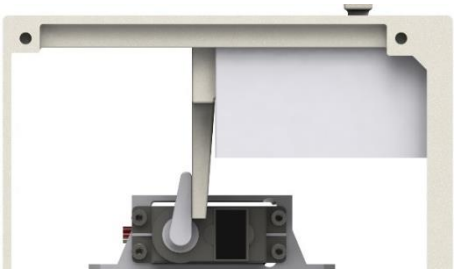

Figure 23: Door closed

4.3.2 Alarm System

A 5 V low-profile active buzzer was used for the alarm system. It has a sound output of 85 dB, which is sufficient to alert the nurse, clinician, or user and it is not damaging at that rating and exposure duration. The alarm for the low number of dosages left is included in the firmware of the MDI delivery system, whereby the microcontroller sends a signal to power the buzzer, activating the alarm, when the number of dosages left is 10 to alert the nurse, clinician, or user to reload the canister. The alarm for when inhalation is not detected activates in the same way if the device does not detect an inhalation for 10 seconds, indicating at least the absence of 2 to 4 breaths (Eldridge, 2022), allowing sufficient time for the nurse, clinician, or close relative to intervene.

4.4 Pulse Oximeter

A Maxim Integrated MAXREFDES117#: Heart rate and Pulse-Oximetry sensor was procured for the pulse oximeter accessory. This sensor was selected for the following reasons: it uses very low power, is very small, suitable for finger placement, works with Arduino, its firmware is basic and open source and is readily available for mass production. A casing was then designed for the sensor by modifying an existing open-source design for a finger pulse oximeter from Thingiverse (Łagiewka, 2021). Figure 24 illustrates the 3D printed pulse oximeter casing, integrated with the sensor.

Figure 24: Pulse oximeter

4.5 User Interface

Based on the UI requirements, an LCD 12864 white on black and a KY-040 - rotary encoder with a push button module is used for the UI to keep the device simple and intuitive to use. Table 5 shows the menu pages on the UI.

Table 5: MDI delivery device menu pages

Item No.	Main Menu	Submenu	Screensaver
1	No. of dosages:		Screensaver Press any button to exit
2	Int btw dosages:		
3	Dosages left:		
4	Deliver 1 dose	Wait for 15 s	
5	Reload canister		
6	Pulse Oximeter	Heart rate: _ bpm SpO2: _ % Press any button to exit	

4.6 Device Electrical System

4.6.1 Microcontroller Selection

After obtaining the main components, it was determined that the microcontroller needed 14 digital pins and 1 analogue pin. An Arduino Mega 2560 R3 was chosen over an Arduino Uno because the Uno has exactly 14 digital pins, additionally, the Mega has greater memory, which is preferable for running large code.

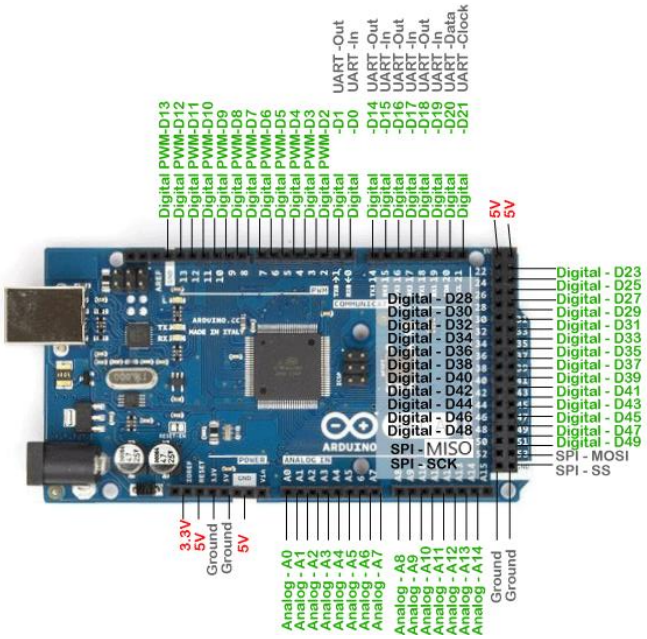

Figure 25: Arduino Mega pin layout

4.6.2 Battery Specifications

The operating voltage of the employed components is 5 V, and their combined current is 0.852 A, as shown in Table 6.

Table 6: Total current consumption

Item No.	Name	Description	Current Rating (A)
1	Alarm	Buzzer 5V Low Profile PCB	0.03
2	Arduino	Mega 2560 Rev 3	0.04
3	Display	LCD 12864 White on Black 3.3V	0.06
4	Flowmeter	Sensirion, SFM3000-200C	0.0055
5	Magnet switch	PS-3150 Magnetic Switch	0.5
6	Pressure sensor	NXP, MPX5010DP	0.005
7	Pulse Oximeter	Maxim Integrated, MAXREFDES117#	0.0015
8	Rotary encoder	KY-040 - Rotary Encoder Module	0.01
9	Servo	Tower Pro, MG995 13 Kg	0.2
		Total Current	0.852

Therefore, based on the components used and the power supply requirement, an 18650 3500 mA 3.7 V Lion battery with a power and charge shield of 5 V, 2 A output was used.

The running time of the battery was calculated to be 4.1 hrs, as shown in Equation 5.

$$Running\ time = \frac{Battery\ capacity}{Current\ Consumption}\ [hrs] \quad \text{Eq. 5}$$

Where:

the battery capacity is 3500 [mAh], and

the current consumption is 0.852 [A].

The charging time of the battery was calculated to be 2.45 hrs, as shown in Equation 6.

$$Charging\ time = \frac{Battery\ capacity + (Battery\ capacity \times 40\%)}{Charging\ current + 1}\ [hrs] \quad \text{Eq. 6}$$

Where:

the battery capacity is 3500 [mAh],

40 % is the average loss during charging, and

the charging current is 1 [A].

Figure 26 illustrates the electrical connection between the electrical system's components, microcontroller, and power supply.

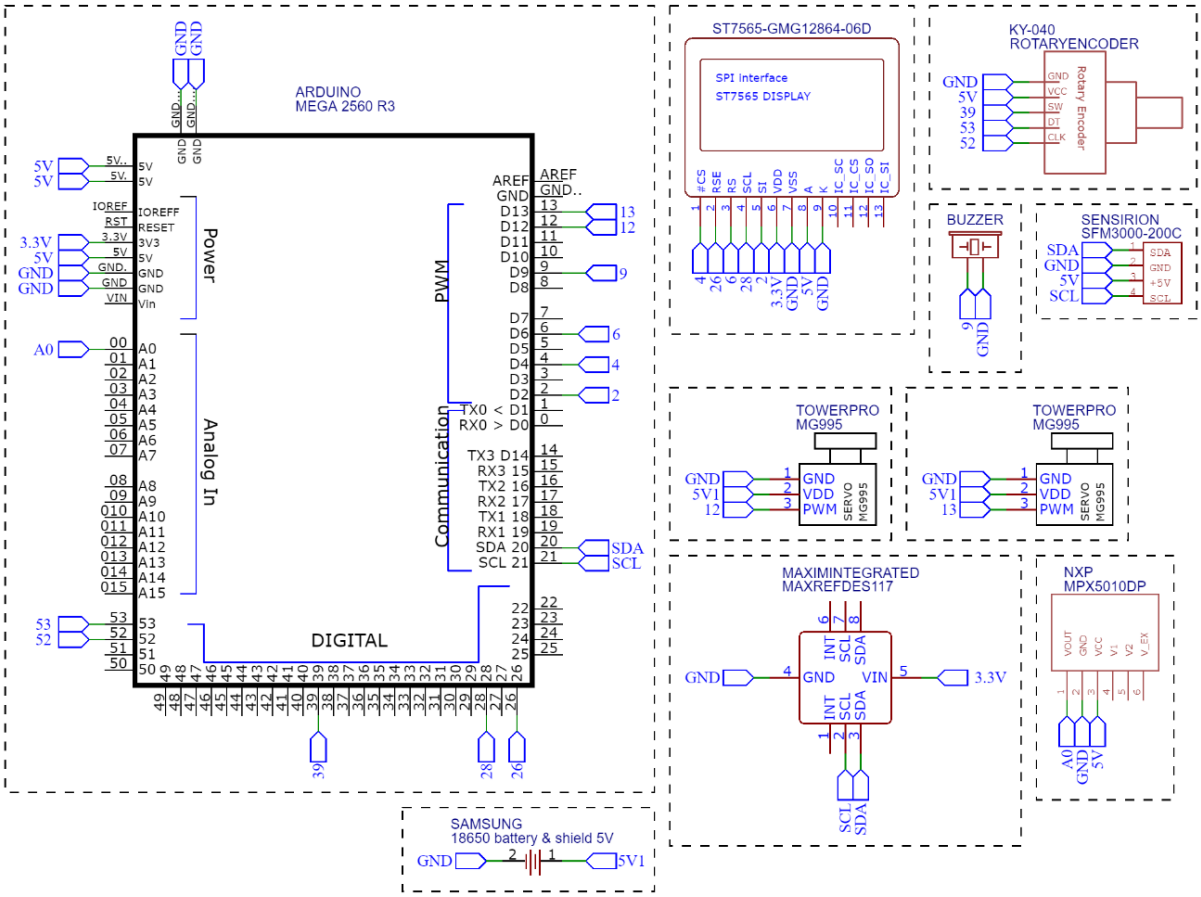

Figure 26: Electrical system

The open-source Arduino integrated development environment software was then used to code the microcontroller to control the system. The necessary software to run all the primary components was sourced from open-source platforms, and the code for the breath detection system was subsequently developed and integrated into this software, refer to Appendix A for the primary code.

4.7 Enclosure

After obtaining all the components and assembling them based on the design layout and electrical system, together with the code compiled on the Arduino, the features and dimensions for the enclosure were determined. The enclosure was then designed, and 3D printed using the Creality Ender 3 Pro. Figure 27 illustrates the rendering of the enclosure design.

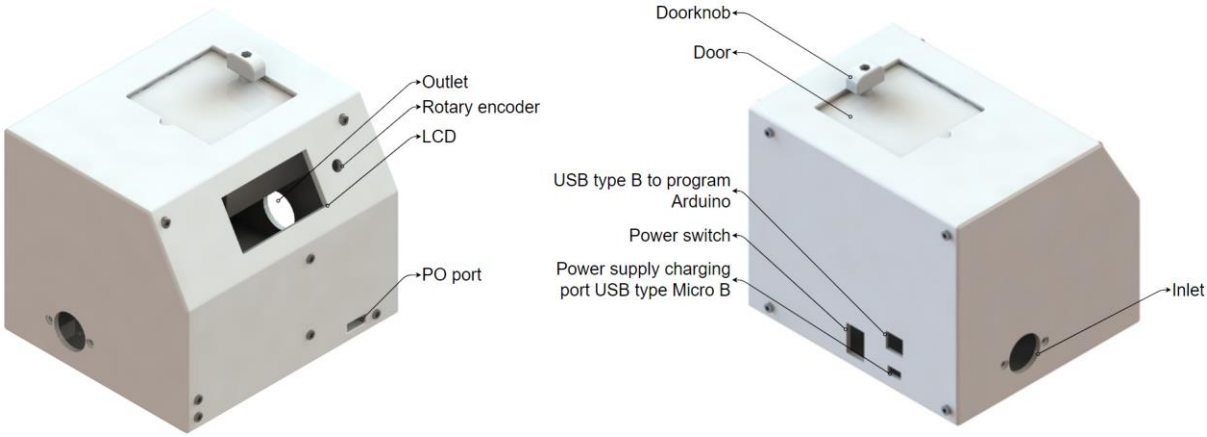

Figure 27: Enclosure

Figure 28 illustrates the rendering of the exploded view of the enclosure, showing the various parts that make up the enclosure and how it will be assembled.

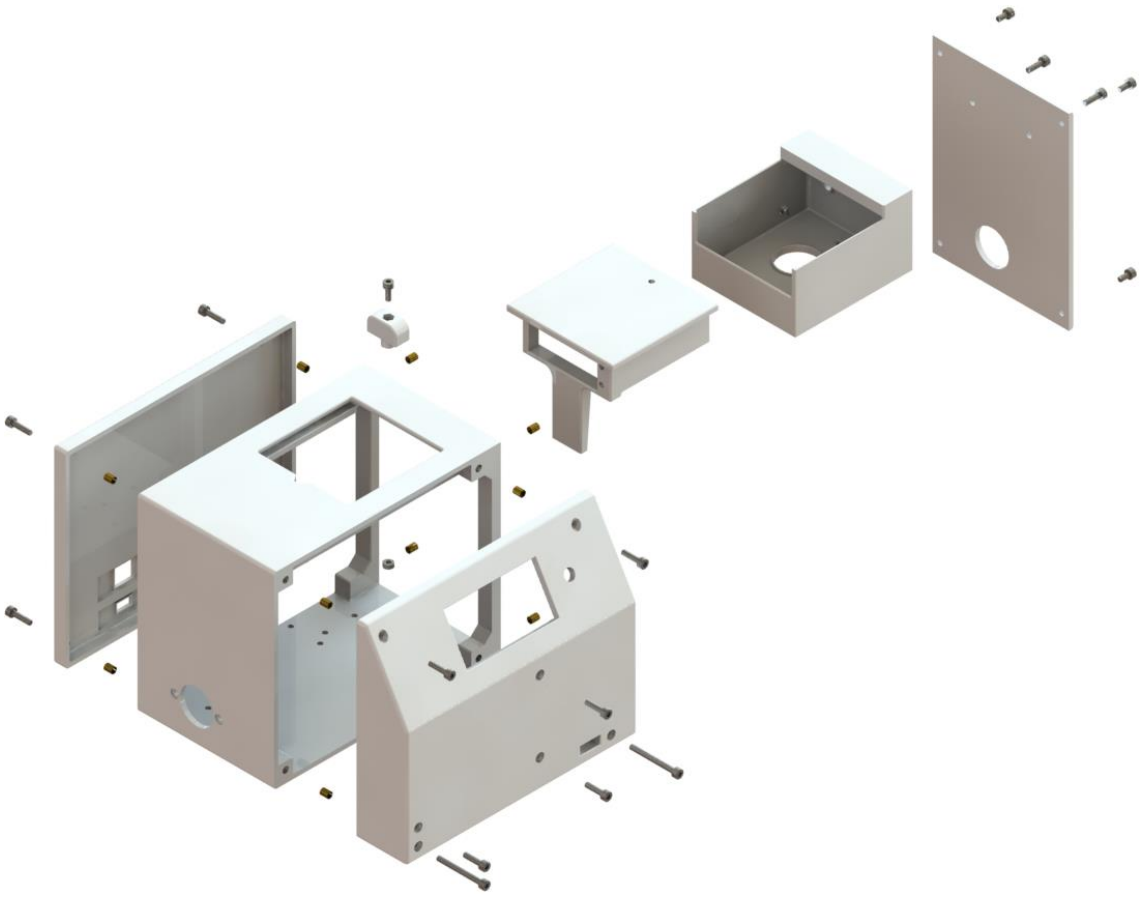

Figure 28: Exploded view of enclosure

4.8 Design specifications

Table 7 details the specifications of the design's subsystem outcomes.

Table 7: Design specifications

Design Requirement	Met?	Specifications
MDI Actuation Mechanism		
Hold the canister vertically	Yes	The canister placement is vertical. See section 4.1.1 MDI Canister Holder
Allow the canister to be easily reloaded	Yes	Easy reloadable by sliding in or out the canister from the holder. See section 4.1.1 MDI Canister Holder
Actuate the canister in-line with the air pathway of the breathing circuit	Yes	The nozzle is in-line with the air pathway. See section 4.1.1 MDI Canister Holder
The cam rotation is not impeded by the door during an actuation	Yes	Cam's base circle is ø21 mm, which fits between the servo mount, allowing for its rotation
The cam is not blocked by the canister when reloading	Yes	There is a 1 mm gap between the cam and the canister to allow the door to be opened when reloading
Exert sufficient force to actuate the canister. 12 kg.cm torque	Yes	Tower PRO MG995. Torque: 13 kg.cm
Allow the canister to be easily accessed without any dismantling	Yes	Servo mount is integrated into the device’s door, allowing easy access to the canister when opened
Breath Detection System		
Measure pressures between 3 and 20 cmH_2O	Yes	NXP MPX5010DP. Read pressures between 0 to 100 cmH2O
Measure flow rates up to 60 L/min,	Yes	Sensirion SFM3000-200C. Read up to 200 L/min
Detect inhalation effectively	Yes	See section 4.2 Breath Detection System
Safety		
The door must be locked	Yes	A limit switch is used near the closing position of the door, signaling a servo, which locks the door
The number of dosages left is low	Yes	Alarm is activated when the number of dosages left is 10
There is a power failure	Yes	A relay switch is used to activate the alarm in case of power failure during use
Inhalation is not detected over a short period	Yes	Alarm is activated if the device does not detect an inhalation for 10 s

Pulse Oximeter		
Connect to the device via a data cable	Yes	See section 4.4 Pulse Oximeter
User Interface		
Allow the user to deliver a dose when required	Yes	See section 4.5 User Interface
Display the number of dosages left and pulse oximeter readings	Yes	See section 4.5 User Interface
A selection to unlock the door for reloading the canister	Yes	See section 4.5 User Interface
Microcontroller		
Provide processing power required to control the functions of all the electronic components	Yes	Arduino Mega 2560 Rev 3. Operating voltage: 5 V, flash memory: 256 KB, SRAM: 8 KB, and clock speed: 16 MHz
Has enough digital and analogue pins. 14 digital and 1 analogue pins	Yes	Has 54 digital and 16 analogue input pins
Power Supply		
Integrated inside the device	Yes	ESP32S 18650 battery shield V3 and battery. Compact, enabling integration inside the device
Rechargeable	Yes	Fully charged in 2.45 hrs
Operate for a minimum of 4 hours	Yes	Can operate for 4 hrs on battery power
Supply required voltage and current. 5 V and 0.812 A	Yes	Output voltage: 5 V and current: 2 A
Enclosure		
Lightweight, compact, and have no sharp edges or corners	Yes	The casing was 3D printed with a thickness of 3 mm, density of 40 %, and overall dimensions of

4.9 Conclusion

In conclusion, the design outcome in this chapter has presented the developed device that meets all the technical specifications and design requirements. The design incorporates features that enhance the device's safety and user-friendliness, making it suitable for use in medical settings. The next chapter will present the validation methodology, which outlines the testing process used to validate the device’s design and functionality that will confirm the device's intended use.

CHAPTER 5: VALIDATION METHODOLOGY

This chapter outlines the validation methodology followed to validate the design and functionality of the device, from the Failure Modes and Effects Analysis, experimental setup, test methodology, and the test deliverables.

5.1 Failure Modes and Effects Analysis (FMEA)

A design FMEA is conducted on the device to identify where and how it might fail during the design process, in terms of specific component failure or failure related to the device's use, the resulting hazardous situation, evaluate the risks and determine the risk controls that must be implemented. As a result, a risk register was drawn up to record and identify any potentially hazardous situations, evaluate the risks, and determine risk controls. The outcomes of this analysis are to avoid any potentially hazardous situations during the design process or during use, to allow for early detection of failures to keep costs low, and to transition a safer and better device from design to manufacturing.

Table 8 shows the probability of a risk occurring, scored on a scale of one to five, based on the probability of occurrence.

Table 8: Probability rating

Probability Rating	Probability of Occurrence [%]
Frequent (5)	81 to 100
Probable (4)	41 to 80
Occasional (3)	11 to 40
Remote (2)	1 to 10
Improbable (1)	<1

Table 9 shows the severity of a risk, scored on a scale of one to five, based on its severity.

Table 9: Severity rating

Severity Rating	Severity Description
Catastrophic (5)	Potential fatality
Critical (4)	Results in lifelong disability or serious injury
Serious (3)	Results in injury or disability that requires expert medical attention
Minor (2)	Results in temporary injury or disability not requiring expert medical attention
Negligible (1)	Inconvenience or short-term discomfort

Table 10 shows the acceptability index, which is the multiplication of the risk's probability and severity.

Table 10: Acceptability index

	Probability				
Severity	Improbable (1)	Remote (2)	Occasional (3)	Probable (4)	Frequent (5)
Catastrophic (5)	5	10	15	20	25
Critical (4)	4	8	12	16	20
Serious (3)	3	6	9	12	15
Minor (2)	2	4	6	8	10
Negligible (1)	1	2	3	4	5

High Risk	>8	Not Acceptable
Medium Risk	>=6 & <= 8	Not Acceptable
Low Risk	<6	Acceptable

The technical approach for the risk analysis conducted on the device involves identifying the hazards, assessing the risks, and mitigating the potential risks associated with its use. The steps involved in the technical approach for risk analysis of the device are as follows:

1. **Identify Hazards:** This first step involves thoroughly examining the device and its intended use to identify all potential hazards, including failures, malfunctions, and misuse.
2. **Risk Analysis**: Once hazards are identified, they are analysed to assess the probability and severity of harm associated with each hazard. This assessment helps in quantifying the risks with a risk index allowing for a more objective comparison of different hazards.
3. **Risk Evaluation:** After assessing the risks, they are evaluated to determine their acceptability. This involves considering factors such as the severity of potential harm, the likelihood of occurrence, and the benefits of the device's use. The risks that exceed acceptable levels may require further mitigation.
4. **Risk Control:** For risks that are deemed unacceptable, appropriate control measures are implemented to mitigate or eliminate them. This may involve redesigning the device, adding safety features, providing warnings or instructions to users, or implementing quality control measures during manufacturing. Even after implementing control measures, some level of risk may remain, or new hazards may be introduced. These risks should be addressed, documented, and communicated to users.

Table 11 shows the risk register of the device, comprising of the risk analysis, evaluation, and control.

Table 11: FMEA analysis

Risk Analysis				Risk Evaluation				Risk Control			
Hazard	**Foreseeable sequence of events / Failure cause**	**Hazardous Situation**	**Harm**	**Probability**	**Severity**	**Risk Index**	**Acceptable?**	**Required Control**	**Control Implemented**	**New hazard introduced?**	**Description of the introduced hazard**
Device does not work as intended	User requirements are not clearly defined	Underperformance of the device	Compromised therapy, potential fatality	2	5	10	No	Define all possible user requirement and test if all requirements are met	Validate the device at the highest settings	No	N/A
Incorrect configurations	User is not familiar with the UI	Insufficient or excess medication delivery	Compromised therapy, lung damage, potential fatality	1	4	4	Yes	N/A	N/A	N/A	N/A
Device transferred from one patient to another or between rooms	Device handled roughly when moving around	Damage to device	Compromised therapy	1	3	3	Yes	N/A	N/A	N/A	N/A
Functionality of device	Non-conforming pressure and flow sensors	Device does not perform as intended	Compromised therapy, potential fatality	2	3	6	No	The sensors must be tested before incorporating in the device	Validate the sensors readings	No	N/A
User accidental input error	Rotary encoder may accidentally be moved, changing its setting	Device produces incorrect output	Compromised therapy	1	4	4	Yes	N/A	N/A	N/A	N/A
Sharp edges on enclosure	Manufacturing error could leave sharp edges	User bumps against the sharp edges	Injury	2	2	4	Yes	N/A	N/A	N/A	N/A
Noise level of device	Excess noise during actuation	Interference with hospitals' sound level policy	Discomfort for the patient or user	5	1	5	Yes	N/A	N/A	N/A	N/A
Access door to canister is not closed and locked	Actuation will not occur ineffectively	Medication is not delivered	Potential fatality	3	1	3	Yes	N/A	N/A	N/A	N/A
Arduino pin stop functioning	Excess current drawn causing pin to blow out	Device does not perform as intended	Compromised therapy, potential fatality	2	4	8	No	Current consumption must be less than supply current	Validate current consumption against supply current	No	N/A
Canister is not available at hand for reloading	User did not hear the alarm for low dosage left	Medication is not delivered	Compromised therapy, potential fatality	2	3	6	No	Activate an alarm first before the low dosage left's alarm	Activate an alarm when 50 dosages are left	No	N/A

5.2 Testing Methodology

5.2.1 Device Description

The device to be tested is an automated Metered Dose Inhaler delivery system. The users of the device are nurses and patients for home use. The device's intended use is to automatically actuate an MDI canister when inhalation is detected, based on the user input settings. The parameters that must be specified on the UI are the number of dosages and the interval between the dosage. The device is connected between the ventilator outlet and the patient mask, along the inhalation limb of the breathing circuit. The device monitors the ventilator's air flow rate and pressure output to detect inhalation. Any 5 V micro-USB charger can power the device, and it also has a built-in rechargeable battery.

5.2.2 Test Strategy

5.2.2.1 Test objectives

The objectives of the test are to validate the following:

1. The breath detection system by comparing the inhalation signal from the device to the breathing simulator’s signal.
2. The accuracy of the actuation mechanism by testing the timing of the actuation against the time at which inhalation is detected.
3. The operation of the device by comparing its operation to the user-specified settings.
4. The effectiveness of the automated solution by comparing the synchrony of the actuation between the automated solution and the current manual solution with inhalation.

5.2.2.2 Scope of testing

Only the developed automated MDI delivery device and a standard MDI in-line adapter will be used in the testing.

5.2.2.3 Type of testing

5.2.2.3.1 Functional testing

This testing will be conducted to validate the device's functionality to show that it works as intended under various configurations.

5.2.2.3.2 Performance testing

This testing will be conducted to evaluate the device's performance to ensure it meets the functional requirements. This testing will address any component or design flaws as well as evaluate the device’s ability to work consistently over long hours.

5.2.2.3.3 Unit testing

This software testing will be used to validate the breath detection system as a unit to ensure that the device's software works effectively to detect inhalation.

5.2.2.3.4 Graphical User Interface (GUI) testing

This testing will validate that the device's operation corresponds to the user input settings on the UI. This test can also identify any coding error in the UI and UI complexity.

5.2.3 Test Cases

Table 12 below shows the test cases for validating the device.

Table 12: Test cases

Test No.	Type of Testing	Description	Test Step		Expected Result
1	Functionality & Unit	Inhalation must be effectively detected	Run the test at the maximum value for the number of dosages and a low actuation interval	Log the breath detection signals from the device and the inhalation signals from the BS	The device accurately detects inhalation in conjunction with the inhalation signals from the BS
2	Performance	Actuation must occur concurrently when inhalation is detected		Log the breath detection signals and the actuation signals from the device, and the inhalation signals from the BS	The actuations must occur within a range of 0.2 s when inhalation is detected
3	Functionality, Performance & GUI	Number of actuations and the interval between the actuations correspond to the user input settings			The signals for the two test variables must correspond to the user input settings
4	Performance: manual vs automated	Perform manual test concurrently while the automated test is running to collect data on actuation time		Log the inhalation signals from the BS and the actuation signals during each test	Actuation during the automated test is more synchronous with inhalation compared to the manual test

5.2.3.1 Test variables

The breathing simulator is a variable where the configuration will vary based on the breathing characteristic parameters similar to the target patients. The breath detection system is directly dependent on this variable as the breathing characteristics will determine the breathing pattern, on which the breath detection relies to detect inhalation.

5.2.3.2 Test controls

The number of dosages and the actuation interval will be kept constant at the maximum value for the number of dosages and a low actuation interval for the first three test cases for the device to undergo a stress test and also to generate sufficient data to analyse the results. The maximum value for the number of dosages and the minimum actuation interval similar to a real use case will be used for the last two cases, to simulate the maximum breath detections and actuations.

The CPAP configuration will also be kept constant. It will be configured with the average settings required for the target patients. This is used as the test control as changing its configuration will not affect the outcomes of the testing as it will only shift the pressure and flow waveforms.

5.2.3.3 Test limitations

The breathing simulator used for the testing was designed and built by the Medical Devices Laboratory (MDL) for testing respiratory care devices. However, due to the technical limitations of the breathing simulator's design, respiratory rates above 30 bpm cannot be configured on the breathing simulator. This will still enable testing in the lower to middle range of the breathing characteristics of the target patients but not close to the upper limit of the range.

5.3 Test Methodology

5.3.1 Test case 1

This test will be conducted to validate the breath detection functionality of the device by validating that it effectively detects inhalation at the same time as the inhalation signal from the breathing simulator. Figure 29 below shows the test setup for test case 1.

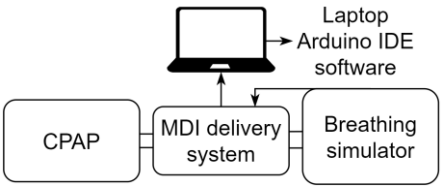

Figure 29: Automated test setup

The following is the test methodology followed for test case 1:

1. The MDI delivery device will be connected between the CPAP device and the breathing simulator as shown in Figure 29.
2. The CPAP device will be configured with the average settings required for the target patients.
3. The MDI delivery system will be configured with the maximum value for the number of dosages and a low actuation interval.
4. The breathing simulator will be configured with characteristic parameters similar to the target patients.

5. The Arduino IDE software will be used to log the inhalation signals from the MDI delivery device and the inhalation signals from the breathing simulator.
6. The device will then be validated by verifying if the device accurately detects inhalation in conjunction with the breathing simulator's inhalation signal.
7. A positive test of step 6 means a pass. If it is a failure, the coding must be troubleshot and re-conduct the validation.

5.3.2 Test case 2

This test will be conducted to validate that the actuation signal occurs concurrently or within an acceptable lag compared to the time when the inhalation is detected from the breathing simulator.

The test steps are the same as in test case 1, except that the actuation signals from the MDI delivery device and the inhalation signals from the breathing simulator will be logged. The test will be positive if the actuation occurs within 0.2 s of when inhalation is detected. If it fails, the coding must be troubleshot and re-conduct the validation.

5.3.3 Test case 3

This test will be conducted to validate the operation of the device by validating its operation with the user-specified settings.

This test will coincide with test case 2 as the same data is collected. The test will be positive if the number of actuations and the interval between the actuations correspond to the user-specified settings. If it fails, the coding must be troubleshot and re-conduct the validation.

5.3.4 Test case 4

This test will be conducted to answer the research question of the thesis: Would an automated MDI delivery system be more effective than the present manual MDI delivery method?

This test will be conducted to compare the effectiveness of the automated solution vs the current manual solution in terms of the delay of the actuation with respect to when inhalation is detected. The literature review concluded that the medication effectiveness is associated with synchronous actuation of the canister with inhalation, which is most effective when it is actuated within 0.2 s from the exact start of inhalation. Thus, this test aims to validate the effectiveness of the automated solution by validating the synchrony of the actuation between the automated solution and the current manual solution with inhalation.

5.3.4.1 Automated test setup

The following is the test methodology for test case 4 in the automated test:

1. The MDD will be connected between the CPAP device and the breathing simulator.
2. The CPAP device will be configured with the average settings required for the target patients.
3. The MDI delivery system will be configured with the maximum value for the number of dosages.
4. The breathing simulator will be configured with breathing characteristic parameters similar to the target patients.
5. The Arduino IDE software will be used to log the time at which the inhalation is detected from the MDI delivery device and when the actuation occurred. The automated test setup is the same as shown in Figure 29.

5.3.4.2 Manual test setup

The following is the test methodology followed for test case 4 in the manual test:

1. The same parameters for the breathing simulator and MDI delivery settings will be used to concurrently run the manual test.
2. The CPAP device will be configured with the average settings required for the target patients.
3. The MDI canister is connected along the breathing circuit using an MDI in-line adapter.
4. A push button will be placed on the MDI canister. The push button will be pressed when the canister is manually actuated and this will send a signal to the Arduino, which will be logged as the actuation signal.
5. The user in the manual test will have to visually monitor the breathing simulator, to check if inhalation is indicated, and then actuate the canister.
6. The user will then manually time 15 s for the next actuation and repeat step 5.
7. Repeat step 6 until the total number of dosages is delivered.
8. The Arduino IDE software will be used to log the time at which the inhalation is detected from the MDI delivery device and when the manual actuation occurred. Figure 30 shows the manual test setup.

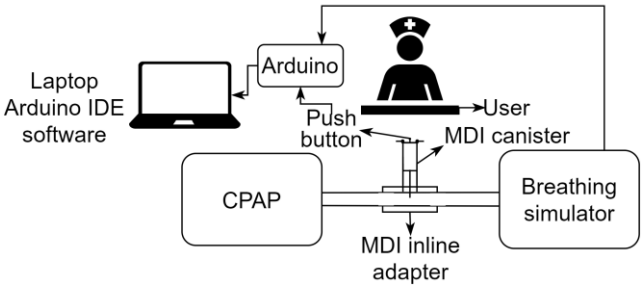

Figure 30: Manual test setup

9. The device will then be validated by verifying the timing of the actuation in each test setup against the time at which inhalation was detected.

10. If the delay between the actuation and the inhalation detection signal in the automated test is less than in the manual test, it will result in a positive result, demonstrating the effectiveness of the device. If the test fails, it will result in a negative test result, indicating the automated solution is not more effective than the manual solution.

5.4 Technical Values of Test Devices

5.4.1 CPAP Device

The setting for the CPAP device was inferred by reviewing the settings typically used on the target patients. Table 13 summarises the initial CPAP settings typically used on COPD or Asthma patients requiring ventilation.

Table 13: CPAP settings

Study	Value [cmH_2O]
(Ediboglu, 2021)	8 to 10
(Ahmed & Athar, 2015)	10
(Masip & Mas, 2014)	8 to 10
(Lopes et al., 2011)	8
(Phipps & Garrard, 2003)	3 to 8

Based on Table 13, a CPAP setting of 8 cmH_2O is selected for the validation test. As mentioned in section 5.2.3.2 Test controls, it is kept constant as changing its configuration will not have any effect on the outcomes of the testing as it will only shift the pressure and flow waveforms.

5.4.2 Breathing Simulator

The settings required for the breathing simulator are the respiratory rate and the I:E ratio, which were drawn based on the breathing characteristics of COPD and Asthma patients. A respiratory rate of more than 25 breaths per minute is considered one of the COPD exacerbation signs (Al-Halhouli et al.,

2021), whereas acute to severe Asthma patients have a respiratory rate of more than 30 breaths per minute (Papiris et al., 2002). A respiratory rate greater than 35 bpm in the target patients is a clinical indication for invasive ventilation (Mowery, 2017). However, due to the technical limitations of the breathing simulator designed for lab testing, respiratory rates above 30 bpm cannot be configured on the breathing simulator. In terms of the I:E ratio, COPD and Asthma patients are characterized by the dynamic hyperinflation of the lung, affecting the expiratory phase, where it can shorten or prolong the exhalation phase (Demoule et al., 2020). Therefore, for the validation tests, a respiratory rate of 25 and 30 bpm and an I:E ratio of 1:1, 1:2 and 1:3 will be configured.

5.5 Summary of Test Steps

Table 14 shows the configurations for test conditions for each test cases 1, 2 and 3.

Table 14: Configurations for each test condition

<table>
<tr><th></th><th></th><th>Ventilator Parameters</th><th colspan="2">Breathing Simulator Parameters</th><th colspan="2">MDI Delivery Device Settings</th></tr>
<tr><th>Test Case No.</th><th>Test Condition No., i</th><th>Mode and Value</th><th>RR [bpm]</th><th>I:E ratio</th><th>No. of dosages</th><th>Int. btw dosages</th></tr>
<tr><td rowspan="6">1, 2 & 3</td><td>1</td><td rowspan="12">CPAP at 8 cmH_2O</td><td rowspan="3">25</td><td>1:1</td><td rowspan="12">10</td><td rowspan="6">5 mins</td></tr>
<tr><td>2</td><td>1:2</td></tr>
<tr><td>3</td><td>1:3</td></tr>
<tr><td>4</td><td rowspan="3">30</td><td>1:1</td></tr>
<tr><td>5</td><td>1:2</td></tr>
<tr><td>6</td><td>1:3</td></tr>
<tr><td rowspan="6">4</td><td>7</td><td rowspan="3">25</td><td>1:1</td><td rowspan="6">-</td></tr>
<tr><td>8</td><td>1:2</td></tr>
<tr><td>9</td><td>1:3</td></tr>
<tr><td>10</td><td rowspan="3">30</td><td>1:1</td></tr>
<tr><td>11</td><td>1:2</td></tr>
<tr><td>12</td><td>1:3</td></tr>
</table>

For test cases 1, 2, and 3, the maximum number of dosages, 10, is used and the interval between the dosages used is 5 mins, which is less than the technical specifications, this is used to collect the maximum data. For test case 4, the maximum number of dosages, 10, is used, and only 1 set is collected as it provides the data required for the analysis.

Figure 31 shows the test steps followed for test cases 1, 2 and 3 and Figure 32 shows the test steps followed for test case 4. The test is initiated with the first test condition i = 1 and is iterated after each pass test case for all the test conditions. In test case 4, the data, after each test condition, on the actuation signals from the manual and automated test, the inhalation signals from MDD and their timing, respectively are collected, and later collated and analysed to determine the effectiveness of the device in terms of the delay in the actuation.

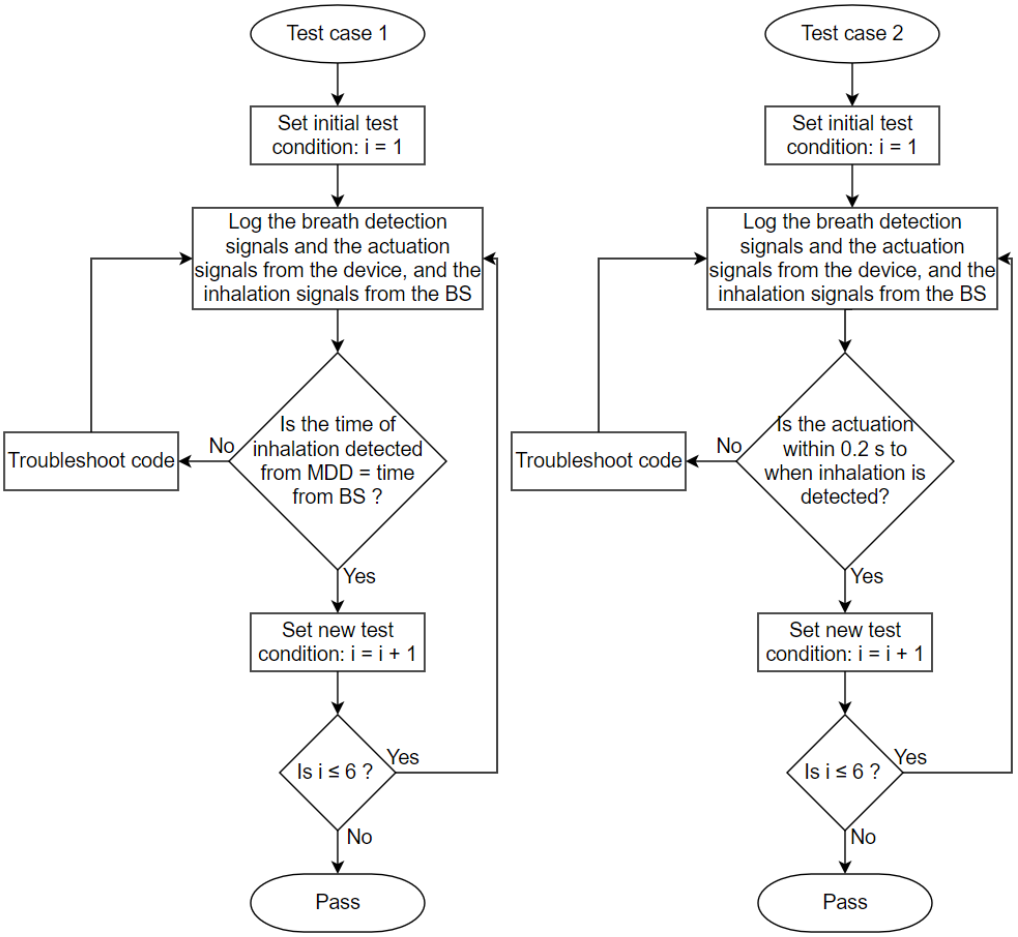

Figure 31: Flowchart of test steps for test cases 1 & 2

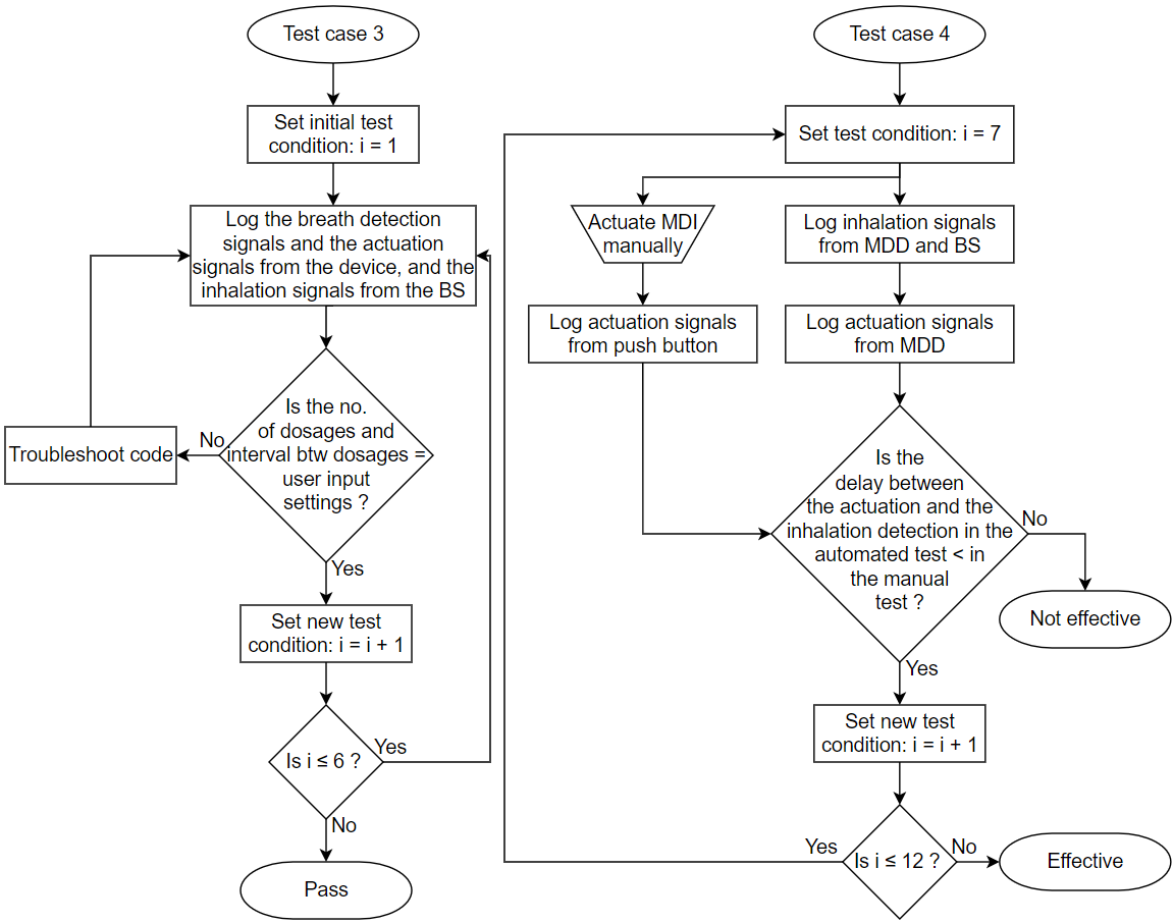

Figure 32: Flowchart of test steps for test cases 3 & 4

5.6 Equipment Allocation and Test Environment

Table 15 shows the equipment required for the testing and their source.

Table 15: Equipment and Source

Equipment	Source
CPAP device	Device designed in Medical Device Design 1
Breathing Simulator	UCvenT
MDI canister	Purchase at pharmacy
In-line MDI adapter	3D print
Laptop	Personal

The test will be conducted in the Medical Devices Laboratory. All the health and safety protocols of the lab will be followed.

5.6.1 CPAP Device

Figure 33 illustrates the CPAP device used for the validation tests.

Figure 33: CPAP device

The device was previously built during the Medical Device Design 1 course. The output pressure of the device was validated using the Medical Devices Lab's Ventilator Assessment Tool (VAT), which is a test instrument to validate various output parameters of a ventilator.

5.6.2 Breathing Simulator

Figure 34 illustrates the breathing simulator used for the validation tests.

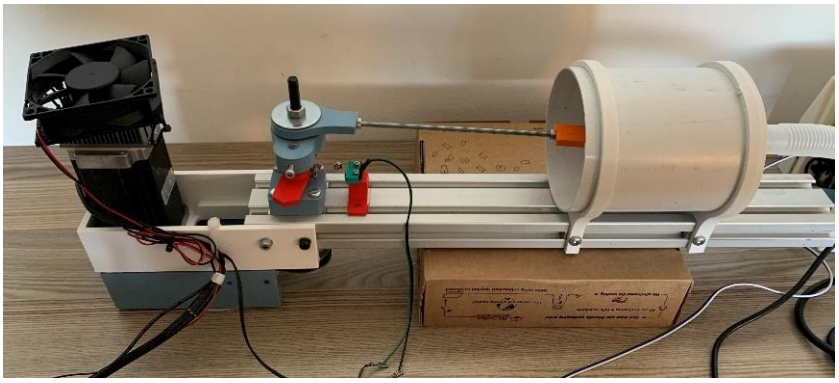

Figure 34: Breathing simulator

The MDL designed and developed the breathing simulator using readily available parts. The breathing simulator simulates breathing using a piston and cylinder mechanism and a limit switch to detect which phase it is in throughout the breathing cycle, and it also features configurable breaths per minute and I:E ratio.

5.6.3 Test Setup

Figure 35 illustrates the test setup of the validation tests.

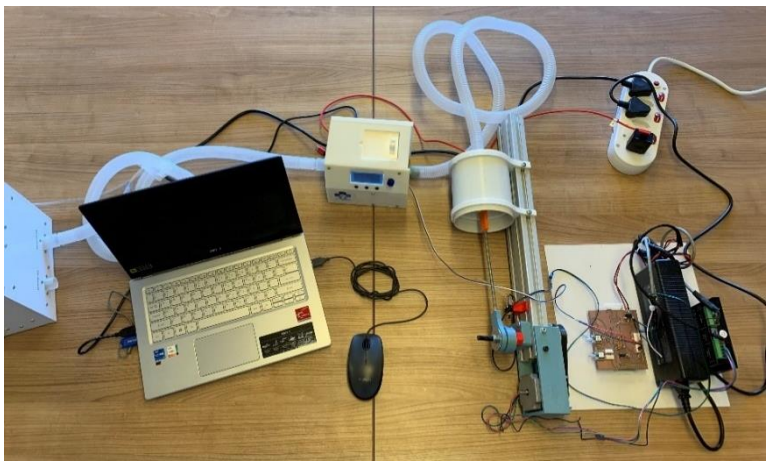

Figure 35: Test setup

5.7 Test Deliverables

Table 16 summarises the test deliverables.

Table 16: Test deliverables

No.	Data Collected	Expected Outcomes
1	Data on breath detection for each test condition, illustrating the timing of the breath detection signals from the device corresponding with the inhalation signals from the breathing simulator	Device accurately detects inhalation
2	Data on the inhalation and actuation signals timing for each test condition, illustrating the difference between the timing of the two to be within an acceptable range	Actuations occur within a range of 0.2 s when inhalation is detected
3	Data on the number of actuations and the interval between the actuations for each test condition illustrating, their correspondence to the user input settings	Device works as intended showing the number of actuations and the interval between the actuations corresponding to the user input settings
4	Data on the timing of the actuation and inhalation detected signals from the manual and automated test	Delay between the actuation and the inhalation signal is less in the automated test compared to the manual test

5.8 Conclusion

In conclusion, the validation methodology of this chapter has outlined the testing process that will be used to validate the design and functionality of the device. The validation methodology comprised several stages, including FMEA, testing methodology, experimental setup, and test deliverables. The next chapter will present the results and discussions, which will provide a comprehensive analysis of the data obtained during the validation process.

CHAPTER 6: RESULTS AND DISCUSSIONS

This chapter details and discusses the design of the device and the results of each test case from the testing methodology section.

6.1 Device Design

Figure 36 illustrates the MDI delivery device after 3D printing the enclosure and assembling all the components.

Figure 36: MDI delivery device

The device is 160 x 125 x 130 mm in size. The ergonomics of the design are considered by filleting all the edges to make them smooth and to avoid any injury, and the user interface panel is angled at 60° to allow for an ergonomic viewing angle. The door to access the canister uses a sliding door mechanism for simplicity and ease of use. There is a USB type A female port at the bottom of the front face to connect the pulse oximeter. The UI is simple and intuitive to use, whereby no additional training is required to operate the device. The device meets all the design requirements.

However, there are some drawbacks to the design of the device which are described below:

- The device is quite large, whereby it will need to be placed on a bedside table or an overbed table depending on factors such as the bed setting and the distance at which the device will be inserted along the breathing circuit from the mask, which is 15 cm (Dhand, 2017).
- The components inside the device are very sensitive and the device is not impact resistant due to the 3D printing material, making the device prone to mechanical failure if the device falls.

- The combined sound of the servo and the canister during an actuation can be considered intrusive by some patients.
- The device can only be used with canisters that do not require shaking before actuation, such as the QVAR RediHaler® and Alvesco® inhalers.

6.2 Accuracy of the Breath Detection System

The ideal relationship between the breath detection system of the device and the inhalation signal from the breathing simulator would be a linear relationship, starting at 0 and equal to each other, which is the same as the relationship of y = x. However, it was expected that there will be a very small difference in the timing of the breath detection signal compared to the inhalation signal from the breathing simulator, considering the weight of the filter used for the breath detection signals.

Nonetheless, a negative time difference between the timing of the breath detection signal and the inhalation signal from the breathing simulator, meaning breath is detected before the inhalation signal from the BS, is preferable, considering the time the servo takes to actually actuate the canister.

Figure 37, Figure 38, Figure 39, Figure 40, Figure 41, and Figure 42 illustrate the results of test case 1, where the timing of the inhalation signal from the device is plotted against the inhalation signal from the breathing simulator for each test condition.

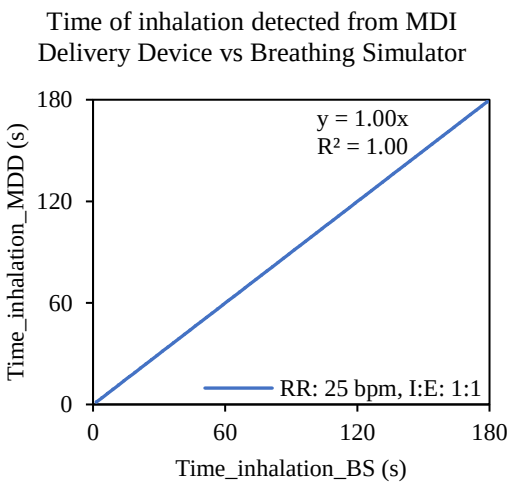

Figure 37: Inhalation detected time from MDD vs BS at 25 bpm & I:E 1:1

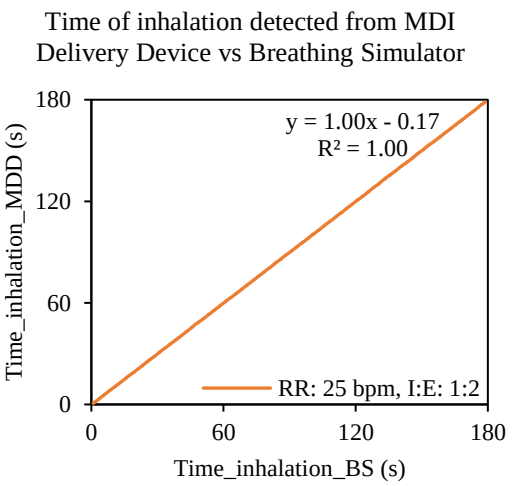

Figure 38: Inhalation detected time from MDD vs BS at 25 bpm & I:E 1:2

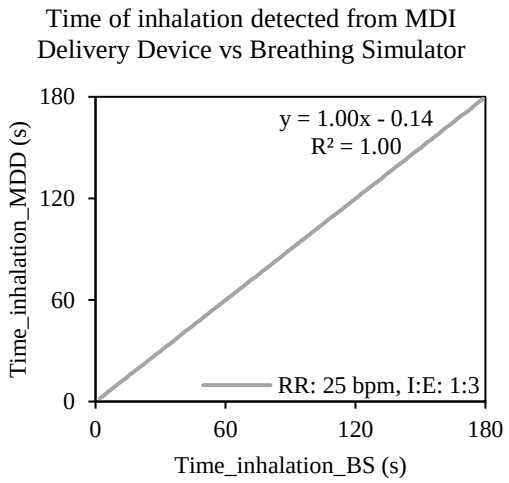

Figure 39: Inhalation detected time from MDD vs BS at 25 bpm & I:E 1:3

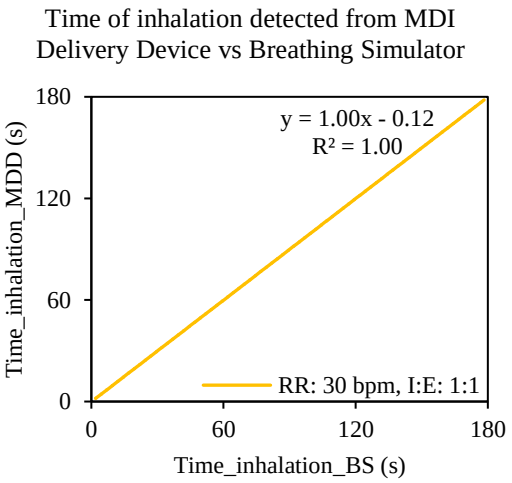

Figure 40: Inhalation detected time from MDD vs BS at 30 bpm & I:E 1:1

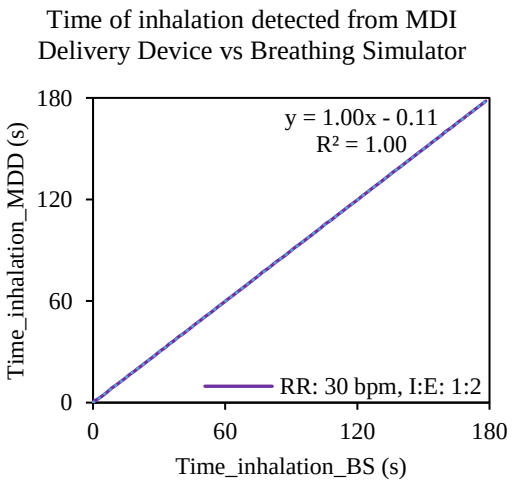

Figure 41: Inhalation detected time from MDD vs BS at 30 bpm & I:E 1:2

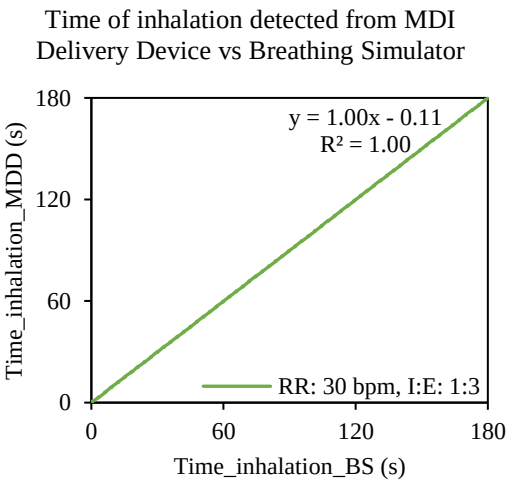

Figure 42: Inhalation detected time from MDD vs BS at 30 bpm & I:E 1:3

The results show a relationship of y = x in all the tests with an average y-intercept of 0.11, which is the difference between the timing of the inhalation signal from the device and the inhalation signal from the breathing simulator. The results also have an R^2 value of 1, indicating a strong positive correlation between the two variables. The negative difference indicates that the device detects inhalation, on average, 0.11 s before the BS's inhalation signal is logged. The servo takes 0.25 s to actuate the canister, and this time difference allows enough time for the actuation, ensuring the medication is delivered within the desired range after the onset of inhalation. Thus, this test is positive, showing that that device accurately detects inhalation.

6.3 Time Difference between Actuation and Inhalation

As described in the literature review, the desired range between the actuation and the onset of inhalation is between 0 to 0.2 s, for the optimum effectiveness of the bronchodilator medication. Thus, for an effective treatment, the time at which the canister is actuated must fall within this range.

The test was conducted as described in section 5.3.2 Test case 2 and the time difference was calculated as shown in Equation 7.

$$\Delta\ Time = Actuation_{time} + 0.25 - Inhalation_{time_{device}} - 0.11\ [s] \qquad \textit{Eq. 7}$$

Where, 0.25 [s] is the time taken for the servo to actuate the canister.

Figure 43 illustrates the results of test case 2, where the time difference between the 3 sets of 10 actuations and the inhalation signal from the device is plotted against the actuation number.

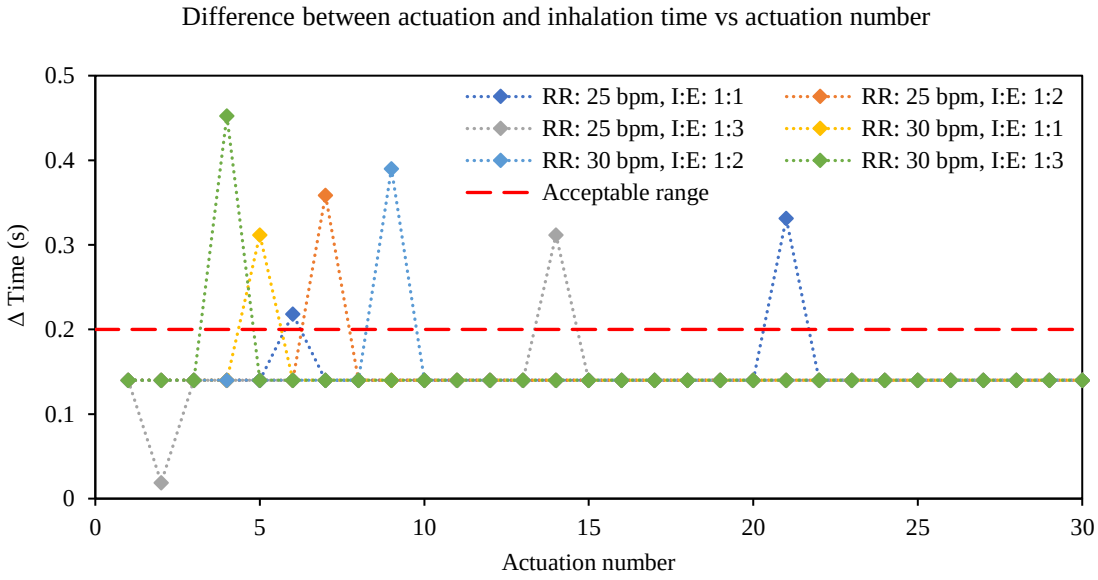

Figure 43: Difference between actuation and inhalation time vs actuation number

Figure 43 shows that for all the test conditions, most of the actuations fall within the acceptable range at 0.14 s. There is a maximum of one or two actuations that fall outside the acceptable range in each test condition and are considered as an actuation asynchrony.

Figure 44 illustrates the number of actuation asynchrony per 3 sets of 10 actuations vs breathing characteristics of the test conditions.

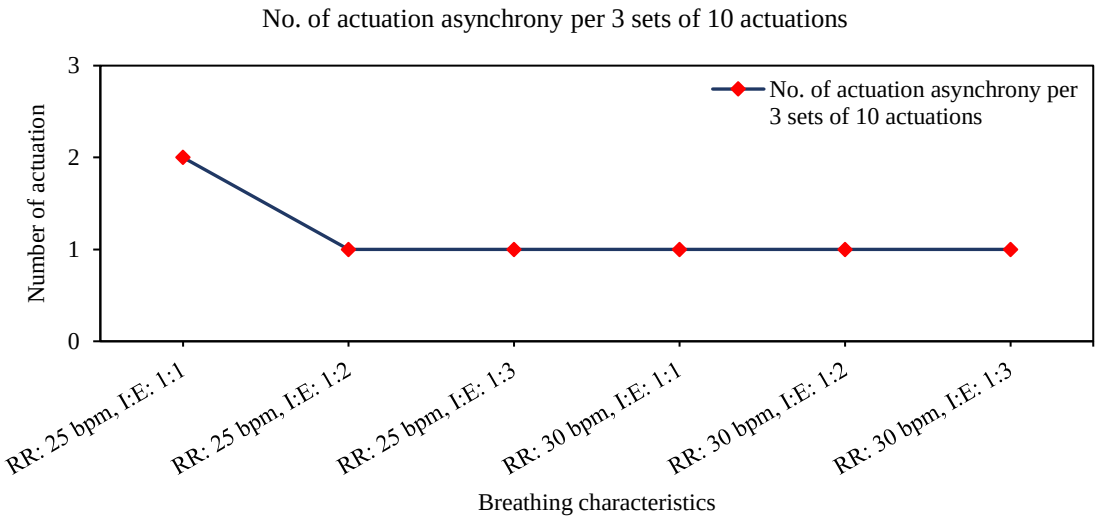

Figure 44: Number of actuation asynchrony per 3 sets of 10 actuations vs breathing characteristics

Figure 44 shows that there was only one actuation asynchrony in all the test conditions, except for the test at RR: 25 bpm and I:E 1:1 which had 2 asynchronous actuations. The test was reconducted with an actuation number of five to understand the asynchronous actuations.

Figure 45 illustrates the number of actuation asynchrony per 3 sets of 5 actuations vs breathing characteristics of the test conditions.

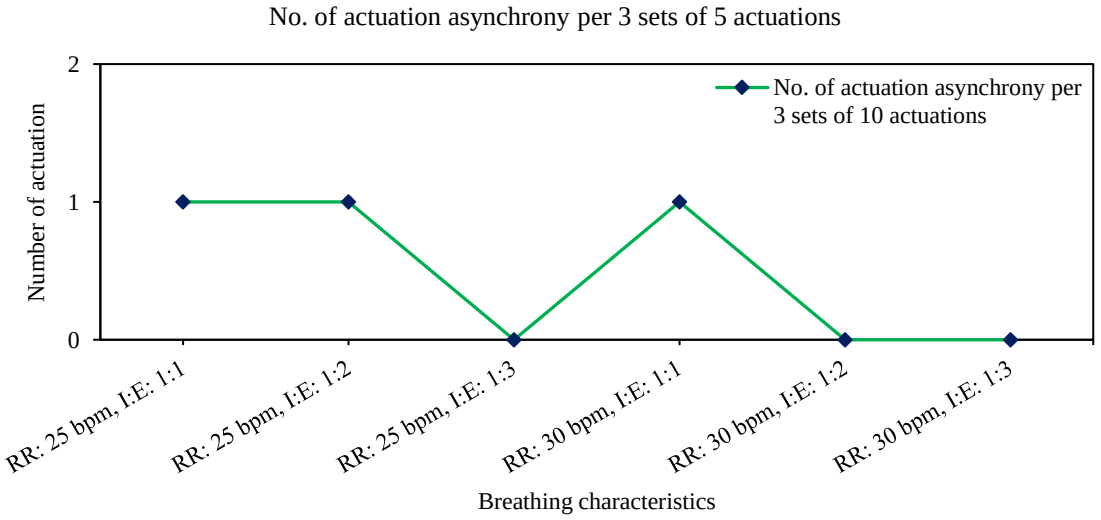

Figure 45: Number of actuation asynchrony per 3 sets of 5 actuations vs breathing characteristics

Figure 45 shows that there was only one actuation asynchrony in three of the conditions and none in the others. It was also noted in this test that the average delay between the BS's inhalation signal and the device's inhalation signal is also 0.11 s. Thus, this value can be used as the average delay between the

two inhalations' signals. The actuation asynchrony seems to occur randomly, at a maximum of one, in any of the tests and no possible source of error was found in the code. Therefore, to address this issue, the following steps were added to the code:

1. Log the time, $t_{inhalation}$, at which inhalation is detected.
2. Log the time, $t_{actuation}$, at which an actuation occurs.
3. If $t_{actuation}$ + 0.25 s - $t_{inhalation}$ – 0.11 s ≤ 0.2 s, then actuate.

The test was reconducted under the same conditions. The results obtained did not show any asynchronous actuations. The time difference between the actuation and the onset of inhalation in all the tests is 0.14 s, which is within the range for the optimum effectiveness of the bronchodilator medication. Thus, this test is positive, showing that the device enables an effective treatment with respect to the actuation and inhalation synchrony.

6.4 Device Operates According to User Input Settings

The test was conducted as described in section 5.3.3 Test case 3 at 10 actuations every 5 mins. This test is conducted to show that the device works as intended showing the number of actuations and the interval between the actuations correspond to the user input settings, and the interval between each actuation in a set is 15 s. Figure 46, Figure 47, Figure 48, Figure 49, Figure 50, and Figure 51 illustrate the results of test case 3, where the actuation time is plotted against the actuation number for each test condition.

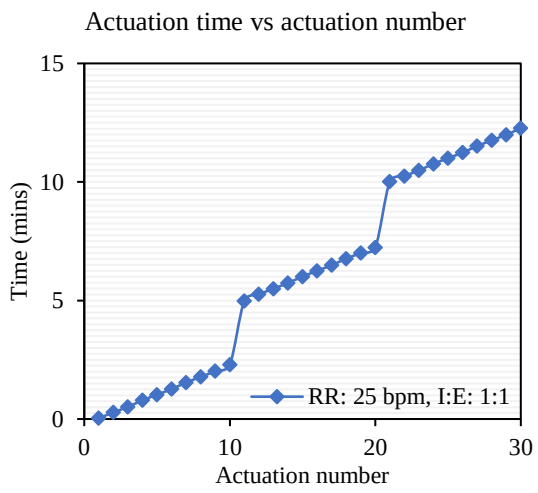

Figure 46: Actuation time vs actuation number at 25 bpm & I:E 1:1

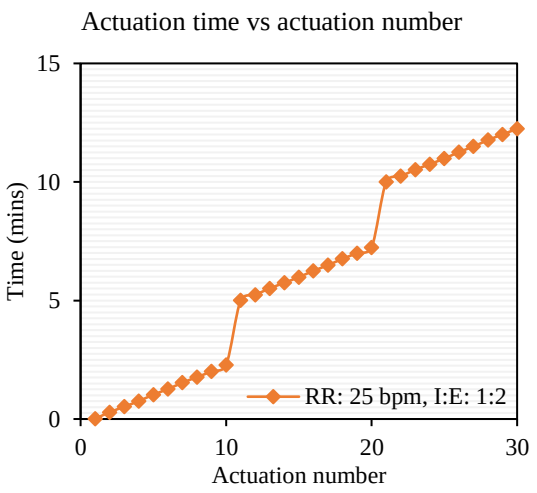

Figure 47: Actuation time vs actuation number at 25 bpm & I:E 1:2

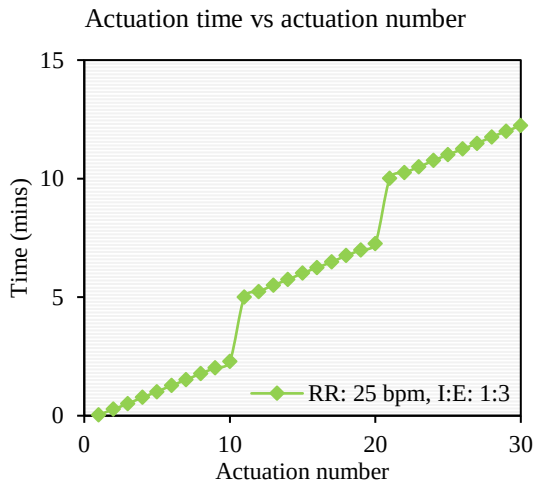

Figure 48: Actuation time vs actuation number at 25 bpm & I:E 1:3

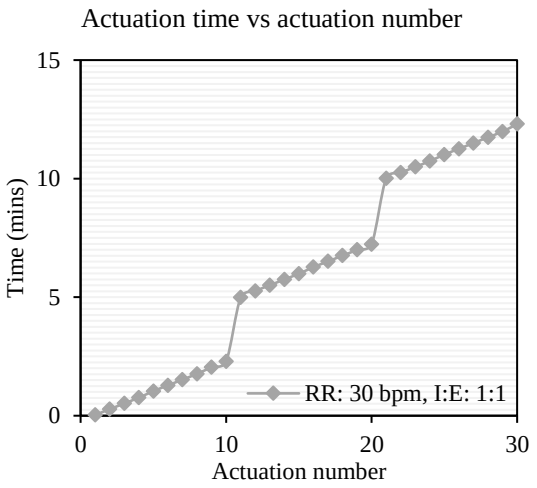

Figure 49: Actuation time vs actuation number at 30 bpm & I:E 1:1

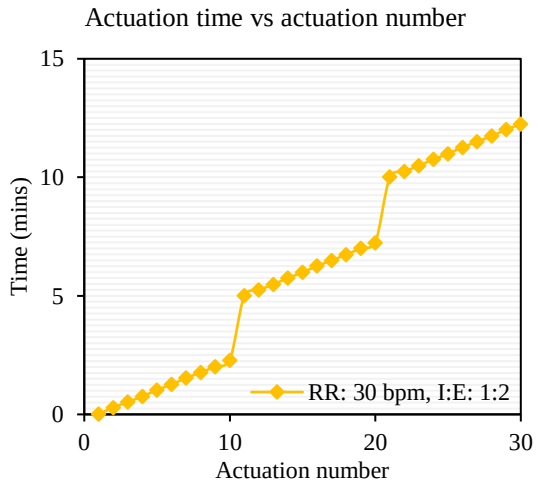

Figure 50: Actuation time vs actuation number at 30 bpm & I:E 1:2

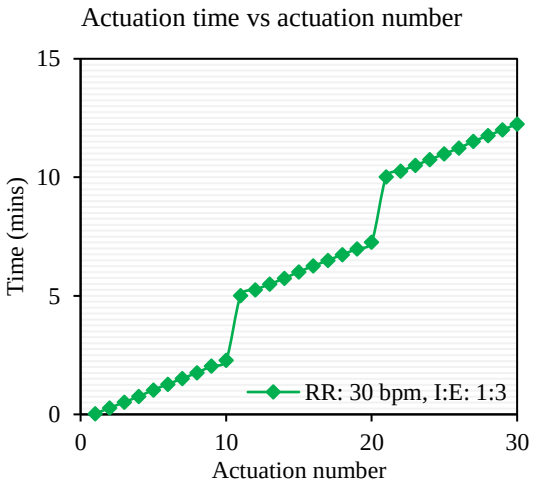

Figure 51: Actuation time vs actuation number at 30 bpm & I:E 1:3

The findings demonstrate that the device effectively actuates 10 times per 5 minutes for all test conditions when the user input settings of 10 actuations every 5 minutes are used.

Figure 52 illustrates the time interval between the actuations in each set.

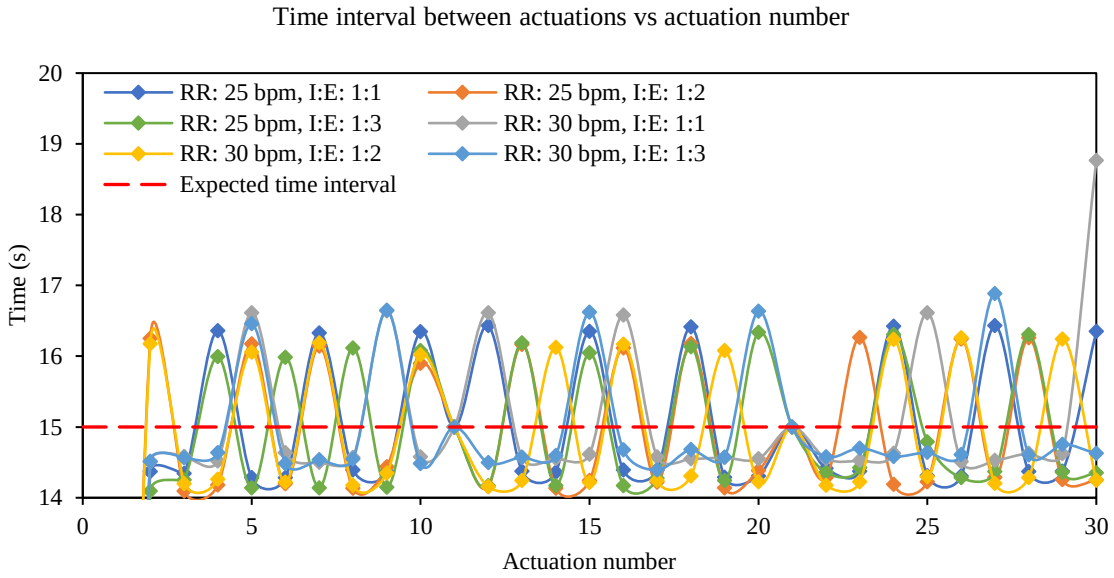

Figure 52: Time interval between the actuations in each set

Figure 52 shows that the interval fluctuates at approximately ±1 s around the expected 15 s.

Figure 53 illustrates the average time interval between the actuations and the time difference from 15 s for each test.

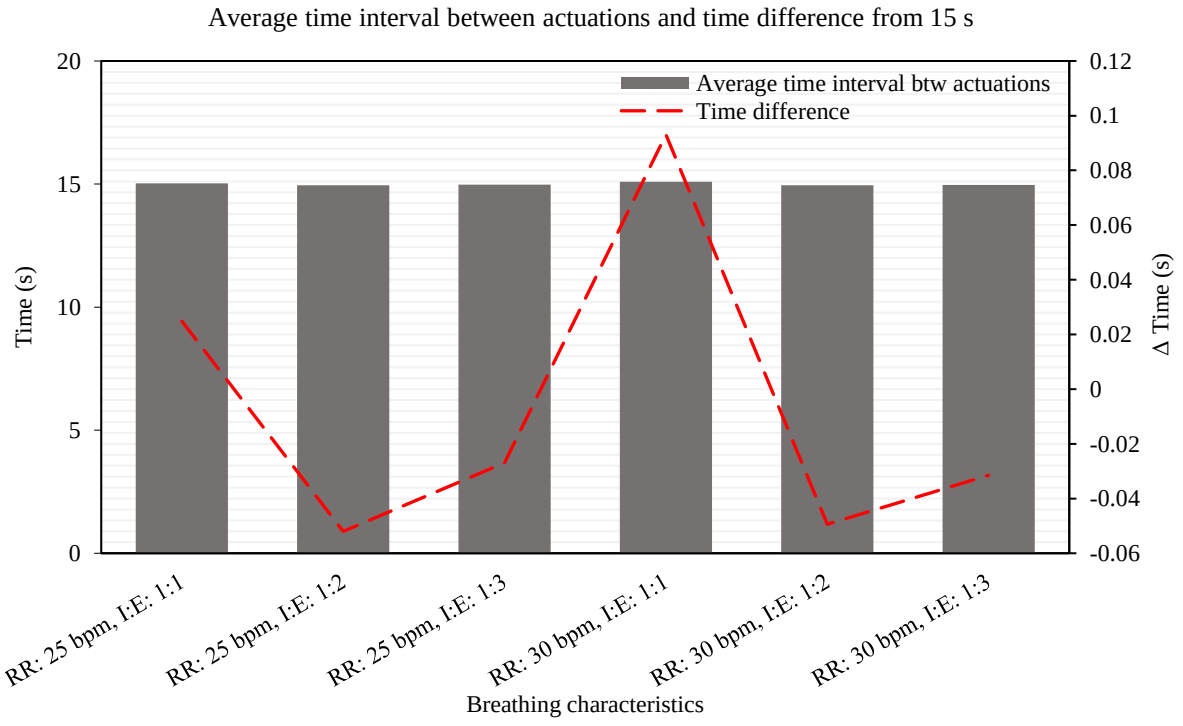

Figure 53: Average time interval btw actuations and time difference from 15 s vs breathing characteristics

Figure 53 shows the average is approximately equal to 15 s and that the time differences from 15 s are within an acceptable range, allowing sufficient time for the medication from the previous actuation to take effect. Thus, this test is positive, showing that the device works as intended by validating the number of actuations and the interval between the actuations with the user input settings, and the interval between each actuation in a set is ≈15 s.

6.5 Synchrony of the Actuation with Inhalation Between Manual and Automated Operation

This test is conducted to compare the effectiveness of the automated solution vs the current manual solution in terms of the delay of the actuation with respect to when inhalation is detected. The automated and manual tests were conducted concurrently. For the manual test, a stopwatch was used. When the first inhalation was indicated, the timer was started, and the canister was actuated. After every 15 s, the canister was again actuated. This was repeated until a total of 10 actuations were delivered for each test condition.

Figure 54 shows the results of the time delay between the actuation and inhalation for the automated and manual tests for 10 actuations.

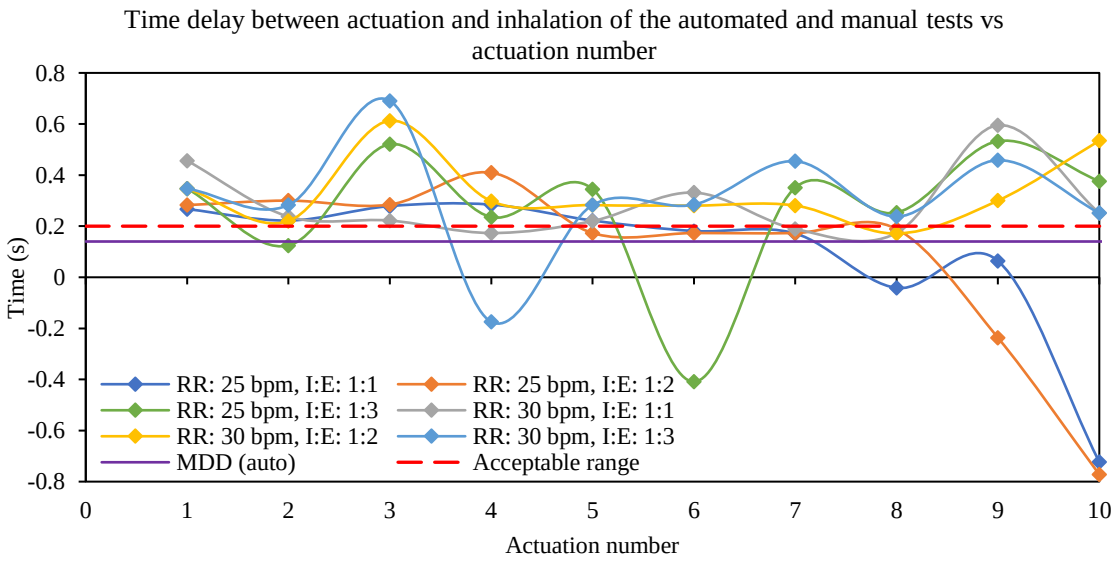

Figure 54: Time delay between actuation and inhalation of the automated and manual tests vs actuation number

The results show that the time difference between the actuation and the onset of inhalation in all the automated tests is again 0.14 s, as obtained in section 6.3 Time Difference between Actuation and Inhalation, which is within the range for the optimum effectiveness of the bronchodilator medication. The results for the manual test are varying and are mostly out of the acceptable range. This is mainly due to reaction time. Thus, this test is positive, showing that the automated solution is more effective by validating that the delay between the actuation and the inhalation signal in the automated test is less than in the manual test.

CHAPTER 7: CONCLUSIONS AND RECOMMENDATIONS

This chapter concludes the design of the device and the outcomes, and recommendations are made based on the outcomes.

7.1 CONCLUSIONS

This study aimed to design and develop an automated MDI delivery system with breath detection that can improve the synchrony of the actuation with inhalation during bronchodilator therapy by detecting inhalation and subsequently actuating an MDI canister to improve the effectiveness of the MDI delivery. The aim has been met by satisfying the objectives set for the study's successes.

The specifications of the device meet all the design requirements. According to the device's technical specifications, the actuation mechanism can actuate up to 10 times with 15 s intervals between each actuation, and the interval between each set of actuations can range from 1 to 10 hours. The breath detection system can also detect pressures ranging from 3 to 20 cmH2O and flow rates of up to 60 L/min. The device can also run for 4 hours on battery power and charges in 2.45 hours. The device is currently set up to work with CPAP therapy. The sensors used in the breath detection system have higher specifications than what is required for CPAP therapy. This is advantageous because it allows for future device modifications to make it compatible with other ventilator modes.

The design of the device is ergonomic and holds all the components securely and safely. However, there are some drawbacks to the design such as the device's size, which can create a hurdle for its placement and the enclosure is not impact resistant, making the device prone to mechanical failure if the device falls.

The door mechanism design is simple, allowing for easily reloading the canister and the device has features to prevent compromised therapy, such as the door lock and the alarm. Another downside of the device’s system is that the device can only be used with canisters that do not require shaking before actuation, which will require additional procurement logistics to obtain the canisters that do not require shaking before each actuation. One possible solution to this problem is incorporating a shaking mechanism, such as a vibrating module. This solution was investigated and determined to be unfeasible due to the negative effects of the vibration on the device and more importantly, to the patients' comfort.

Also, the MDI holder, the inlet and the outlet connection were not printed with a biocompatible material, as it was only for lab testing purposes. However, these components are in direct contact with the air along the air pathway and thus, in real-life applications, the material must be strictly biocompatible and adhere to the relevant standards. The pulse oximeter add-on feature has also been added, it can be connected to the device via a USB type A port and the readings can then be viewed on the device’s display.

The two most important parts of this study were the actuation mechanism and the breath detection system, which are the two main subsystems that can together ensure the intended use of the device in terms of detecting inhalation and actuating the canister only. The actuation mechanism of the device effectively

actuates the MDI canister. The servo selected is a 13 kg.cm metal gear servo, which provides the high torque needed to actuate the canister. However, the gear mechanism causes a considerable noise level during an actuation, which can be considered intrusive by some patients or can disturb other patients.

The breath detection system accurately detects inhalation with an average lead of 0.11 s between the device and the peak of inhalation, allowing enough time for the actuation, and ensuring the medication is delivered within the desired range after the onset of inhalation. The device works as intended, whereby the number of actuations and the interval between the actuations corresponds with the user input settings, and the interval between each actuation is ≈ 15 s. The research question was answered by comparing the automated solution to the existing manual solution. The manual solution was conducted by manually actuating the canister and recording the timing. The validation results showed that the automated solution is more effective than the existing manual solution, as the delay between the actuation and the inhalation signal in the automated test is 0.14 s, which is less than in the manual test. The delay in the manual operation is mostly out of the acceptable range compared to the automated solution which is within the acceptable range of 0 to 0.2 s.

Therefore, it can be concluded that the device enables an effective treatment with respect to the actuation and inhalation synchrony as the device accurately actuates the canister when inhalation is detected with a time difference of 0.14 s between the actuation and the onset of inhalation, which is within the range for the optimum effectiveness of the bronchodilator medication. It was also found that the delay of 0.14 s between the actuation and the inhalation is primarily due to the time taken for the servo to move from its rest position to the actuation position. This factor is dependent on the operating speed of the servo, which is the degree moved per second.

Hence, the developed device meets the aim of this study as it is more effective than the existing manual solution, which will benefit the patients and nurses, by providing an automated and improved solution to deliver bronchodilator therapy, thus, increasing the effectiveness of the medication delivery, which will overall benefit the healthcare system.

7.2 RECOMMENDATIONS

The developed device met the aim and objectives of the study, however, there were some drawbacks to the design, which can be improved and there is scope for future work on the validation results to further validate the effectiveness of the solution.

7.2.1 Device Design

The design of the enclosure can be revised to make the device smaller in size, making it easier to be placed in the ward setting and the material of the enclosure must be changed to an impact-resistant material such as polycarbonate.

The current actuation mechanism used in the device takes up much space as it is situated on top of the canister. The mechanism can be placed on the side of the canister and use force transfer to actuate the canister, or a smaller high-torque servo can be used. The noise caused by the actuation can be mitigated by lining the inside of the device with soundproofing material.

The delay between the actuation and the inhalation can be improved by using a servo with a lower operating speed. If necessary, a servo with a low operating speed enables the nurse to adjust the delay between actuation and inhalation within the 0.2 s range if necessary. A battery level indicator must be added to the device for home users to monitor the battery level.

The device's functionality can be modified to make it compatible with other ventilator modes. The pressure sensor used, NXP MPX5010DP, can read pressures of up to 100 cmH2O and the flowmeter, Sensirion SFM3000-200C, can read flows of up to 200 L/min. Using these sensors in the device makes this modification very simple to implement, as it will only require a coding change and no additional hardware or dismantling of the device. The software is easily updated via the USB type B port connected to the microcontroller.

7.2.2 Device Validation

The validation results can be improved by adding additional test conditions to increase the accuracy of the test results. The current tests are limited to 25 bpm and 30 bpm due to the technical limitations of the breathing simulator used.

A commercially available off-the-shelf breathing simulator can be used to increase the range of breathing rates for the validation tests. The data will allow for a better understanding of the timing at high breathing rates and improve the test results' accuracy.

The validation results can also be further validated by using nurses to assess the solution's effectiveness and add value to the overall solution.

REFERENCES

Agache, I., & Akdis, C. A. (2016). Endotypes of allergic diseases and asthma: An important step in building blocks for the future of precision medicine. *Allergology International*, *65*(3), 243-252. https://doi.org/10.1016/j.alit.2016.04.011

Ahmed, S. M., & Athar, M. (2015). Mechanical ventilation in patients with chronic obstructive pulmonary disease and bronchial asthma. Indian Journal of Anaesthesia, 59(9), 589. https://doi.org/10.4103/0019-5049.165856

Al-Halhouli, A., Al-Ghussain, L., Khallouf, O., Rabadi, A., Alawadi, J., Liu, H., Al Oweidat, K., Chen, F., & Zheng, D. (2021). Clinical evaluation of respiratory rate measurements on COPD (male) patients using wearable inkjet-printed sensor. Sensors, 21(2), 468. https://doi.org/10.3390/s21020468

Ari, A. (2015). Aerosol therapy in pulmonary critical care. Respiratory Care, 60(6), 858–879. https://doi.org/10.4187/respcare.03790

Avdeev, S., Moiseev, S., Brovko, M., Yavorovskiy, A., Umbetova, K., & Akulkina, L. et al. (2020). Low prevalence of bronchial asthma and chronic obstructive lung disease among intensive care unit patients with COVID-19. Allergy, 75(10), 2703-2704. https://doi.org/10.1111/all.14420

Biccard, B., Gopalan, P., Miller, M., Michell, W., Thomson, D., & Ademuyiwa, A. et al. (2021). Patient care and clinical outcomes for patients with COVID-19 infection admitted to African high-care or intensive care units (ACCCOS): a multicentre, prospective, observational cohort study. The Lancet, 397(10288), 1885-1894. https://doi.org/10.1016/s0140-6736(21)00441-4

Biswas, R., Hanania, N., & Sabharwal, A. (2017). Factors Determining In Vitro Lung Deposition of Albuterol Aerosol Delivered by Ventolin Metered-Dose Inhaler. *Journal Of Aerosol Medicine And Pulmonary Drug Delivery*, *30*(4), 256-266. https://doi.org/10.1089/jamp.2015.1278

Broeders, M. E. A. C., Molema, J., Hop, W. C. J., & Folgering, H. T. M. (2003). Inhalation profiles in asthmatics and COPD patients: Reproducibility and effect of instruction. Journal of Aerosol Medicine, 16(2), 131–141. https://doi.org/10.1089/089426803321919898

Broeders, M. E. A. C., Vincken, W., & Corbetta, L. (2011). The admit series — issues in inhalation therapy. 7) ways to improve pharmacological management of COPD: The Importance of Inhaler Choice and inhalation technique. Primary Care Respiratory Journal, 20(3), 338–343. https://doi.org/10.4104/pcrj.2011.00062

Brusasco, C., Corradi, F., Ferrari, A., Ball, L., Kacmarek, R. M., & Pelosi, P. (2015). CPAP devices for emergency prehospital use: A bench study. Respiratory Care, 60(12), 1777–1785. https://doi.org/10.4187/respcare.04134

Capstick, T. G. D., & Clifton, I. J. (2012). Inhaler technique and training in people with chronic obstructive pulmonary disease and asthma. Expert Review of Respiratory Medicine, 6(1), 91–103. https://doi.org/10.1586/ers.11.89

Cardin, D. (2021, May). Albuterol dosage, forms, and strengths - singlecare.com. Retrieved November 24, 2022, from https://www.singlecare.com/prescription/albuterol-sulfate/dosage

Chan, J., Yuan, S., Kok, K., To, K., Chu, H., & Yang, J. et al. (2020). A familial cluster of pneumonia associated with the 2019 novel coronavirus indicating person-to-person transmission: a study of a family cluster. The Lancet, 395(10223), 514-523. https://doi.org/10.1016/s0140-6736(20)30154-9

Chen, Z., Hu, Z., & Dai, H. (2012). Control system design for a continuous positive airway pressure ventilator. *BioMedical Engineering OnLine*, *11*(1), 5. https://doi.org/10.1186/1475-925x-11-5

Chhiba, K., Patel, G., Vu, T., Chen, M., Guo, A., & Kudlaty, E. et al. (2020). Prevalence and characterization of asthma in hospitalized and nonhospitalized patients with COVID-19. Journal Of Allergy And Clinical Immunology, 146(2), 307-314.e4. https://doi.org/10.1016/j.jaci.2020.06.010

Choi, Y., Park, J., Lee, H., Suh, J., Song, J., & Byun, M. et al. (2020). Effect of asthma and asthma medication on the prognosis of patients with COVID-19. European Respiratory Journal, 57(3), 2002226. https://doi.org/10.1183/13993003.02226-2020

Cho-Reyes, S., Celli, B. R., Dembek, C., Yeh, K., & Navaie, M. (2019). Inhalation technique errors with metered-dose inhalers among patients with obstructive lung diseases: A systematic review and meta-analysis of U.S. studies. Chronic Obstructive Pulmonary Diseases: Journal of the COPD Foundation, 6(3), 267–280. https://doi.org/10.15326/jcopdf.6.3.2018.0168

Coronavirus and pneumonia. (2020, March 30). WebMD. https://www.webmd.com/lung/covid-and-pneumonia#1

De Tratto, K., Gomez, C., Ryan, C. J., Bracken, N., Steffen, A., & Corbridge, S. J. (2014, May). Nurses' Knowledge of Inhaler Technique in the Inpatient Hospital Setting. *Clinical Nurse Specialist, 28*(3), 156–160. https://doi.org/10.1097/nur.0000000000000047

De Wilde, A. H., Snijder, E. J., Kikkert, M., & Van Hemert, M. J. (2017). Host factors in coronavirus replication. *Roles of Host Gene and Non-coding RNA Expression in Virus Infection*, 1-42. https://doi.org/10.1007/82_2017_25

Demoule, A., Brochard, L., Dres, M., Heunks, L., Jubran, A., Laghi, F., Mekontso-Dessap, A., Nava, S., Ouanes-Besbes, L., Peñuelas, O., Piquilloud, L., Vassilakopoulos, T., & Mancebo, J. (2020). How to ventilate obstructive and asthmatic patients. Intensive Care Medicine, 46(12), 2436–2449. https://doi.org/10.1007/s00134-020-06291-0

Dhand, R. (2017). How should aerosols be delivered during invasive mechanical ventilation? Respiratory Care, 62(10), 1343–1367. https://doi.org/10.4187/respcare.05803

Dhand, R., & Tobin, M. (1997). Inhaled Bronchodilator Therapy in Mechanically Ventilated Patients. American Journal Of Respiratory And Critical Care Medicine, 156(1), 3-10. https://doi.org/10.1164/ajrccm.156.1.9610025

Dhand, R., Jubran, A., & Tobin, M. J. (1995). Bronchodilator delivery by metered-dose inhaler in ventilator-supported patients. American Journal of Respiratory and Critical Care Medicine, 151(6), 1827–1833. https://doi.org/10.1164/ajrccm.151.6.7767526

Dhar Chowdhury, S., & Oommen, A. M. (2020). Epidemiology of covid-19. Journal of Digestive Endoscopy, 11(01), 03–07. https://doi.org/10.1055/s-0040-1712187

Dhont, S., Derom, E., Van Braeckel, E., Depuydt, P., & Lambrecht, B. N. (2020). The pathophysiology of 'happy' hypoxemia in COVID-19. *Respiratory Research, 21*(1). https://doi.org/10.1186/s12931-020-01462-5

Docherty, A., Harrison, E., Green, C., Hardwick, H., Pius, R., & Norman, L. et al. (2020). Features of 16,749 hospitalised UK patients with COVID-19 using the ISARIC WHO Clinical Characterisation Protocol. https://doi.org/10.1101/2020.04.23.20076042

Ediboglu, O. (2021). Mechanical ventilation for patients with COPD. Chronic Obstructive Pulmonary Disease - A Current Conspectus. https://doi.org/10.5772/intechopen.96633

Ehrmann, S., Roche-Campo, F., Sferrazza Papa, G., Isabey, D., Brochard, L., & Apiou-Sbirlea, G. (2013). Aerosol therapy during mechanical ventilation: an international survey. Intensive Care Medicine, 39(6), 1048-1056. https://doi.org/10.1007/s00134-013-2872-5

Eldridge, L. (2022). Normal respiratory rate for adults and children. Verywell Health. Retrieved October 20, 2022, from https://www.verywellhealth.com/what-is-a-normal-respiratory-rate-2248932

Fekete, M., Szarvas, Z., Fazekas-Pongor, V., Feher, A., Dosa, N., Lehoczki, A., Tarantini, S., & Varga, J. T. (2022). COVID-19 infection in patients with chronic obstructive pulmonary disease: From pathophysiology to therapy. mini-review. *Physiology International*, *109*(1), 9-19. https://doi.org/10.1556/2060.2022.00172

Fernández Tena, A., & Casan Clarà, P. (2012). Deposition of inhaled particles in the lungs. Archivos De Bronconeumología (English Edition), 48(7), 240–246. https://doi.org/10.1016/j.arbr.2012.02.006

Galanis, P., Vraka, I., Fragkou, D., Bilali, A., & Kaitelidou, D. (2021, March 25). Nurses' burnout and associated risk factors during the COVID-19 pandemic: A systematic review and meta-analysis. *Journal of Advanced Nursing*. https://doi.org/10.1111/jan.14839

Galiatsatos, P. (2022, February 28). *COVID-19 lung damage*. Johns Hopkins Medicine, based in Baltimore, Maryland. https://www.hopkinsmedicine.org/health/conditions-and-diseases/coronavirus/what-coronavirus-does-to-the-lungs#:~:text=If%20COVID%2D19%20pneumonia%20progresses,a%20form%20of%20lung%20failure

Gattinoni, L., Chiumello, D., Caironi, P., Busana, M., Romitti, F., Brazzi, L., & Camporota, L. (2020). COVID-19 pneumonia: Different respiratory treatments for different phenotypes? *Intensive Care Medicine*, *46*(6), 1099-1102. https://doi.org/10.1007/s00134-020-06033-2

Georgopoulos, D., Mouloudi, E., Kondili, E., & Klimathianaki, M. (2000). Bronchodilator delivery with metered-dose inhaler during mechanical ventilation. Critical Care, 4(4), 227. https://doi.org/10.1186/cc698

Gerayeli, F., Milne, S., Cheung, C., Li, X., Yang, C., & Tam, A. et al. (2021). COPD and the risk of poor outcomes in COVID-19: A systematic review and meta-analysis. Eclinicalmedicine, 33, 100789. https://doi.org/10.1016/j.eclinm.2021.100789

Ghassemi, A. E. (2021, October 25). Burnout in nurses during the COVID-19 pandemic: the rising need for development of evidence-based risk assessment and supportive interventions. *Evidence Based Nursing*, *25*(3), 94–94. https://doi.org/10.1136/ebnurs-2021-103438

GINA. (2016). (rep.). Pocket Guide For Asthma Management And Prevention. Retrieved September 15, 2022, from https://ginasthma.org/wp-content/uploads/2016/05/WMS-GINA-2016-main-Pocket-Guide.pdf.

Glover, G., & Fletcher, S. J. (2009). Assessing the performance of the Whisperflow® continuous positive airway pressure generator: a bench study. British Journal of Anaesthesia, 102(6), 875–881. https://doi.org/10.1093/bja/aep077

Grandbastien, M., Piotin, A., Godet, J., Abessolo-Amougou, I., Ederlé, C., & Enache, I. et al. (2020). SARS-CoV-2 Pneumonia in Hospitalized Asthmatic Patients Did Not Induce Severe Exacerbation. The Journal Of Allergy And Clinical Immunology: In Practice, 8(8), 2600-2607. https://doi.org/10.1016/j.jaip.2020.06.032

Hansen, E., Moeller, A., Backer, V., Andersen, M., Kober, L., Kragholm, K., & Torp-Pedersen, C. (2020). Severe outcomes of COVID-19 among patients with COPD and asthma. ERJ Open Research, 7(1), 00594-2020. https://doi.org/10.1183/23120541.00594-2020

Helmy, Y., Fawzy, M., Elaswad, A., Sobieh, A., Kenney, S., & Shehata, A. (2020). The COVID-19 Pandemic: A Comprehensive Review of Taxonomy, Genetics, Epidemiology, Diagnosis, Treatment, and Control. Journal Of Clinical Medicine, 9(4), 1225. https://doi.org/10.3390/jcm9041225

How Lungs Work. Lung.org. (2022). Retrieved 21 September 2022, from https://www.lung.org/lung-health-diseases/how-lungs-work.

Huang, C., Wang, Y., Li, X., Ren, L., Zhao, J., Hu, Y., Zhang, L., Fan, G., Xu, J., Gu, X., Cheng, Z., Yu, T., Xia, J., Wei, Y., Wu, W., Xie, X., Yin, W., Li, H., Liu, M., … Cao, B. (2020). Clinical features of patients infected with 2019 novel coronavirus in Wuhan, China. The Lancet, 395(10223), 497–506. https://doi.org/10.1016/s0140-6736(20)30183-5

Hypoxemia. (2022, June 15). Cleveland Clinic. https://my.clevelandclinic.org/health/diseases/17727-hypoxemia

Jamebozorgi, M. H., Karamoozian, A., Bardsiri, T. I., & Sheikhbardsiri, H. (2022, January 14). Nurses Burnout, Resilience, and Its Association With Socio-Demographic Factors During COVID-19 Pandemic. *Frontiers in Psychiatry*, *12*. https://doi.org/10.3389/fpsyt.2021.803506

Johnson, B. R., Franks, A. S., Bullock, L. N., Dennis, D. L., Heidel, R. E., & Self, T. H. (2022, June 10). Pharmacist-led inhaler training for nurses on an acute care pulmonary unit. *JACCP: JOURNAL OF THE AMERICAN COLLEGE OF CLINICAL PHARMACY*, *5*(7), 660–667. https://doi.org/10.1002/jac5.1656

Karle, S., Lorenz, M., Maslonkowski, E., & Matsick, A. (2007). Automated, in-home delivery of inhaled drugs through portable continuous positive airway pressure (CPAP) system. Retrieved 22 February 2022, from https://bmedesign.engr.wisc.edu/projects/f07/cpap/file/view/cbd3035e-26b9-4c35-8dcb-7b8ed8a1d1b9/BME_400_final_paper.pdf.

Łagiewka, W. (2021). Finger pulse oximeter MAX30102. Thingiverse. Retrieved September 1, 2022, from https://www.thingiverse.com/thing:4847827/files

Leach, C. L., Davidson, P. J., Hasselquist, B. E., & Boudreau, R. J. (2005). Influence of particle size and patient dosing technique on lung deposition of HFA-Beclomethasone from a metered dose inhaler. *Journal of Aerosol Medicine*, *18*(4), 379–385. https://doi.org/10.1089/jam.2005.18.379

Lebret, M., Fresnel, E., Prieur, G., Quieffin, J., Dupuis, J., Lamia, B., Combret, Y., & Medrinal, C. (2021). High O2 flow rates required to achieve acceptable FIO2 in CPAP-Treated patients with Severe COVID-19: a clinically based bench study. Archivos De Bronconeumología, 57(9), 607–610. https://doi.org/10.1016/j.arbres.2021.04.018

Lee, H., & Choi, S. (2022, September 9). Factors Affecting Fatigue among Nurses during the COVID-19 Pandemic. *International Journal of Environmental Research and Public Health*, *19*(18), 11380. https://doi.org/10.3390/ijerph191811380

Lee, S., Son, K., Han, C., Park, S., & Jung, J. (2021). Impact of COPD on COVID-19 prognosis: A nationwide population-based study in South Korea. Scientific Reports, 11(1). https://doi.org/10.1038/s41598-021-83226-9

Leung, J. M., Yang, C. X., Tam, A., Shaipanich, T., Hackett, T., Singhera, G. K., Dorscheid, D. R., & Sin, D. D. (2020). ACE-2 expression in the small airway epithelia of smokers and COPD patients: Implications for COVID-19. *European Respiratory Journal*, *55*(5), 2000688. https://doi.org/10.1183/13993003.00688-2020

Liu, S., Zhi, Y., & Ying, S. (2020). COVID-19 and asthma: Reflection during the pandemic. *Clinical Reviews in Allergy & Immunology*, *59*(1), 78-88. https://doi.org/10.1007/s12016-020-08797-3

Lopes, A. J., Nery, F. P., Sousa, F. C., Guimaraes, F. S., Dias, C. M., Oliveira, J. F., & Menezes, S. L. (2011). CPAP decreases lung hyperinflation in patients with stable COPD. Respiratory Care, 56(8), 1164–1169. https://doi.org/10.4187/respcare.01092

Lu, R., Zhao, X., Li, J., Niu, P., Yang, B., & Wu, H. et al. (2020). Genomic characterisation and epidemiology of 2019 novel coronavirus: implications for virus origins and receptor binding. The Lancet, 395(10224), 565-574. https://doi.org/10.1016/s0140-6736(20)30251-8

Lung Volumes. (2016). Pathway Medicine. Retrieved September 27, 2022, from https://www.pathwaymedicine.org/lung-volumes

Maccari, J. G., Teixeira, C., Gazzana, M. B., Savi, A., Dexheimer-Neto, F. L., & Knorst, M. M. (2015). Inhalation therapy in mechanical ventilation. Jornal Brasileiro De Pneumologia, 41(5), 467–472. https://doi.org/10.1590/s1806-37132015000000035

Marianne Belleza, R. (2022). Respiratory System Anatomy and Physiology. Nurseslabs. Retrieved 25 September 2022, from https://nurseslabs.com/respiratory-system/#functions_of_the_respiratory_system.

Martinsen, P. (2016, August 13). *Exponential filter*. MegunoLink. https://www.megunolink.com/documentation/arduino-libraries/exponential-filter/#

Masip, J., & Mas, A. (2014). Noninvasive ventilation in acute respiratory failure. International Journal of Chronic Obstructive Pulmonary Disease, 837. https://doi.org/10.2147/copd.s42664

Mason, R. J. (2020). Pathogenesis of COVID-19 from a cell biology perspective. *European Respiratory Journal*, *55*(4), 2000607. https://doi.org/10.1183/13993003.00607-2020

Matsumoto, K., & Saito, H. (2020). Does asthma affect morbidity or severity of COVID-19?. Journal Of Allergy And Clinical Immunology, 146(1), 55-57. https://doi.org/10.1016/j.jaci.2020.05.017

Maxrefdes117#: Heart-rate and pulse-oximetry monitor. Maximintegrated. (2016). Retrieved October 10, 2022, from https://www.maximintegrated.com/en/design/reference-design-center/system-board/6300.html

Morais-Almeida, M., Pité, H., Aguiar, R., Ansotegui, I., & Bousquet, J. (2020). Asthma and the coronavirus disease 2019 pandemic: A literature review. *International Archives of Allergy and Immunology*, *181*(9), 680-688. https://doi.org/10.1159/000509057

Mouloudi, E., Prinianakis, G., Kondili, E., & Georgopoulos, D. (2000). Bronchodilator delivery by metered-dose inhaler in mechanically ventilated COPD patients: influence of flow pattern. European Respiratory Journal, 16(2), 263. https://doi.org/10.1034/j.1399-3003.2000.16b13.x

Mowery, N. T. (2017). Ventilator strategies for chronic obstructive pulmonary disease and acute respiratory distress syndrome. Surgical Clinics of North America, 97(6), 1381–1397. https://doi.org/10.1016/j.suc.2017.07.006

Naidoo, R., & Naidoo, K. (2021). Prioritising 'already-scarce' intensive care unit resources in the midst of COVID-19: a call for regional triage committees in South Africa. BMC Medical Ethics, 22(1). https://doi.org/10.1186/s12910-021-00596-5

Pandirajan, K. (2022). Mechanics of Breathing. teachmephysiology. Retrieved 21 September 2022, from https://teachmephysiology.com/respiratory-system/ventilation/mechanics-of-breathing/.

Papiris, S., Kotanidou, A., Malagari, K., & Roussos, C. (2002). Clinical review: Severe asthma. Critical Care, 6(1), 30. https://doi.org/10.1186/cc1451

Paraskevis, D., Kostaki, E. G., Magiorkinis, G., Panayiotakopoulos, G., & Tsiodras, S. (2020). Full-genome evolutionary analysis of the novel Corona virus (2019-ncov) rejects the hypothesis of emergence as a result of a recent recombination event. https://doi.org/10.1101/2020.01.26.920249

Patone, M., Thomas, K., Hatch, R., Tan, P., Coupland, C., & Liao, W. et al. (2021). Mortality and critical care unit admission associated with the SARS-CoV-2 lineage B.1.1.7 in England: an observational cohort study. The Lancet Infectious Diseases, 21(11), 1518-1528. https://doi.org/10.1016/s1473-3099(21)00318-2

Pérez-Malagón, C. D., Barrera-Rodríguez, R., Casillas, N. G. M., Casillas-Muñoz, J. P., Silva-Sánchez, G., & Macías-Limón, C. (2021, February 28). Competence in Metered-Dose Inhaler Technique among Healthcare Workers of Three General Hospitals in Mexico: It is Not Good after All These Years. *Advances in Respiratory Medicine*, *89*(1), 8–14. https://doi.org/10.5603/arm.a2021.0027

Phipps, P., & Garrard, C. S. (2003). The pulmonary physician in critical care * 12: Acute severe asthma in the intensive care unit. Thorax, 58(1), 81–88. https://doi.org/10.1136/thorax.58.1.81

Rajbanshi, L., & KC, S. (2017, February 20). Nurses' competency on use of metered dose inhaler. *Journal of Chitwan Medical College*, *6*(2), 33–37. https://doi.org/10.3126/jcmc.v6i2.16686

Samudrala, P. K., Kumar, P., Choudhary, K., Thakur, N., Wadekar, G. S., Dayaramani, R., Agrawal, M., & Alexander, A. (2020). Virology, pathogenesis, diagnosis and in-line treatment of COVID-19. *European Journal of Pharmacology*, *883*, 173375. https://doi.org/10.1016/j.ejphar.2020.173375

Shaker, M. S., Oppenheimer, J., Grayson, M., Stukus, D., Hartog, N., Hsieh, E. W. Y., Rider, N., Dutmer, C. M., Vander Leek, T. K., Kim, H., Chan, E. S., Mack, D., Ellis, A. K., Lang, D., Lieberman, J., Fleischer, D., Golden, D. B. K., Wallace, D., Portnoy, J., … Greenhawt, M. (2020). Covid-19: Pandemic contingency planning for the allergy and immunology clinic. The Journal of Allergy and Clinical Immunology: In Practice, 8(5). https://doi.org/10.1016/j.jaip.2020.03.012

Sheleme, T., Bekele, F., & Ayela, T. (2020). Clinical presentation of patients infected with coronavirus disease 19: A systematic review. *Infectious Diseases: Research and Treatment*, *13*, 117863372095207. https://doi.org/10.1177/1178633720952076

Simons, S. O., Hurst, J. R., Miravitlles, M., Franssen, F. M., Janssen, D. J., Papi, A., Duiverman, M. L., & Kerstjens, H. A. (2020). Caring for patients with COPD and COVID-19: A viewpoint to spark discussion. *Thorax*, *75*(12), 1035-1039. https://doi.org/10.1136/thoraxjnl-2020-215095

Skevaki, C., Karsonova, A., Karaulov, A., Xie, M., & Renz, H. (2020). Asthma-associated risk for COVID-19 development. *Journal of Allergy and Clinical Immunology*, *146*(6), 1295–1301. https://doi.org/10.1016/j.jaci.2020.09.017

Spandorfer, M. & iDTx Systems, Inc. (2008). Drug delivery and monitoring system for a ventilator (US20080308101A1). U.S. Patent and Trademark Office. https://patentimages.storage.googleapis.com/57/a1/09/b26a8917769e9c/US20080308101A1.pdf

Spandorfer, M., Gilbert, M. P., & iDTX Systems, Inc. (2015). Compact self-contained automated MDI adapters or units for ventilators (US 9216267B2). U.S. Patent and Trademark Office. https://patentimages.storage.googleapis.com/88/f5/d6/34c656259fb1b5/US9216267.pdf

Spandorfer, M., Niese, B. A., Arnett, J. D., Butters, J. A., Johnson, L. M., & iDTx Systems, Inc. (2019). Automated drug delivery systems (US10173025B2). U.S. Patent and Trademark Office. https://patentimages.storage.googleapis.com/28/24/b3/ed1b3312092a41/US10173025.pdf

Stasi, C., Fallani, S., Voller, F., & Silvestri, C. (2020). Treatment for COVID-19: An overview. European Journal of Pharmacology, 889, 173644. https://doi.org/10.1016/j.ejphar.2020.173644

Swami, V., Cho, J. G., Smith, T., Wheatley, J., & Roberts, M. (2021, January 1). Confidence of nurses with inhaler device education and competency of device use in a specialised respiratory inpatient unit. *Chronic Respiratory Disease*, *18*, 147997312110022. https://doi.org/10.1177/14799731211002241

Tabassum, T., Rahman, A., Araf, Y., Ullah, M. A., & Hosen, M. J. (2022). Management of asthma patients during the COVID-19 pandemic: Pathophysiological considerations to address the challenges. *Beni-Suef University Journal of Basic and Applied Sciences*, *11*(1). https://doi.org/10.1186/s43088-022-00204-4

Talaat, M., Si, X., & Xi, J. (2022). Effect of MDI Actuation Timing on Inhalation Dosimetry in a Human Respiratory Tract Model. *Pharmaceuticals*, *15*(1), 61. https://doi.org/10.3390/ph15010061

Villamañán, E., Sobrino, C., Carpio, C., Moreno, M., Arancón, A., & Lara, C. et al. (2021). Inhaled bronchodilators use and clinical course of adult inpatients with Covid-19 pneumonia in Spain: A retrospective cohort study. Pulmonary Pharmacology & Therapeutics, 69, 102007. https://doi.org/10.1016/j.pupt.2021.102007

Villarreal, M. R. (2007). Respiratory system complete. Respiratory system. Wikipedia. Retrieved September 27, 2022, from https://en.wikipedia.org/wiki/File:Respiratory_system_complete_en.svg.

Vincent, J., & Creteur, J. (2020). Ethical aspects of the COVID-19 crisis: How to deal with an overwhelming shortage of acute beds. European Heart Journal: Acute Cardiovascular Care, 9(3), 248-252. https://doi.org/10.1177/2048872620922788

Volsko, T. A. (2019). Devices used for CPAP delivery. *Respiratory Care*, *64*(6), 723-734. https://doi.org/10.4187/respcare.06625

Wahlster, S., Sharma, M., Lewis, A., Patel, P., Hartog, C., & Jannotta, G. et al. (2021). The Coronavirus Disease 2019 Pandemic's Effect on Critical Care Resources and Health-Care Providers. Chest, 159(2), 619-633. https://doi.org/10.1016/j.chest.2020.09.070

WHO. (2020). Coronavirus disease 2019 (COVID-19) Situation Report. Retrieved September 15, 2022, from https://www.who.int/docs/default-source/coronaviruse/situation-%E2%80%8Ereports/20200304-sitrep-44-covid-19.pdf?sfvrsn=783b4c9d_2%E2%80%8E.

Wisnu Wardana, V. A., & Rosyid, A. N. (2021). Inflammatory mechanism and clinical implication of asthma in COVID-19. *Clinical Medicine Insights: Circulatory, Respiratory and Pulmonary Medicine*, *15*, 117954842110427. https://doi.org/10.1177/11795484211042711

World Health Organization. (2022). COVID-19 Weekly Epidemiological Update Edition 109 published 14 September 2022. World Health Organization. Retrieved September 21, 2022, from https://www.who.int/publications/m/item/weekly-epidemiological-update-on-covid-19---14-september-2022

Wu, F., Zhou, Y., Wang, Z., Xie, M., Shi, Z., Tang, Z., Li, X., Li, X., Lei, C., Li, Y., Ni, Z., Hu, Y., Liu, X., Yin, W., Cheng, L., Ye, F., Peng, J., Huang, L., & Ran, P. (2020). Clinical characteristics of COVID-19 infection in chronic obstructive pulmonary disease: A multicenter, retrospective, observational study. *Journal of Thoracic Disease*, *12*(5), 1811-1823. https://doi.org/10.21037/jtd-20-1914

Zhang, M., Wang, S., & Yang, Y. (2016). Experiment of aerosol-release time for a novel automatic metered dose inhaler. Advances In Mechanical Engineering, 8(5), 168781401664788. https://doi.org/10.1177/1687814016647886

Zhao, Q., Meng, M., Kumar, R., Wu, Y., Huang, J., Lian, N., Deng, Y., & Lin, S. (2020). The impact of COPD and smoking history on the severity of COVID-19: A systemic review and meta-analysis. *Journal of Medical Virology*, *92*(10), 1915-1921. https://doi.org/10.1002/jmv.25889

Zhou, P., Yang, X., Wang, X., Hu, B., Zhang, L., & Zhang, W. et al. (2020). A pneumonia outbreak associated with a new coronavirus of probable bat origin. Nature, 579(7798), 270-273. https://doi.org/10.1038/s41586-020-2012-7

APPENDIX A – Arduino Code

```
// Arduino libraries
#include <MegunoLink.h>               // Exponential filter library
#include <Wire.h>
#include <Filter.h>
#include <Servo.h>
#include <LCDMenuLib2.h>
#include <Arduino.h>
#include <U8g2lib.h>
#include <MAX3010x.h>
#include "filters.h"

// Added libraries
#include <sfm3000wedo.h>
// https://github.com/dwerne/Sensirion_SFM3000_arduino/tree/master

// LCD & MENU_____________________________________________________________________
// https://github.com/Jomelo/LCDMenuLib2

#ifdef U8X8_HAVE_HW_SPI
#include <SPI.h>
#endif
#ifdef U8X8_HAVE_HW_I2C
#include <Wire.h>
#endif

// LCD pins
U8G2_ST7565_EA_DOGM128_F_4W_SW_SPI u8g2(U8G2_R0, /* clock=*/ 33, /* data=*/ 2, /*
cs=*/ 6, /* dc=*/ 4, /* reset=*/ 35);

// settings for u8g lib and LCD
#define _LCDML_DISP_w                 128            // LCD width
#define _LCDML_DISP_h                 64             // LCD height
// font settings
#define _LCDML_DISP_font              u8g2_font_profont11_tf  // u8glib font (more
fonts under u8g.h line 1520 ...)
//TimesNewPixel_tr
//missingplanet_tf
//wqy12_t_chinese1
//profont11_tf
//finderskeepers_tf
//mozart_nbp_tf
#define _LCDML_DISP_font_w            6              // font width
#define _LCDML_DISP_font_h            12             // font height
// cursor settings
#define _LCDML_DISP_cursor_char       ">"            // cursor char
int cursorState;
```

```
#define _LCDML_DISP_cur_space_before  2              // cursor space between
#define _LCDML_DISP_cur_space_behind  4              // cursor space between
// menu position and size
#define _LCDML_DISP_box_x0            5              // start point (x0, y0)
#define _LCDML_DISP_box_y0            0              // start point (x0, y0)
#define _LCDML_DISP_box_x1            128            // width x  (x0 + width)
#define _LCDML_DISP_box_y1            64             // height y  (y0 + height)
#define _LCDML_DISP_draw_frame        0.5            // draw a box around the menu
// scrollbar width
#define _LCDML_DISP_scrollbar_w       2  // scrollbar width (if this value is < 3,
the scrollbar is disabled)

// nothing change here
#define _LCDML_DISP_cols_max          ((_LCDML_DISP_box_x1-
_LCDML_DISP_box_x0)/_LCDML_DISP_font_w)
#define _LCDML_DISP_rows_max          (((_LCDML_DISP_box_y1-_LCDML_DISP_box_y0-
((_LCDML_DISP_box_y1-
_LCDML_DISP_box_y0)/_LCDML_DISP_font_h))/_LCDML_DISP_font_h)+1)

// rows and cols
// when you use more rows or cols as allowed change in LCDMenuLib.h the define
"_LCDML_DISP_cfg_max_rows" and "_LCDML_DISP_cfg_max_string_length"
// the program needs more ram with this changes
#define _LCDML_DISP_rows              _LCDML_DISP_rows_max  // max rows
#define _LCDML_DISP_cols              20                    // max cols

// Initialize menu functions
void lcdml_menu_display();
void lcdml_menu_clear();
void lcdml_menu_control();

// Initilialize objects
LCDMenuLib2_menu LCDML_0 (255, 0, 0, NULL, NULL); // root menu element (do not
change)
LCDMenuLib2 LCDML(LCDML_0, _LCDML_DISP_rows, _LCDML_DISP_cols, lcdml_menu_display,
lcdml_menu_clear, lcdml_menu_control);

// Example for dynamic content
// 1. set the string to ""
// 2. use type  _LCDML_TYPE_dynParam   instead of    _LCDML_TYPE_default
// this function type can not be used in combination with different parameters
// LCDMenuLib_addAdvanced(id, prev_layer,     new_num,
condition,   lang_char_array, callback_function, parameter (0-255), menu function
type  )
LCDML_addAdvanced (0 , LCDML_0         , 1  , NULL,          ""                  ,
mDyn_para_1,                0,   _LCDML_TYPE_dynParam);                    //
NULL = no menu function
```

```
// Example for dynamic content
// 1. set the string to ""
// 2. use type  _LCDML_TYPE_dynParam   instead of    _LCDML_TYPE_default
// this function type can not be used in combination with different parameters
// LCDMenuLib_addAdvanced(id, prev_layer,     new_num,
condition,   lang_char_array, callback_function, parameter (0-255), menu function
type  )
LCDML_addAdvanced (1 , LCDML_0         , 2  , NULL,          ""                  ,
mDyn_para_2,                0,   _LCDML_TYPE_dynParam);                    //
NULL = no menu function

LCDML_addAdvanced (2  , LCDML_0         , 3  ,
NULL,          ""                   ,
mDyn_para_3,                0,   _LCDML_TYPE_dynParam);


// Menu setup LCDML_add(id, prev_layer, new_num, lang_char_array,
callback_function)
LCDML_add         (3  , LCDML_0         , 4  , "Deliver 1 dose"        ,
mFunc_manual_actuate);        // this menu function can be found on
"LCDML_display_menuFunction" tab
LCDML_add         (4  , LCDML_0         , 5  , "Reload canister"        ,
mFunc_reload);        // this menu function can be found on
"LCDML_display_menuFunction" tab
LCDML_add         (5  , LCDML_0         , 6  , "Pulse Oximeter"      ,
mFunc_information);       // this menu function can be found on
"LCDML_display_menuFunction" tab


//LCDML_addAdvanced (6  , LCDML_0_6         , 1  ,
NULL,          ""                   ,
mDyn_para_4,                0,   _LCDML_TYPE_dynParam);
//LCDML_add         (7 , LCDML_0_6       , 2  , "Back"             ,
mFunc_back);              // this menu function can be found on
"LCDML_display_menuFunction" tab
//


// Example for conditions (for example for a screensaver)
// 1. define a condition as a function of a boolean type -> return false = not
displayed, return true = displayed
// 2. set the function name as callback (remove the braces '()' it gives bad
errors)
// LCDMenuLib_addAdvanced(id, prev_layer,     new_num,
condition,   lang_char_array, callback_function, parameter (0-255), menu function
type  )
LCDML_addAdvanced (6 , LCDML_0         , 7  , COND_hide,  "screensaver"        ,
mFunc_screensaver,        0,   _LCDML_TYPE_default);       // this menu function
can be found on "LCDML_display_menuFunction" tab
```

```
// menu element count - last element id
// this value must be the same as the last menu element
#define _LCDML_DISP_cnt    6

// create menu
LCDML_createMenu(_LCDML_DISP_cnt);

uint8_t g_dynParam_1 = 1;             // variable defn for dosageNumber
uint8_t g_dynParam_2 = 1;             // variable defn for dosageInterva

uint8_t g_dynParam_3;             // variable defn for dosagesLeft
uint8_t g_dynParam_4;


// PRESSURE SENSOR_____________________________________________________________
// https://www.instructables.com/How-to-Read-MPX5010-Differential-Pressure-Sensor-
W/

const float ADC_mV = 4.8828125;       // conversion multiplier for ADC to mV
const float SensorOffset = 200.0;     // in mV taken from datasheet
const float sensitivity = 4.413;      // in mV/mmH2O taken from datasheet
const float mmh2O_cmH2O = 10;         // conversion divider for mmH2O to cmH2O
const float mmh2O_kpa = 0.00981;      // conversion multiplier for mmH2O to kPa
unsigned long int previousTime_p;     // time when 1st pressure reading is taken
unsigned long int currentTime_p;      // time when 2nd pressure reading is taken
#define Pressure_Sensor A0            // pressure sensor pin


// FLOWMETER___________________________________________________________________
// https://github.com/dwerne/Sensirion_SFM3000_arduino/tree/master

SFM3000wedo measflow(64);             // call flowmeter library
int offset = 32000;                   // offset for the sensor
float scale = 142.0;                  // scale factor for O2
int flow;
unsigned long int previousTime_f;     // time when 1st flow reading is taken
unsigned long int currentTime_f;      // time when 2nd flow reading is taken

// FILTER______________________________________________________________________
// https://www.megunolink.com/documentation/arduino-libraries/exponential-filter/

long filterWeight1 = 10;                // filter weight = 1
long filterWeight2 = 10;                // filter weight = 1
/* create a new exponential filter with a weight of 5 and an initial value of 0
   for each reading */
ExponentialFilter<long> ADCFilter1(filterWeight1, 0);
ExponentialFilter<long> ADCFilter2(filterWeight2, 0);
```

```
unsigned long int sampleTime_p = 100;
unsigned long int sampleTime_f1 = 200;
unsigned long int sampleTime_f2 = 250;

unsigned long int currentTime_1;
unsigned long int currentTime_2;
unsigned long int currentTime_3;
unsigned long int currentTime_4;
unsigned long int currentTime_5;
unsigned long int currentTime_6;

unsigned long int actuateTime;
unsigned long int inhaleTime;
unsigned long int currentTime;

int x;
int y;
int cpap_pressure;

// SERVO_____________________________________________________________________________
// https://github.com/hadefuwa/elegoo/blob/main/servo.ino

Servo myservo;                          // create servo object to control actuation
servo
Servo myservo1;                         // create servo object to control lock servo
int servoPause_1 = 250;                 // time taken move to each position
int servoPause_2 = 15000;               // servo pauses for 15s after each actuation
to allow medication from the previous delivery to take effect*/
int actuationFlag_num;                  // number flag for actuation
int dosageCounter = 200;                // number of dosages in 1 canister
int actuationCounter = 0;               // initialise number of actuations
unsigned long int timer = 0;            // initialise timer for dosage interval
bool breath_detected = false;           // flag for breath detection
int breath_detectedgradient = 0;

int totalCounter = 0;             // initialise number of actuations

// PIN SETUP
int alarm_pin = 9;                      // alarm/buzzer pin
int alarm_pinValue = 0;                 // set pin to low = alarm off

int door_pin = 11;                      // door switch pin
int door_pinValue = 0;                  // set pin to low = not pushed in

//int power_pin = 12;                     // power relay pin
int power_pinValue = 1;                 // set pin to low = relay open/close

int breath_pin = 12;
```

```
int breath_pinValue = 0;

int button_pin = 70;
int button_pinValue = 0;


// PULSE
OXIMETER_____________________________________________________________________
// Imported from Arduino library
// Sensor (adjust to your sensor type)

MAX30105 sensor;
const auto kSamplingRate = sensor.SAMPLING_RATE_400SPS;
const float kSamplingFrequency = 400.0;

// Finger Detection Threshold and Cooldown
const unsigned long kFingerThreshold = 10000;
const unsigned int kFingerCooldownMs = 500;

// Edge Detection Threshold (decrease for MAX30100)
const float kEdgeThreshold = -2000.0;

// Filters
const float kLowPassCutoff = 5.0;
const float kHighPassCutoff = 0.5;

// Averaging
const bool kEnableAveraging = false;
const int kAveragingSamples = 5;
const int kSampleThreshold = 5;
// Filter Instances
LowPassFilter low_pass_filter_red(kLowPassCutoff, kSamplingFrequency);
LowPassFilter low_pass_filter_ir(kLowPassCutoff, kSamplingFrequency);
HighPassFilter high_pass_filter(kHighPassCutoff, kSamplingFrequency);
Differentiator differentiator(kSamplingFrequency);
MovingAverageFilter<kAveragingSamples> averager_bpm;
MovingAverageFilter<kAveragingSamples> averager_r;
MovingAverageFilter<kAveragingSamples> averager_spo2;

// Statistic for pulse oximetry
MinMaxAvgStatistic stat_red;
MinMaxAvgStatistic stat_ir;

// R value to SpO2 calibration factors
// See https://www.maximintegrated.com/en/design/technical-documents/app-
notes/6/6845.html
float kSpO2_A = 1.5958422;
float kSpO2_B = -34.6596622;
float kSpO2_C = 112.6898759;
```

```
// Timestamp of the last heartbeat
long last_heartbeat = 0;

// Timestamp for finger detection
long finger_timestamp = 0;
bool finger_detected = false;

// Last diff to detect zero crossing
float last_diff = NAN;
bool crossed = false;
long crossed_time = 0;

int bpm;
float spo2;

//
SETUP_____________________________________________________________________________

void setup() {

  // LCD
SETUP_____________________________________________________________________
  u8g2.begin();
  u8g2.clearDisplay();
  u8g2.display();
  u8g2.setContrast (50);
  u8g2.clearBuffer();                 // clear the internal memory

  // serial init; only be needed if serial control is used
  Serial.begin(9600);                 // start serial

  // LCDMenuLib Setup
  LCDML_setup(_LCDML_DISP_cnt);

  // Enable Menu Rollover
  LCDML.MENU_enRollover();

  // Enable Screensaver (screensaver menu function, time to activate in ms)
  LCDML.SCREEN_enable(mFunc_screensaver, 10000); // set to 10 seconds

  Wire.begin();
  measflow.init();                    // initialize flowmeter
  delay(300);                         // wait 200 ms to initialize sensors

  pinMode(alarm_pin, INPUT);          // set pin as output
  pinMode(door_pin, INPUT);           // set pin as input
  // pinMode(power_pin, OUTPUT);         // set pin as input
```

```
  pinMode(breath_pin, INPUT);
  pinMode(button_pin, INPUT);

  //
SERVO_____________________________________________________________________________
  //myservo.attach(12);                 // attaches the servo on pin 12 to the
servo
  // myservo.write(0);                   // servo initially at 0 deg = rest
position

  myservo1.attach(13);                // attaches the servo on pin 13 to the servo
  myservo1.write(0);                  // servo initially at 0 deg = rest
position*/

  Serial.println("CLEARDATA");
  Serial.println("LABEL, Time, Started Time, Date, cpap_pressure,
inhalation_detect, button, flow, pressure, inhaleTime, MDD, actuateTime, time_dif,
actuation, actuationCounter");
  Serial.println("RESETTIMER");

  currentTime_3 = millis();

  while (millis() <= currentTime_3 + servoPause_1) {
    // time taken for servo to move and avoid bounce
    myservo1.write(130);              // servo moves to actuation pos 130
  }
  myservo1.write(40);
  // PULSE OXIMETER_____________________________________________________________
//  if (sensor.begin() && sensor.setSamplingRate(kSamplingRate)) {
//    Serial.println("Sensor initialized");
//  }
//  else {
//    Serial.println("Sensor not found");
//    while (1);
//  }

}

void actuateServo() {


  currentTime_3 = millis();

  while (millis() <= currentTime_3 + servoPause_1) {
    // time taken for servo to move and avoid bounce
    myservo1.write(130);              // servo moves to actuation pos 130
  }
  myservo1.write(40);                 // servo moves 40 deg
```

```
  breath_detected = false;             // set breath detected to false to allow
for next detection

}

void manualActuateservo() {

  actuationFlag_num = 14;// set an actuation flag number to log the signal, 15
when actuated
  Serial.print("Actuation:"); Serial.print(actuationFlag_num); Serial.print(",");

  currentTime_5 = millis();
  while (millis() < currentTime_5 + servoPause_1) {
    // time taken for servo to move and avoid bounce
    actuationFlag_num = 5;

    myservo1.write(130);              // servo moves to actuation pos 130
  }
  actuationFlag_num = 0;// set an actuation flag number to log the signal, 0 when
not actuated
  Serial.print("Actuation:"); Serial.print(actuationFlag_num); Serial.print(",");

  myservo1.write(45);                 // servo moves to rest position at 0 deg
}

void alarm() {

  // DOOR NOT
CLOSED_____________________________________________________________________
  door_pinValue = digitalRead(door_pin);
  if (door_pinValue == HIGH) {
    alarm_pinValue = HIGH;
  }
  else if (door_pinValue == LOW) {
    alarm_pinValue = LOW;
  }

  // LOW DOSAGE LEFT

  if (dosageCounter <= 10) {
    alarm_pinValue = HIGH;
  }
  else if (dosageCounter > 10) {
    alarm_pinValue = LOW;
  }

  digitalWrite(alarm_pin, alarm_pinValue);
```

```
}


void pulseOximeter() {
  auto sample = sensor.readSample(1000);
  float current_value_red = sample.red;
  float current_value_ir = sample.ir;

  // Detect Finger using raw sensor value
  if (sample.red > kFingerThreshold) {
    if (millis() - finger_timestamp > kFingerCooldownMs) {
      finger_detected = true;
    }
  }
  else {
    // Reset values if the finger is removed
    differentiator.reset();
    averager_bpm.reset();
    averager_r.reset();
    averager_spo2.reset();
    low_pass_filter_red.reset();
    low_pass_filter_ir.reset();
    high_pass_filter.reset();
    stat_red.reset();
    stat_ir.reset();

    finger_detected = false;
    finger_timestamp = millis();
  }

  if (finger_detected) {
    current_value_red = low_pass_filter_red.process(current_value_red);
    current_value_ir = low_pass_filter_ir.process(current_value_ir);

    // Statistics for pulse oximetry
    stat_red.process(current_value_red);
    stat_ir.process(current_value_ir);

    // Heart beat detection using value for red LED
    float current_value = high_pass_filter.process(current_value_red);
    float current_diff = differentiator.process(current_value);

    // Valid values?
    if (!isnan(current_diff) && !isnan(last_diff)) {

      // Detect Heartbeat - Zero-Crossing
      if (last_diff > 0 && current_diff < 0) {
        crossed = true;
        crossed_time = millis();
```

```
      }

      if (current_diff > 0) {
        crossed = false;
      }

      // Detect Heartbeat - Falling Edge Threshold
      if (crossed && current_diff < kEdgeThreshold) {
        if (last_heartbeat != 0 && crossed_time - last_heartbeat > 300) {
          // Show Results
          bpm = 60000 / (crossed_time - last_heartbeat);
          float rred = (stat_red.maximum() - stat_red.minimum()) /
stat_red.average();
          float rir = (stat_ir.maximum() - stat_ir.minimum()) / stat_ir.average();
          float r = rred / rir;
          spo2 = kSpO2_A * r * r + kSpO2_B * r + kSpO2_C;

          if (bpm > 50 && bpm < 250) {
            // Average?
            if (kEnableAveraging) {
              int average_bpm = averager_bpm.process(bpm);
              int average_r = averager_r.process(r);
              int average_spo2 = averager_spo2.process(spo2);

              // Show if enough samples have been collected
              if (averager_bpm.count() >= kSampleThreshold) {
//                Serial.print("Time (ms): ");
//                Serial.println(millis());
//                Serial.print("Heart Rate (avg, bpm): ");
//                Serial.println(average_bpm);
//                Serial.print("R-Value (avg): ");
//                Serial.println(average_r);
//                Serial.print("SpO2 (avg, %): ");
//                Serial.println(average_spo2);
              }
            }
            else {
//              Serial.print("Time (ms): ");
//              Serial.println(millis());
//              Serial.print("Heart Rate (current, bpm): ");
//              Serial.println(bpm);
//              Serial.print("R-Value (current): ");
//              Serial.println(r);
//              Serial.print("SpO2 (current, %): ");
//              Serial.println(spo2);
            }
          }
```

```
          // Reset statistic
          stat_red.reset();
          stat_ir.reset();
        }

        crossed = false;
        last_heartbeat = crossed_time;
      }
    }

    last_diff = current_diff;
  }


}


void loop() {

  Serial.print("DATA, TIME, TIMER, DATE,");

  cpap_pressure = 8;// Serial.print("cpap_pressure:");
  Serial.print(cpap_pressure); Serial.print(",");


  unsigned long int dosageInterval = g_dynParam_1 * 3600000;

  unsigned long int numberOfdosage = g_dynParam_2;

  // LOG INHALATION SIGNAL FROM BREATHING
SIMULATOR_____________________________________
  breath_pinValue = digitalRead(breath_pin);
  // Serial.print("inhalation_detect:"),
  Serial.print(breath_pinValue * 10), Serial.print(",");

  button_pinValue = digitalRead(button_pin);
  // Serial.print("inhalation_detect:"),
  Serial.print(button_pinValue * 20), Serial.print(",");


  // FLOW
METER_____________________________________________________________________
  unsigned int resultcheck = measflow.getvalue();           // read flowmeter
  flow = ((float)resultcheck - offset) / (scale);       // flow reading in Lpm
  //  Serial.print("flow:");
  Serial.print(flow / 4); Serial.print(",");

  ADCFilter1.Filter(flow);                    // filter flow reading
  int flow_filter  = ADCFilter1.Current();
```

```
  // Serial.print("flowfilter:");
  //  Serial.print(flow_filter / 4); Serial.print(",");
  int flow_gradient = 0;

  // PRESSURE SENSOR_____________________________________________________________________
  int pressure = (analogRead(A0) * ADC_mV - SensorOffset) / sensitivity
                / mmh2O_cmH2O; // pressure reading in cmH2O
  //Serial.print("pressure:");
  Serial.print(pressure); Serial.print(",");

  // SETTING BASELINE
PRESSURE_____________________________________________________
  ADCFilter2.Filter(pressure);                    // filter pressure reading
  int baseline_pressure  = ADCFilter2.Current();

  //Serial.print("baseline_pressure:");
  //  Serial.print(baseline_pressure); Serial.print(",");

  // BREATH DETECTION_____________________________________________________________________
  if (flow_filter < flow && baseline_pressure > pressure && flow < 0) {
    breath_detected = true;

    inhaleTime = millis();
    Serial.print(inhaleTime); Serial.print(",");

    int w = 12;  // Identifier for breath detection in data recorded
    Serial.print(w); Serial.print(",");
  }

  else {
    breath_detected = false;

    inhaleTime = 0;
    Serial.print(inhaleTime); Serial.print(",");

    int w = 0;   // Identifier for breath detection in data recorded
    Serial.print(w); Serial.print(",");
  }


  if (millis() >=  currentTime_4) {
    // servo pauses for 15 seconds after each actuation to allow medication from
the previous delivery to take effect
    if (breath_detected && (actuationCounter < numberOfdosage)) {

      actuateTime = millis();
      Serial.print(actuateTime); Serial.print(",");

      x = actuateTime - inhaleTime + servoPause_1 - 110;
```

```
    Serial.print(x); Serial.print(",");

    if   (x <= 200) {
      actuationFlag_num = 14; // Identifier for actuation in data recorded
      Serial.print(actuationFlag_num); Serial.print(",");

      actuateServo();

      actuationCounter++;
      totalCounter++;
      dosageCounter--;
    }

    else {
      actuationFlag_num = 5;  // Identifier for no actuation in data recorded
      Serial.print(actuationFlag_num); Serial.print(",");
    }
    currentTime_4 += servoPause_2;
  }
}

else {

  actuateTime = millis();
  Serial.print(actuateTime); Serial.print(",");

  currentTime = millis();

  x = actuateTime - currentTime + servoPause_1 - 110;
  Serial.print(x); Serial.print(",");

  actuationFlag_num = 0;
  Serial.print(actuationFlag_num); Serial.print(",");
}

Serial.println(totalCounter);

if (millis() >= timer) {
  actuationCounter = 0;
  timer += dosageInterval;
  currentTime_4 = millis();
}

alarm();


LCDML.loop();
```

```
}


// ************************************************************************
// check some errors - do not change here anything
// ************************************************************************
# if(_LCDML_glcd_tft_box_x1 > _LCDML_glcd_tft_w)
# error _LCDML_glcd_tft_box_x1 is to big
# endif

# if(_LCDML_glcd_tft_box_y1 > _LCDML_glcd_tft_h)
# error _LCDML_glcd_tft_box_y1 is to big
# endif
```